

CRANFIELD UNIVERSITY

Tasneem Bhaiji

Enhancing Microalgae Attachment for Biofilm-Based
Photobioreactors

School of Aerospace, Transport and Manufacturing

PhD

Academic Year: 2012 - 2015

Supervisor: Qi Zhang and Paul Kirby
February 2016

CRANFIELD UNIVERSITY

School of Aerospace, Transport and Manufacturing

PhD

Academic Year 2012 - 2015

Tasneem Bhaiji

Enhancing Microalgae Attachment for Biofilm-Based Photobioreactors

Supervisor: Dr Qi Zhang and Dr Paul Kirby
February 2016

This thesis is submitted in partial fulfilment of the requirements for the
degree of PhD

© Cranfield University (2016). All rights reserved. No part of this
publication may be reproduced without the written permission of the
copyright owner.

Acknowledgements

I would like to thank my supervisor Dr Qi Zhang for his help and guidance throughout this project. I would also like to thank Dr Paul Kirby and Dr Zsussanna Libor for their contribution and interest towards the study.

I would also like to acknowledge all the members of the ALGADISK consortium for their collaborations and discussions throughout the project. Thank you also to colleagues and friends at Cranfield University especially Faruk, Kasia, and Rebecca.

I would like to thank my family and friends, in particular, Ananda, Shaheena, Yasin, Amna, and Rick for their immense help and support throughout my studies.

Finally, the financial support of the European Union's Seventh Framework Program (FP7/2007-2013) is thankfully acknowledged.

Abstract

The potential of algal biofuels has been technically and experimentally confirmed with laboratory- and pilot-scale studies in past literature. However, the most important factor now is to confirm that algal cultivation for biofuels and other end-products is economically feasible on the large, commercial scale. The ALGADISK project aimed to produce a novel biofilm-based photo-bioreactor with the aims of CO₂ capture and making valuable products such as biofuel, economically viable. This thesis aimed to investigate and provide substrates in which algae biofilm is stimulated and increased. Polyelectrolyte (PE) coatings adsorbed onto cost-effective polymers were investigated, based on the strategy of electrostatic attraction. It was found that the algae species charge density and cell wall functional groups composition affected attachment onto charged PE coatings. Two coatings labeled C1 and C3 were selected due to their promising growth results with the strains *C.sorokiniana*, *C.vulgaris* and *S.obliquus*. Harvesting growth results showed inconsistent regrowth due to the lack of textured structure. Sandpapering the surface with certain grades was found to improve regrowth and consistency. Surface roughness did not show correlation to initial attachment of algae or strength of attachment. It was shown instead that surface roughness improved long-term growth

As part of the aims of the ALGADISK project, the coatings large scale potential and cost was optimized. It was found that airbrushing rather than dip-coating, reduced the amount of PE solution needed drastically. Furthermore, photo-cross-linking with UV exposure enhanced the strength of C1 according to scratch and wear data.

Lastly, the physico-chemical properties of both algae and substrates were examined in order to examine the thermodynamic model for algae adhesion prediction. It was found that the two thermodynamic approaches tested did not predict algae adhesion results with good accuracy. However, it was revealed that there could be a possible link between the substrate physico-chemistry and lipid content found in the biofilm attached. It was found that the less favorable the predicted thermodynamic conditions the higher the lipid content.

Table of Contents

Chapter 1	1
1.0 Introduction.....	1
1.1 Algal Biofuel Production	1
1.2 Project development	5
1.3 Objectives of research.....	8
1.4 Thesis outline	8
Chapter 2	10
Literature review.....	10
2.1 Current Algae Cultivation Techniques	10
2.1.1 Suspended algae production	10
2.1.2 Non-suspended algae production.....	18
2.2 Algal attachment and biofilm formation.....	22
2.3 Cell to Substrata and Cell to Cell Interactions.....	25
2.4 Methods for harvesting algae.....	31
2.5 Algae as a potential Biofuel.....	35
2.6 Algae and Biofuel Production.....	41
Chapter 3	50
Encouraging algae biofilm formation using polyelectrolyte coated polymers ..	50
Abstract.....	50
3.1 Introduction.....	51
3.2 Materials and Methods.....	52
3.2.7 Contact angle measurements.....	57
3.2.8 Zeta potential measurements and charge density.....	57
3.2.9 Determining cell wall functional groups.....	58
3.2.10 Data analysis and Statistics	58
3.3 Results and Discussion	58
3.3.1 Testing PEM coatings adsorbed onto polymers on different algae species.....	58
3.3.3 Cell viability assays	64
3.4 Conclusion	70
Chapter 4	72
Cost-effective methods to improve regrowth between harvests	72

Abstract.....	72
4.1 Introduction.....	73
4.2 Methodology.....	74
4.2.1 Algae culture and growth studies.....	74
4.2.2 Substrate preparation and PE deposition	74
4.2.3 Surface characterization using microscopy.....	74
4.2.4 Dektak surface profiler	75
4.2.6 Data analysis and Statistics.....	75
4.3 Results and discussion	76
4.3.1 Examining use of C1 and C3 in long term growth studies	76
4.3.2 Optimizing regrowth on coated substrates between harvests	82
4.3 Conclusions.....	89
Chapter 5	90
Optimisation of coating and application for large scale production for the ALGADISK system.....	90
5.1 Introduction.....	91
5.2 Materials and methods	93
5.2.1 Algae culture and growth studies.....	93
5.2.2 Substrate preparation and PE deposition	93
5.2.3 Contact angle measurements, Hysteresis and Surface energy measurements.....	93
5.2.7 Coating application via spraying	95
5.2.8 Ultraviolet (UV) treatment.....	95
5.2.9 Determining optimal number of AB layers in C1.....	96
5.2.10 Determining optimal polymer concentration for AB application ...	96
5.2.11 Determining optimum ionic strength.....	96
5.2.12 Disk coating method for ALGADISK prototype.....	96
5.3 Results and Discussion	97
5.3.1 Investigating alternative substrate pre-treatments.....	97
5.3.2 Investigating spraying as method of coating application.....	102

5.3.4	Photo-cross linking with Ultraviolet (UV).....	107
5.3.5	Determining optimal polymer concentration	112
5.3.6	Determining optimal number of layers	115
5.3.7	Determining optimum ionic strength	118
5.3.8	Finalized method for ALGADISK prototype, cost analysis and results	124
5.4	Conclusions.....	127
Chapter 6	129
	Influence of physico-chemical properties on algae adhesion and lipid production	129
	Abstract.....	129
6.1	Introduction.....	130
6.2	Methodology.....	131
6.3	Results and discussion	135
6.3.1.	Thermodynamic modeling results.....	135
6.2.1	Experimental growth results and evaluation of the thermodynamic model	139
6.2.2	Investigating the influence of physico-chemical properties of algae and substrata on lipid content.	148
6.4	Conclusion	152
Chapter 7	154
	Conclusions and Recommendations	154
	Nomenclature.....	158

List of Tables

1.1 - Advantages and Disadvantages of open ponds and photobioreactors compared to the ALGADISK system (Wootsch et al. 2012).....	7
2.1: List of properties and known applications for PEs selected.....	47
3.2.1: Coating labels used and their PE composition.....	57
3.3.1 Contact angle measurements (°) taken with water of all coated substrates.....	60
3.3.2: Summary of coatings and substrates with the highest biofilm growth....	68
3.3.3: Charge density of algae.....	69
3.3.4 Amount of acidic sites found in the cell walls of <i>C. sorokiniana</i> , <i>C. vulgaris</i> and <i>N. oculata</i>	70
4.3.1: Elemental analysis of C1 PETG after harvest 6 via EDX.....	79
4.3.2: Contact angle (°) measurements taken before and after harvesting.....	80
5.3.1: Contact angle and surface tension measurements of substrate PET.....	98
5.3.2: Pretreatment and resulting coating thickness.	99
5.3.3: Contact angle measurements and film thickness of airbrushed and dip coated methods of C1 application.....	103
5.3.4: Contact angles and surface energy measurements of surfaces exposed to UVC.....	109
5.3.5: Contact angle and coating thickness measurements of C1 with different PE concentrations.....	112
5.3.6: Contact angle and film thickness measurements of C1 with differing number of layers.....	116
5.3.7: Contact angle and film thickness measurements of C1 made with differing levels of salt	121
5.3.8: Contact angle measurements taken before and after wetting.....	125
6.3.1: Surface tension measurements of liquids (mJ m^{-2}) (Van & Good, 1992).	137
6.3.2: Physico chemical properties of algae.....	137

6.3.3: Physico chemical properties of surfaces.....	137
6.3.4 Interaction energy between substrate and algae.	138
6.3.5: Comparison of model prediction and experimental results.....	146
6.3.6: Correlation coefficients calculated from data presented in Figures 6.3.3.....	147
6.3.7: Correlation coefficients calculated from data presented in Figure 6.3.4.....	151

List of Figures

1.1: Worldwide total energy consumption 1971 to 2012 (IEA, 2014)	1
1.2: Algae cultivation and the potential products (adapted from Markou and Nerantzis, 2013).....	3
2.1: Overhead view of a raceway pond system (Chisti.,2007).....	12
2.2: Schematic drawing of tubular horizontal photobioreactor (A); and a flat-plate photobioreactor (B) (Jorquera et al. 2009)	16
2.3: Stirred tank photobioreactor (Gupta et al. 2015)	17
2.4 - Proposed versatility of algae as biofuels compared to current sources (Adapted from Jones and Mayfield, 2012).....	38
2.5: Microscopic images of BAEC growth and adhesion on different polyelectrolyte films.....	43
3.2.1: (A) Schematic diagram showing algae adhesion assay set up for absorption and desorption tests. (B) Schematic drawing of Ibidi 0.2 Luer Sticky-slides.....	53
3.2.2: Microscopic images taken of <i>C. sorokiniana</i> before (left) and after flushing with water (right).....	54
3.2.3: Long-term growth experiment set-up. Image shows example of static and non-static (rotating table) growth tests. All samples are placed directly beneath two florescent light tubes (15 W).....	54
3.2.4: Schematic diagram showing steps in PEM formation onto a substrate.	56
3.3.1. (A) Static growth results of <i>C.sorokiniana</i> .(B)non-static growth results of <i>C. sorokiniana</i> . A & B show algae dry weight harvested at day 7 on surfaces tested. (C) Adhesion of <i>C. sorokiniana</i> found on surfaces after wash-out, calculated as a percentage. Error bars represent standard deviation of the mean (n=3).....	61
3.3.2. (A) Static growth results of <i>S. obliquus</i> . (B) Non-static growth results of <i>S. obliquus</i> . A & B show algae dry weight harvested at day 7 on surfaces tested. (C)	

Adhesion (%) of *S. obliquus* found on surfaces after wash-out, calculated as a percentage. Error bars represent standard deviation of the mean (n=3).
.....62

3.3.3. (A) Static growth results of *C.vulgaris*. (B) Non-static growth results of *C.vulgaris*. A & B show algae dry weight harvested at day 7 on surfaces tested. (C) Adhesion (%) of *C.vulgaris* found on surfaces after wash-out, calculated as a percentage. Error bars represent standard deviation of the mean (n=3).
.....63

3.3.4 displays the % of viable cells found on all surfaces after 72 hours for all 3 algal species. C4 and C6 for *C. sorokiniana* had the lowest observable viable algal cells. 64

3.3.5: Graph shows average biofilm growth for *C.sorokiniana*, *S.obliquus* and *C.vulgari* plotted against contact angle of substrate. Error bars represent standard deviation of the mean (n=9)..... 65

3.3.6. (A) Effect of pH on zeta potential of all three algae species. (B) Effect of pH and corresponding zeta potential on algal adhesion on C1 PETG and C3 PETG. (C) Effect of charge density on 5 different algal species on C3 PETG. Error bars represent standard deviation of the mean (n=3)
.....69

4.3.1. AFM (left) and ESEM images (right). (A) PETG C0. (B) PETG C1 (C) PETG C3.....78

4.3.2. ESEM images taken after harvest 6 (A) PETG C0. (B) PETG C1 (C) PETG C3.....79

4.3.4: (A) Schematic representation of the ALGADISK lab scale reactor. D= disk, M= motor, C- container, T= temperature control system, BT= buffer tank. (B) Average productivities of four growth harvest cycles at 11 rpm. Due to technical issues with disk one, productivity results were not presented. (C) Biofilm progression of lab scale experiment before and after harvest on day 10. Error bars represent standard deviation of the mean (n=3). The following surfaces were tested: Rough mesh (45 um) (steel), fine mesh (15 um) (steel) and Polycarbonate with coating 1, on *C.sorokiniana*. Error bars show standard deviation of the mean. (Blanken et al. 2014). (D) CLSM characterization of rough and fine steel mesh obtained from WU.....81

4.3.5: (A) Optical microscopy images of polypropylene mesh (PPM) with 200 um sized gaps (I & ii) and 100 um sized gaps (iii & iv) before and after harvest.

(B) Average harvest weight from 5 harvest cycles for <i>C.sorokiniana</i> . (C) Average harvest weight from 5 harvest cycles for <i>C.vulgaris</i> . Harvesting took place every 7 days.....	83
4.3.6: (A) Dry <i>Chlorella</i> strain weight found on polyethylene with and without coating 3. (B) Biofilm thickness (um). (C) Lipid productivity found on coated and uncoated disk material. (D) Image of lab scale ALGADISK reactor at BAYBIO.	84
4.3.7: Topographical analysis using CLSM (A& C) and AFM (B & D). (A & B) PETG Grit blasted. (C & D) PETG sandpapered with grade p90. (E& F) Microscopic images of sandpapered PETG C1 after harvest (Objective: X 20 & X 5 respectively). (G) Average harvested weight for 8 harvest cycles. Harvesting was undertaken every 7 days. Error bars show standard deviation of the mean.....	85
4.3.8: (A) Number of algal cells measured in initial attachment adhesion test. (B) % of remaining cells measured after wash-out via adhesion assays (C) Average growth results taken for 4 harvest cycles. Harvesting was undertaken every 7 days.....	88
5.2.1. Diagram showing how advancing and receding contact angles are measured.....	93
5.3.1. Hysteresis values calculated for differing pre-treated PETG with and without C1. Error bars represent standard deviation of the mean.....	98
5.3.2. (A) ESEM images (1000 x) of C1 on different pre-treated substrates. (I) Substrate charging. (II) Hydrolysatation. (III) Plasma etching. (B – D) Scratch and wear testing on differently pre-treated substrates followed by C1.	100
5.3.3. (A) Adhesion of <i>C. sorokiniana</i> found on surfaces with C1 with different pre-treatments after flushing. (B) Number of cells counted after 6 hours of incubation followed by washing. (C) Biofilm density harvested after 7 days. Error bars represent standard deviation of the mean (n=3)	101
5.3.4: ESEM images at 1000x taken of substrates PET with AB C1 (A) Fine mist. (B) Medium mist. (C) Large mist.....	103
5.3.5: Hysteresis values calculated for PETG with and without C1. Error bars represent standard deviation of the mean (N =3)	103

5.3.6. Comparison of DC ad AB methods. (A – C) Scratch and wear testing on different airbrush gun application.....104

5.3.7. (A) Number of attached cells counted after incubation with *C. sorokiniana* followed by washing. (B) Adhesion (%) of *C. sorokiniana* found on tested coated surfaces at 72 hrs after flushing. (C) Biofilm density found on tested surfaces. Error bars show standard deviation of the mean (n=3)..... 106

5.3.8: Hysteresis values calculated for PETG with and without C1. Error bars represent standard deviation of the mean (N =3)..... 109

5.3.9: (A&B) ESEM images at 100x (right) and 1000x (left) taken of substrate PETG with coating 1 after UV exposure. (A) AB PETG C1. (B) DC PETG C1. (C) AFM 3D analysis of AB fine mist (5 layers) of C1 after UV exposure.(D) AFM 3D analysis of DC of C1(5 layers) UV exposure. UV exposure: 3hours.109

5.3.10 (A & B) Scratch and wear testing comparing the effect of UV exposure on strength of coating (C) Number of attached cells counted after incubation with *C. sorokiniana* followed by washing. (D) % adhesion found on tested coated surfaces. (E) Biofilm density found on tested surfaces. *C. sorokiniana* algae used. Error bars show standard deviation of the mean (n=3) 111

5.3.11: Hysteresis values calculated for PETG made with varying concentrations of PE in C1. Error bars represent standard deviation of the mean (N =3).....113

5.3.12. (A) Number of attached cells counted after incubation with algae followed by washing. (B) Adhesion (%) found on PETG C1 formulated with differing PE concentration after 72 hrs incubation with algae followed by flushing. (B) Biofilm density found on tested surfaces. *C. sorokiniana* algae used. Error bars show standard deviation of the mean (n=3).113

5.3.13. (A – D) Scratch and wear testing on C1 PETG using different PE concentration (A) 0.5 mg/ml (B) 1.0 mg/ml. (C) 1.5 mg/ml, (D) 2.5 mg/ml.114

5.3.14. (A) Adhesion (%) found on C1 PETG with different number of layers. (B) Number of attached cells counted after incubation with algae followed by washing (C) Biofilm density found on tested surfaces. *C. sorokiniana* algae used. Error bars show standard deviation of the mean (n=3) 116

5.3.15: (A – D) Scratch and wear data investigating effect of number of PE layers on coating strength (PETG C1). (A) 5 layers. (B) 7 layers. (C) 9 layers. (D)	117
5.3.16. (A) Hysteresis values observed on different number of PE layers. (B) AFM 3D analysis of 9 layers (C1 PETG). (C) ESEM image (1000 x) of PETG C1 9 layers.....	118
5.3.17: (A-F) AFM 3D analysis characterising the effect of ionic strength (NaCl conc.) on C1 PETG. (A) 0 M. (B) 0.1 M. (C) 0.5 M. (D) 1 M. (E) 2 M. (F) Adhesion (%) of <i>C.sorokiniana</i> (N=3). Error bars show standard deviation of the mean.	122
5.3.18. (A - D) Scratch and wear data investigating effect of ionic strength of PE solution on coating strength (PETG C1). A) 0 M. (B) 0.1 M. (C) 0.5 M. (D) 1 M. (E) 2 M (F) Hysteresis found with varying salt content.	123
5.3.19. (A) Image of prototype disk before and after harvest. (B) Prototype reactor growth results for up to 10 harvesting cycles showing total dry matter (g).	127
6.3.1. Bars show initial attachment of algae after 2h on different surfaces. Error bars show standard deviation of the mean (n=3). ΔG_{adh} is the free energy of adhesion according to AB and LW components. W-d and W-p is the work of attachments due dispersive and polar forces respectively. W is the total work of attachment due to polar and dispersive forces and substrate surface energy.	143
.6.3.2. Bars show percentage of algal cells after flushing with water on different surfaces. Error bars show standard deviation of the mean (n=3). ΔG_{adh} is the free energy of adhesion according to AB and LW components. W-d and W-p is the work of attachments due dispersive and polar forces respectively. W is the total work of attachment due to polar and dispersive forces and substrate surface energy.	144
6.3.3. Bars show weighted biofilm density found on tested surfaces on different surfaces after 7 days. Error bars show standard deviation of the mean (n=3). ΔG_{adh} is the free energy of adhesion according to AB and LW components. W-d and W-p is the work of attachments due dispersive and polar forces respectively. W is the total work of attachment due to polar and dispersive forces and substrate surface energy.....	145

6.3.4. Bars show lipid content (%) found on tested surfaces on different surfaces after 7 days. Error bars show standard deviation of the mean (n=3). ΔG_{adh} is the free energy of adhesion according to AB and LW components. W is the total work of attachment due to polar and dispersive forces and substrate surface energy.....150

6.3.5. Bars show correlation coefficient (refer to table 6.3.7). ΔG_{adh} is the free energy of adhesion according to AB and LW components. W is the total work of attachment due to polar and dispersive forces and substrate surface energy.....151

Chapter 1

1.0 Introduction

1.1 Algal Biofuel Production

While there is debate regarding the status of the world's oil reserves, overall world energy consumption has risen in correlation with the increase in population, industrialisation and globalisation. International Energy Agency (IEA) data shows an increasing trend in the consumption of total energy worldwide over a period of 40 years, with increases in fossil fuel usage especially prominent (Figure 1.1) (IEA, 2014). Growth in the consumption of oil, coal and nuclear power accelerated in 2013, with an overall increase in usage worldwide by 2.3% (BP, 2014). Global policy makers have determined that global temperature should not rise by more than 2 °C above pre-industrial measurements in order to reduce the effects of global warming (UNFCCC, 2009). In order for this to be accomplished, a recent study concluded that one third of oil reserves, half of natural gas reserves, and over 80% of coal reserves should remain in the ground (McGlade & Ekins, 2015). Therefore, it is clear that alternative, renewable and clean sources of energy are required.

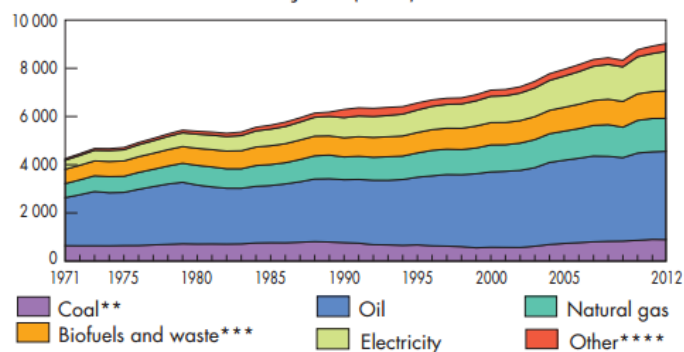


Figure 1.1 - Worldwide total energy consumption 1971 to 2012 (IEA, 2014)

The extraction of biofuels from agricultural, forestry and aquatic biomass have been considered for a number of years due to their renewable, carbon-neutral nature. However, the first generation biofuels derived from food crops and oils have repercussions on land available for food supply, food prices, and even increased emissions from clearing forestry for their cultivation (Ragauskas et al. 2006; Wiley et al. 2011). The second generation biofuels can be extracted from lignocellulose material, woody crops, or agricultural residues which require extensive processing; meaning capital and logistics costs are therefore high and a barrier to widespread use (Greenergy, 2010). Therefore algal biomass has been identified as a promising alternative. This promise results from a number of inherent advantages; firstly, algae have little to no competition with agricultural food and feed production (Behera et al. 2015); second, they have higher photosynthetic efficiency compared to terrestrial crops (Wiley et al. 2011); and third, they can be cultivated in arable, saline, and wastewater conditions throughout the year (Gendy and El-Temtamy, 2013). Algae are noted to require less land for cultivation: if transport fuel use for a single year in the United Kingdom (UK) was met solely with biodiesel from rapeseed oil, this would require 17.5 Mha (million hectares) of land, which is over 50% of the total land area of the UK. If these requirements were met with algae, assumed productivity estimates suggest that only 0.6 Mha of land would be required (Scott et al. 2010). The varying molecular contents of different algal species leads to a variety of products that can potentially be produced; including biofuels, animal feed, high-value cosmetics and food supplements, along with industrial applications such as wastewater treatment (Figure 1.2) (Markou and Nerantzis, 2013).

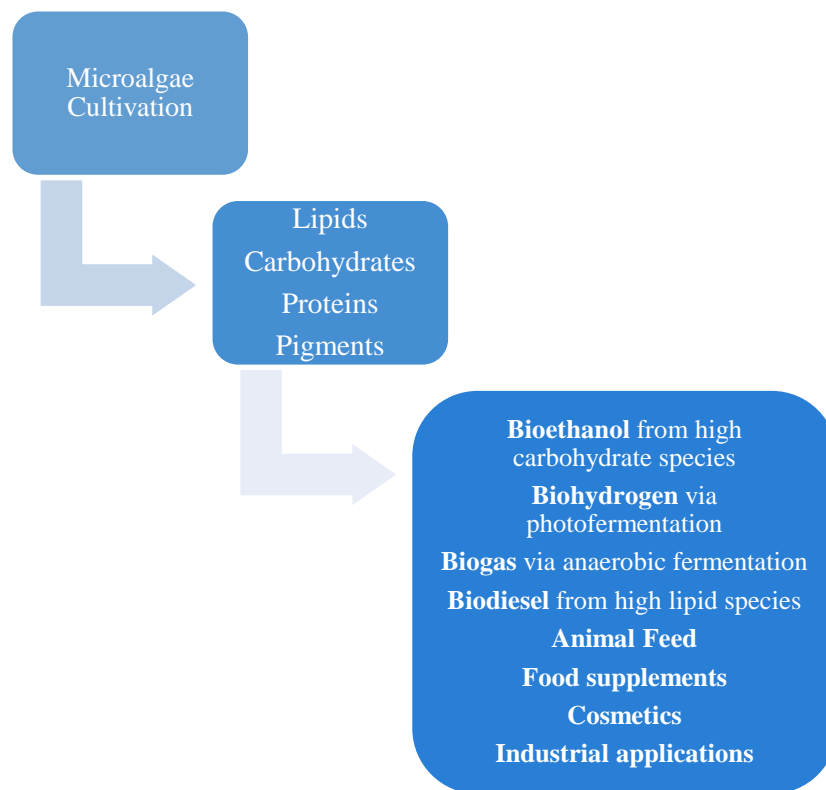


Figure 1.2 - Algae cultivation and the potential products (adapted from Markou and Nerantzis, 2013).

Algae cultivation, harvesting and processing into useful end-products is promising in small- and pilot-scale studies (Rodolfi et al. 2009; Vanthoor-Koopmans et al. 2013). A criticism of contemporary research is that potential growth yields from pilot studies are frequently overestimated (Moody et al. 2014). A recent study combining a large-scale growth model with worldwide meteorological data found that a number of countries in South America, Asia and Africa could potentially supplement 30% of their fuel consumption from microalgae cultivation with the lowest estimates of productivity (Moody et al. 2014). Therefore, even conservative estimates highlight the potential of algae as a biofuel.

The concept of utilising algae to make fuel was first discussed around half a century ago. In the 1970s, The US Department of Energy’s Office of Fuels Development funded

an Aquatic Species Program (ASP), aimed at producing biodiesel from pond algae (Sheehan et al. 1998). This program led to the development of open production systems (raceway ponds) and photobioreactors (PBRs) (Sheehan et al. 1998; Wijffels & Barbosa, 2010). Both open production systems and PBRs have advantages, however there are a number of significant drawbacks which make scaling up production to the level required for significant biofuel production difficult. Open ponds are prone to contamination, require more land, and do not allow manipulation of environmental factors such as light intensity, pH, and carbon dioxide delivery (Scott et al. 2010). PBRs allow for controlled conditions, and generally show good productivity on the small- to pilot-scale (Ugwu et al. 2008). However, they require higher investment and operating costs. These costs have been reducing over the past 15-20 years resulting from improvements in PBR design, materials and efficiency (Ugwu et al. 2008). Regardless, sensitivity analysis of current PBR production costs (accounting for prospective improvements in efficiency) estimate that in 10 years costs can reduce from € 5-6 per kg biomass to € 0.70 per kg dry weight (Norsker et al. 2011). This is close to the US € 0.23 kg⁻¹ recommended cost for economic fuel production (Darzins et al. 2010). This 10 to 15 year projection is confirmed by other research (Rodolfi et al. 2009; Wijffels & Barbosa, 2010).

An alternative method of algae production explored in light of these limitations is the non-suspended cultivation of algae in a polymeric matrix or from a biofilm. These solid carrier systems can potentially offer greater biomass yields, reduce water consumption, and be easier to scale up (Gross et al. 2015). In addition, biofilm growth systems can reduce costs related to harvesting, which is an expensive process (Ugwu et al. 2008; Gross et al. 2015). A variety of surfaces and reactor configurations have been tested to facilitate biofilm formation and overall biomass yield: surface biomass productivity

ranges from 1.8 to 20.1 g m⁻² day⁻¹ depending on reactor design, attachment material and algal species (Blanken et al. 2014; Gross et al. 2015).

Bio-refining of algae to simultaneously produce and extract bulk chemicals, feed, and high-value cosmetic and food materials is noted to be one of the most efficient and effective ways to make algae production economically viable (Wijffels & Barbosa, 2010; Vanthoor-Koopmans et al. 2013; Li et al. 2015). For this to occur, current research need to focus on first finding the optimum algae species for the desired end-product, with regards to biofuels these are generally high lipid-containing species. A promising avenue for future research is the genetic modification of algae species (Wijffels & Barbosa, 2010). In addition, proficient cell disruption, extraction and harvesting technologies are necessary (Vanthoor-Koopmans et al. 2013). With regards to biofilm cultivation, the optimum configuration of bioreactor, along with the most effective surface materials are areas that need to be explored. These factors, when combined with longer duration pilot-studies and intensive cost analyses, will ideally allow algae to fulfil its promising potential as a biofuel.

1.2 Project development

This project is part of the ALGADISK project, funded by the European Union's Seventh Framework Program (FP7/2007-2013) under grant agreement no.286887. The ALGADISK project aims to develop a biofilm reactor for algal biomass production. The ALGADISK reactor will additionally be modular and automatic, which will facilitate scaling of the system to meet industrial needs (Wootsch et al. 2012).

The ALGADISK system uses biofilm technology on Rotating Biological Contractors (RBCs), which are commonly used for industrial wastewater treatment (Safa et al. 2014). Flat plates or discs are coated with a biocompatible surface which the cultivated algal species adhere to. These discs are rotated and submerged regularly in the liquid

and gaseous media. The system itself utilises captured carbon dioxide from industrial emissions to cultivate algae on both biocompatible surfaces and in aqueous environments. This means carbon dioxide is absorbed from both the liquid and the gaseous phase, increasing the overall productivity of the reactor while minimising water requirements. Excess algae on the surfaces of the rotating discs are harvested automatically, without disturbing production. For the reactor to be scaled-up or down, this requires the addition or removal of discs. Artificial light is provided and manipulated by the use of an LED lamp system (Wootsch et al. 2012).

This design has the additional advantage of a reduced footprint; a criticism frequently found in other suspended and non-suspended algae production systems (Jones & Mayfield, 2002; Gross et al 2015). Other advantages of the ALGADISK system over conventional open-pond and photobioreactor (PBR) systems are capital costs on par with open-ponds, and lower than those of PBRs (Wootsch et al. 2012) Operating costs are further reduced as oxygen removal and cooling are unnecessary (Table 1.1).

Table 1.1 - Advantages and Disadvantages of open ponds and photobioreactors compared to the ALGADISK system (Wootsch et al. 2012)

	Open pond	Photo Bio Reactor (PBR)	ALGADISK
Required space (footprint)	very high	lower than open pond	Due to the large surface area of rotating disks, the space required for algae production is minimized. Space requirements are equivalent to photobioreactors.
Water loss	very high	low	Lower than PBR due to a higher algae concentration.
Capital cost	high, depending on the pond depth	low	In case of closed ALGADISK system, low; in the case of opened system, it would be higher, than but not as high as for the opened pond system.
O₂ concentration	usually low due to spontaneous out-gassing	high, built up in closed system, requires gas exchange (O ₂ prohibits photosynthesis).	In the case of an opened ALGADISK system, it would be negligible, in the case of a closed system, O ₂ can be easily removed from the gas phase, due to its lower molar weight compared to CO ₂ .
Temperature	highly variable, some control is possible using pond depth	cooling is often required (usually by spraying water on PBR)	The temperature can be controlled in two ways: increased water flow, and increased disk rotation speed.
Shear	usually low	usually high (fast turbulent flows required for good mixing)	very good mixing due to the rotating disks
Cleaning	no issue	required due to pronounced wall growth that reduces light intensity. Cleaning reduces the reactor lifetime	cleaning is required only when changing alga cultivation, however cleaning is easier than that of PBR.
Contamination risk	high (that is why only limited number of species can be grown)	medium or low	medium or low, depending on the manner of usage
Biomass quality	variable	reproducible	reproducible
Biomass concentration	0.1-0.5 g/l	0.5-8 g/l	5-10 g/l
Process control	limited (flow speed, mixing, temperature)	possible with tolerance	an excellent and precise control is designed
Weather dependence	high (light intensity, temperature, rainfall)	Medium	no weather dependence in closed system equipped with artificial lighting
Capital cost	high, about 100.000 €/hectare	very high, about 250.000 to 1.000.000 €/hectare, plus equipment cost	lower than PRB, and comparable with opened pond. For 1t/year production the target is 50.000€. The required land would be less than 1 hectare for this size.
Operating cost	low	high (CO ₂ addition, oxygen removal, cooling, cleaning maintenance)	low, no oxygen removal, no cooling, slightly higher than for an open pond
Harvesting cost	high, species dependent	lower than opened pond due to the higher concentration	lower than PRB due to the high concentration. The automatic harvesting system can remove biomass from the rotating disks while the liquid phase remains saturated with algae. The process does not have to be stopped when harvesting takes place, as opposed to Ponds or PBR.

1.3 Objectives of research

The overall aim of this research was to contribute towards the production of an economically viable algae-based solution of CO₂ capture from industrial emissions and biomass production.

1. To produce a low-cost novel coating based on the strategy of electrostatic attraction of algal cells to promote algae biofilm formations intended for the ALGADISK reactor.
2. To optimise the selected surface coating for large scale production.
3. To investigate the potential of the thermodynamic approach for the prediction of algae attachment.
4. To investigate the role of carrier materials on algal lipid content.

1.4 Thesis outline

Chapter 2 reviews current algae cultivation techniques and evaluates algae as a potential source of biofuel. Chapter 2 also provides insight into previous algae attachment research and the physico-chemical properties that have been found to influence this.

Chapter 3 focusses on the potential of employing polyelectrolyte multilayers as a surface coating in order to attract and increase algae attachment. The coating selected was then tested with a lab-scale ALGADISK reactor, in order to determine possible further modifications needed. These lab-scale reactors were located and tested at

Wageningen University (WU) (Netherlands) and at the Bay Zoltan Foundation for Applied Research Institute (BAYBIO) (Hungary). Chapter 4 investigates and tests these modifications in terms of implementing surface roughness and texture to the selected substrate in order to improve regrowth. Chapter 5 looks at optimizing the PE coating selected for large-scale production, and tests the newly devised method on a pilot scale ALGADISK reactor. The main aim of chapter 5 was to reduce coating production and

application costs, increase the selected coating strength and performance and reduce the need for highly trained end-users. Chapter 6 aimed to examine the physico-chemical influence of substrates on biofilm formation and lipid content.

Chapter 2

Literature review

2.1 Current Algae Cultivation Techniques

2.1.1 Suspended algae production

The majority of conventional algae production systems are suspended systems, where algae cells are suspended in a nutrient-rich liquid medium. These can be further subdivided into open or closed systems: Open systems, meaning that the algae and the medium are exposed to the atmosphere. Closed systems, also termed photobioreactors (PBR), involve algae cultivation in controlled systems.

2.1.1.2 Open systems

Open-pond systems for the production of biofuels from algae were first introduced conceptually in the 1950s. This was in response to a range of factors including the rising world population and subsequent need for alternative food sources (Spolaore et al. 2006) and the possible utilisation of microalgae as sources of biologically active compounds, including antibiotics (Borowitzka, 1995). The hypothesised use of algae as a source of biomass for methane developed during the 1970s-1990s in projects funded by the US Department of Energy (Sheehan et al. 1998). Initially, a paddlewheel-mixed shallow raceway pond was developed. These systems are built as individual ponds or as groups of ponds arranged in a series connection, and typically are made of concrete or compacted earth. These artificial are ponds approximately 0.3 m deep in the shape of a raceway (Fig.2.1) where a paddlewheel continuously circulates the liquid around the

raceway, ensuring the algae is maintained in a well-mixed suspension. Overall, this mimics the natural way algae grows in the environment.

Advantages of these systems are their low build and operational costs. In addition, they are easier to scale up when compared to PBR systems (Shen et al. 2009; Wiley et al. 2011), partly due to the few electrical and mechanical components required for operation. With regards to commercial production of algae, the most common open systems currently in use are raceway ponds and tanks. Examples are Cyanotech Corporation in Kailua-Kona, Hawaii and Earthrise Nutritionals, California which produce *Spirulina* algae for their value as food and nutritional supplements (Pulz and Gross, 2004).

However there are disadvantages. Open ponds are limited in the species of microalgae that can be grown, the larger land area required, the reduced efficiency of light utilisation, and the high risk of culture contamination (Pulz, 2001; Richmond, 2004; Carvalho et al., 2006). A method to limit culture contamination is through the use of highly selective conditions which favour dominance of the desired species (Wiley et al. 2011). Therefore, commercial use is restricted to species that can be cultivated under conditions of extreme pH or salinity: Examples of some microalgae that can grow at low pH environments are:

Dunaliella acidophila, *Chlamydomonas acidophila*, *Chlorella saccharophila*,

Pseudococcomyxa simplex, *Stichococcus bacillaris*, and *Viridiella fridericana*.

Chaetoceros grafilis and *Tetraselmis tetrathele* can be cultivated in saline conditions.

Algae and cyanobacteria such as *Spirulina platensis* can also grow in saline alkaline environments (Razeghifard, 2013).

In addition, target algae species are frequently replaced by more rapidly-growing wild species (Tamburic et al. 2011). Due to the exposed nature of open systems;

temperatures and exposure to natural sunlight fluctuates according to diurnal variation and season. Also, evaporation losses are noted to be as high as $10 \text{ L m}^{-2} \text{ day}^{-1}$ (Sheehan et al. 1998). This amounts to approximately 410 kg of water lost per kg of produced algal biodiesel, thus necessitating large volumes of freshwater to be continuously supplied to the raceway ponds. Lastly, raceway ponds require energy-intensive harvesting and dewatering techniques in order for the algae to be separated, extracted and processed; with costs of biomass production accounting for up to 30% of the total cost of production (Gudin and Therpenier, 1986). Overall, while operating costs of open systems are amongst the lowest of any algae production systems, they generally result in low final densities of microalgae (Suh and Lee, 2003).

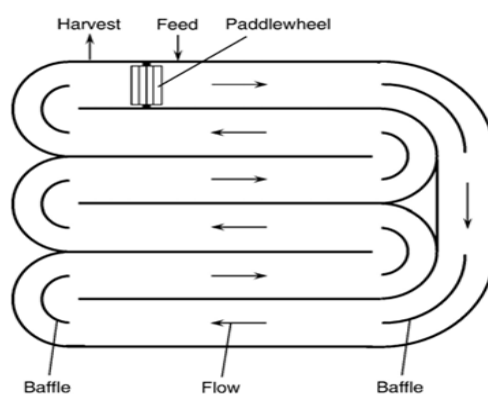


Figure 2.1 - Overhead view of a raceway pond system (Chisti, 2007)

2.1.1.2 Closed Systems

To address some of the aforementioned limitations of open systems, closed photobioreactors (PBR) were developed. Here, algae are cultivated in bags, tubing or other transparent materials and are therefore not directly exposed to the atmosphere. A PBR involves a four phase system composed of the algal cells, the liquid growth medium, the gaseous H_2 product, and the superimposed artificial light field (Tamburic et al. 2011). The closed configuration allows cultivation of a single species of algae, as well as specific control of temperature, pH, light intensity and nutrient composition of

media. The ideal PBR should have uniform illumination, along with quick mass transfer of carbon dioxide and oxygen (Gupta et al. 2015). Therefore, the ideal PBR will have optimised the interaction between environmental parameters, i.e. the light field and fluid dynamics, and biomass production.

The artificial light field must be optimised to match the growth kinetics of the cultivated algae strain, as many algae are adapted to low light intensities (Posten, 2009). The carbon dioxide transfer rate of the culture can be calculated based on the carbon content of the biomass (Posten, 2009). To supply the specified amount of carbon dioxide, carbon dioxide-enriched gas bubbles are bubbled constantly to the reactor at the optimum partial pressure, which is generally 0.1-0.2 kPa in the fluid phase (Spalding 2008; Posten, 2009). Mixing ensures algae cells are kept in suspension in the nutrient-rich media and improves gas-liquid mass transfer. In addition, mixing induces periodic light/dark cycles as algae are consistently exposed to the light rich surfaces of the PBR and to the darker interior regions (Spalding 2008; Gupta et al. 2015). Research shows that enhancing light/dark cycles has direct effects on productivity and biomass field, with the light fraction (ratio between the light period and the cycle time) having the highest effect on growth rates (Barbosa et al. 2003).

Various forms of PBR have been developed based on the morphology of the illuminated surface. Horizontal tubular PBRs are among the most popular closed systems (Fig.2.2 A) (Gupta et al. 2015). Tubular photobioreactors incorporate small (1cm to 6cm) diameter tubes with turbulent flow around the tubes maintained by mechanical pumps. The various orientations include horizontal, inclined, spiral and helical. Tube length, circulation system, light and flow velocity also differ between systems. A key advantage of the tubular layout using small diameter tubes is the high surface to volume ratio conferred by the design. In addition, the 'lens' effect of the small diameter tubes allows

for a more even distribution of light and can prevent the mutual shading of algal cells from the light source (Posten, 2009). Two PBRs culturing the cyanobacteria *Arthrospira platensis* using 1cm tubes arranged in a horizontal orientation resulted in biomass output rates of 2.1 to 2.7 g L⁻¹ d⁻¹ (Carlozzi, 2003). A study comparing the culturing of *Haematococcus pluvialis* in tubular and bubble column PBRs found that the tubular design resulted in higher biomass productivity with greater carotenoid content (Lopez et al. 2006).

However, the high surface to volume ratio of PBRs means that for large scale production extensive cooling is required. Another disadvantage is the accumulation of oxygen, which at high levels inhibits algae growth (Gupta et al. 2015). Therefore, tubular PBRs may be a more suitable choice for high value compounds (such as carotenoids) rather than energy products (Posten, 2009). Additionally, tubular PBRs also require more land use than other PBR designs. The largest tubular PBR is located in Klötze, Germany with tubes of 500 km length in total (Posten, 2009).

Vertical tubular PBRs are composed of transparent vertically-arranged tubes with the cultured circulated via an airlift system or an air pump. Two subtypes of vertical PBRs are bubble column and airlift. Bubble column PBRs use gas sparging to achieve agitation and mixing. The lack of moving parts and the efficiency of sparging allows for good mixing and low shear stress (Ugwu et al. 2008; Gupta et al. 2015). These types of reactors have wide commercial use for wastewater treatment, along with the production of beer, vinegar, and baker's yeast (Gupta et al. 2015).

Airlift PBRs physically separate the column either through an internal loop, an internal tube, or an external loop. This means that there is separation of the up-flowing (riser) stream and the down comer stream. The gas is sparged through the riser stream, and then the heavier now bubble-free liquid at the top of the vessel subsequently recirculates

through the down comer. This induced circular mixing pattern theoretically exerts a light/dark cycle on the algal cells (Sanchez Miron et al. 2002; Gupta et al 2015).

A study culturing *Phaeodactylum tricornutum* in both an airlift PBR and a bubble column PBR (19cm diameter) concluded that final biomass concentrations and growth rates were comparable to narrow (3cm) tubular PBRs (Sanchez Miron et al. 2002). The authors also noted that oxygen inhibition of photosynthesis is less than that of tubular PBRs. However, they are generally suited to small-scale production at present, as increasing the diameter of the column leads to areas of high dark fraction in the centre of the cylinder (Posten, 2009). In addition, scaling up may be difficult as the surface area exposed to illumination is relatively small, and construction of airlift PBRs requires sophisticated materials (Ugwu et al. 2008).

Flat plate or plate photobioreactors (Fig.2.2 B) are composed of flat, translucent panels which can be oriented and tilted at varying angles to increase exposure to artificial or natural light. The flat panels confer a high surface to volume ratio. Similar to tubular PBRs, pumps circulate the algae cell suspension. Advantages of this design are the larger surface area exposed to light, suitability for outdoor culturing, and relatively low cost. Oxygen accumulation is also noted to be lower than that of horizontal PBRs.

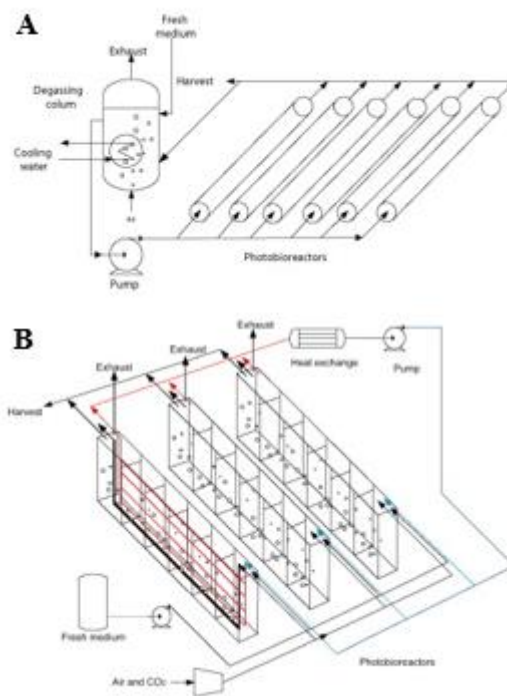


Figure 2.2: Schematic drawing of tubular horizontal photobioreactor (A); and a flat-plate photobioreactor (B) (Jorquera et al. 2009)

However, flat panel systems generally result in lower areal yields (Gupta et al. 2015). This is likely due to the short light penetration depths. Other limitations include: control of culture temperature and aeration of flat panel PBRs that can result in hydrodynamic stress (Ugwu et al. 2008). The overall consensus is that flat plate PBRs are more suited to research or small-scale production, and thus are unsuitable for the production of biofuel (Ugwu et al. 2008; Posten, 2009; Gupta et al. 2015).

Stirred tank PBRs (Fig.2.3) consist of a tank with a motor-driven agitator. This agitator results in mechanical agitation of the algae cell media, along with aeration and heat and mass transfer (Gupta et al. 2015). The agitator generally requires a higher energy input per unit volume, however the stirring mechanism means that light dispersion throughout the medium and mass transfer rates are high (Gupta et al. 2015). This subsequently leads to good biomass productivity, although, productivity is hindered by the low surface to

volume ratio. In addition, the energy-intensive motor-driven agitation leads to high costs and inefficiency, ultimately meaning that stirred tank PBRs are difficult to scale up.

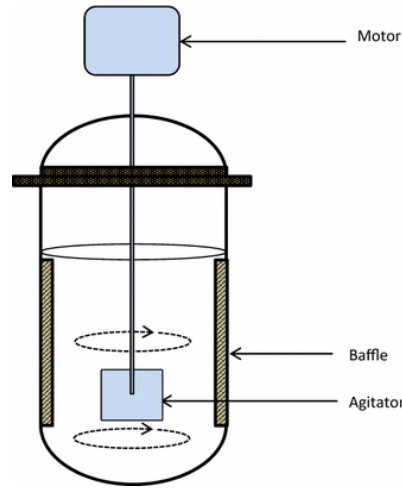


Figure 2.3: Stirred tank photobioreactor (Gupta et al. 2015)

Overall, the higher investment and operating costs of PBRs are significant barriers to industrial use (Carvalho et al. 2006), therefore closed reactors are predominantly utilised for high-value products that require cultivation in controlled environments. The various cultivation systems of PBRs are promising on the smaller scale, but are generally difficult to scale up.

Typically, PBRs do show greater volumetric productivity when compared to open ponds. This is secondary to enhanced capture of light energy and more optimal use of land area. There is wide variation in energy use for mixing and gas/liquid mass transfer according to the type of PBR: Values of 55 W/M^3 for flat plates and from $800\text{--}3000 \text{ W/m}^3$ for horizontal tubular reactors have been suggested (Carvalho et al., 2006 and Sierra et al., 2008). A significant drawback of flat plate PBRs is the vulnerability to stress by aeration (Tamburic et al. 2011). Both forms of PBR have been scaled up to volumes of over 1000 L (Sierra et al. 2008), and recent advanced in PBR

design focusing on photosynthetic efficiency and automated process control systems are aiming to bring costs of PBRs down.

Recent analysis showed that PBRs at a capital cost of US € 452,690 ha⁻¹ must decrease to less than US € 90,540 ha⁻¹ in order to compete with raceway ponds (Darzins et al. 2010). Overall, both open and closed systems are not feasible in their present ability to produce biofuels from microalgae. Operating costs significantly hinder PBRs, even with the research on current systems like the Simgaetm and the GWP-II which show construction costs similar to lined ponds (Borowitzka and Moheimani, 2012). The present cost of biomass production is US € 4.53 kg⁻¹, which is 20 times the price suggested for economic fuel production (US € 0.23 kg⁻¹) (Darzins et al. 2010). Norsker and colleagues (2011) calculated monthly biomass production costs for open pond, horizontal tubular PBRs, and flat panel PBRs in Dutch conditions. The costs were 4.95, 4.15 and 5.96 € per kg respectively. Sensitivity analysis accounting for enhanced irradiation and photosynthetic efficiency, along with reduced nutrient and mixing costs could potentially reduce costs to € 0.70 per kg dry weight for the two bioreactors and € 1.30 for the raceway in approximately 10 years. Other methods to improve efficiency and economics are the use of flue gases from industrial sources as the carbon dioxide source, along with wastewater as the primary water source (Acien et al. 2012). While the biomass production and controlled conditions that PBRs possess are advantageous, the major issue with regards to large scale biofuel production are scaling up production while simultaneously keeping energy input low, minimising maintenance costs and maximising solar radiation.

2.1.2 Non-suspended algae production

Following on from aforementioned cost and production limitations with suspended algae production methods, there is now an interest in using surface attached algae

systems. These solid carrier systems offer higher biomass yields, are easier to scale-up, offer improved control of contamination and show markedly reduced water consumption (Gross et al. 2015; Katarzyna et al. 2015). With regards to non-suspended production, algae can either be incorporated into a polymeric matrix (enclosure method), or the algae can form a biofilm on the surface (non-enclosure). Algae are noted to be easier to control when encapsulated inside a polymeric matrix. A similar technique has been widely used in the industry for many years for the purpose of enzyme and organelle entrapment (Katarzyna et al. 2015). Hameed and Ebrahim had some success with immobilising algae cells via a matrix of alginate. However, large scale production was difficult due to the high cost of polymeric matrix (Hameed & Ebrahim, 2007). Johnson and Wen recently developed a rocker system with a bottom surface consisting of polystyrene for the attachment of algae. They tested it on *Chlorella* sp and found that the attached culture produced a higher yield than the suspended culture (Johnson & Wen, 2010). However, scaling-up polymeric matrices is highly expensive, and is a major barrier for large-scale non-suspended production of algae.

A biofilm is a layer of eukaryotic or prokaryotic cells which are anchored to a substratum and embedded in an organic biological matrix (Bos et al. 2006). In contrast to suspended production systems, biofilm production shows reduced costs as harvesting is more easily accomplished (Gross et al. 2015). Gross and colleagues used a Revolving Algal Biofilm (RAB) growth system, and found that a raceway-based and a trough-based RAB system were superior (with regards to footprint and surface biomass productivity) to a control raceway pond by 309% and 697%, respectively. In addition, the authors noted reduced costs secondary to improved water efficiency and cheaper harvesting (Gross et al. 2015). Another study combined a Rotating Algal Biofilm Reactor (RABR) with a simple spool harvesting method and found that this technique

was effective at wastewater treatment and biomass production at the small- to medium-scale (Christenson and Sims, 2002). Harvested algae is approximately 10-20% dry content, similar to that of post-centrifuged biomass (Christenson and Sims, 2002; Gross et al. 2013).

As stated, non-enclosure methods are based on biofilm cultures. As a consequence of biofilm formation, cell densities in reactors can increase significantly (Qureshi et al, 2005). There have been several different types of larger scale biofilm systems developed thus far, which vary according to end application, configuration, and attachment materials. A variety of materials have been utilised in the literature: Cao and others produced a floating conveyer belt system for the harvesting of algae from textured steel surfaces (Cao et al. 2009). Torpey and others also had used metal surfaces for their algae and set up illuminated rotating aluminium disks (Torpey et al., 1971). More recently, Christenson and Sims found that cotton rope was the most effective substratum in their novel rotating algal biofilm reactor (RABR). Polyvinyl chloride (Posadas et al. 2013), cellulose acetate (Genin et al. 2014), and glass (Schnurr et al. 2013) have all been successfully used.

Gross and colleagues subdivide the various configurations of algal biofilm systems into stationary and rotating designs (Gross et al 2015). The stationary design uses a pump to transfer liquid over the surface of a biofilm. Algal turf scrubbers (ATS) are an example of this design, where liquid is flowed over a biofilm formed on the horizontal attachment sheet. This method has been successfully used in the treatment of dairy manure effluent (Mulbry et al. 2008). Operational costs of ATS are noted to be below costs cited for upgrade of existing wastewater treatment systems, likely secondary to the minimal use of moving parts (Mulbry et al. 2008). However, scale up is limited by the fact that ATS require a significant foot print (Gross et al. 2015).

Stationary systems can also be orientated vertically, which creates a flat-plate reactor. This configuration has been used to cultivate a range of algae species for feedstock production (Liu et al. 2013) and wastewater treatment (Zamalloa et al. 2013). A parallel flat plate biofilm reactor was noted to have low capital and operating costs with regards to wastewater treatment; approximately 0.5 €/m³. The vertical orientation of plates means that overall land footprint is smaller than that of a horizontal plate reactor, but the vertical orientation does mean that energy is required to maintain liquid circulation. In contrast, rotating algal biofilms (RAB) involve the rotation of the attachment material through the air phase and the liquid medium. As stated previously, harvesting is commonly accomplished by scraping. The attachment materials can be oriented as flat discs (Blanken et al. 2014), a rotating cylindrical drum (Christenson and Sims, 2012) or a conveyor belt (Gross et al. 2013). Whertz and colleague's developed a bacterial biofilm reactor which consisted of trickling filters and a rotating biological contactor (RBC) (Whertz et al, 2004). RBCs have been utilised in wastewater treatment since the 1970s (Hassard et al. 2015).

Two key parameters when discussing the efficiency of algal biofilm reactors are the surface biomass productivity and the footprint biomass productivity. A review conducted by Gross and colleagues (2015) found that surface biomass productivity is generally in the range of 2 - 6 g m⁻² day⁻¹, while footprint productivity varies widely from 0.71 to 80 g m⁻² day⁻¹. The wide range is likely attributed to the differing orientations of biofilm systems, as well as the varying strains and conditions tested.

The major benefits shown by the research are the ease of harvesting when compared to suspension-based systems. However, scaling up production will require an efficient mechanical harvesting method, as manual harvesting is not feasible for large scale production. Light is used more efficiently due to the uniform nature of the biofilm,

especially when compared to the varying light paths and biomass densities in suspended reactors. This is especially true if frequent harvesting is performed. Photosynthetic efficiency is noted to be increased in vertical biofilm reactors, as the biofilm dilutes sunlight throughout the entire surface area, which subsequently reduces photosaturation. This combined with reduced light reflection which occurs on exposed open ponds leads to higher biomass yields within the same footprint area (Gross et al 2015). Carbon dioxide transfer to biofilms is superior to that of open ponds as there is a larger gas-liquid interface. However, carbon dioxide has to diffuse through the interior layers of the biofilm, unlike in suspended systems where carbon dioxide can be adsorbed (Gross et al. 2015). This limiting step can also be alleviated by frequent harvesting which ensures the biofilm remains thin.

Future research on algal biofilm systems needs to focus on developing a surface coating that could potentially enhance algae attachment and optimise biofilm formation. In addition, long-term pilot- and laboratory-scale studies are required to determine the most efficient methods of carbon dioxide transfer, light penetration and harvesting, along with determining the economics of scaling up these systems for large-scale cultivation.

2.2 Algal attachment and biofilm formation

Biofilm formation is altered by a number of factors. Important physiological influences are the microorganism type, growth stage and metabolic activity. Environmental variables include the pH, electrolyte type, ionic strength and temperature. Interface factors are the surface charge, surface energy, chemical nature, wettability, lubricity and surface topography (Bowen et al. 2007; Li et al. 2010; Characklis et al. 1990; Cao et al. 2009). The sequence of events is constant and can be subdivided into two parts: firstly,

the initial attachment, and second, deliberate secondary adhesion (Callow and Fletcher, 1994).

Initially, cells can move towards the conditioned surface in a range of ways; they can move actively via motile mechanisms, be transported by gravity, or be transferred by advection (Ozkan and Berberoglu, 2013). Attachment for most algae is thought to be facilitated by its specialised reproductive propagules which allow initial contact with a substratum. Motile spores are aided by their ability to respond to external stimuli such as surface texture and surface chemistry. Non- motile spores are aided by the adhesive properties of the extracellular residual mucilage. After initial contact is made all spores secrete adhesive materials which allow a permanent attachment to be made (Fletcher & Callow, 1992). The primary colonisers are considered to be diatoms, which are unicells or colonial algae. The spontaneous, often reversible adsorption of organic and inorganic aqueous molecules to the solid surface is followed by a non-reversible secondary adhesion of cells via the production of adhesive EPS (extracellular polymeric substances). These are molecules produced by both algae and other microorganisms in response to physiological stresses encountered in the natural environment (Marvasi et al. 2010).

Algogenic organic matter (AOM) can consist of proteins, peptides, amino sugars, and polysaccharose (Pivokonsky et al., 2006). AOM consists of multicomponent, mucilaginous, organic bioadhesive complexes that can found on the exterior of algal plasma membranes (Evans, 2000). The major molecular components are acidic polysaccharides, proteins, and an actin-based cytoskeleton. The binding strength of EPS found in AOM is thought to occur by hydrogen bonding, electrostatic interactions and van der Waals forces between functional groups (Ozkan and Berberoglu, 2013). Computer derived models showed that charged groups are present on the exterior of the

molecular chains, and so can easily interact with other charged molecules (Sutherland, 2001).

Research focusing on biofouling has focused on the only variable that can be altered artificially, namely the properties of solid surface. The strength of adhesion of both micro- and macro-organisms is generally thought to be lower on hydrophobic surfaces with a low surface free energy (Brady and Singer, 2000; Li et al. 2010), where minimal bioadhesion occurs at 22-24 mJ/m² (Li et al. 2010). However, a number of studies have shown unexpected behaviours regarding surface energy and adhesion. Certain diatom species adhere more strongly to hydrophobic surfaces. This is in contrast to the adhesion behaviour of other marine fouling organisms, like green algal spores (Ista et al. 2004). A study investigating the adhesion properties of the diatom *Nitzschia closterium* on self-assembled monolayers (SAMs) with hydrophobic methyl (CH₃-SAM) and hydrophilic carboxylic (COOH-SAM) end groups on glass slides found that attachment densities were much greater on hydrophobic CH₃-SAMs with smaller free energy, and lower on mixed SAMs (Li et al. 2010). However, the percentage of removed adhered cells was larger for hydrophobic surfaces, overall indicating weaker adhesion strength.

Alteration of wettability using mixed mercaptoundecanol (–OH) and dodecanethiol (–CH₃) SAMs on a gold surface, showed that *Ulva* zoospores settled less on hydrophilic surfaces (Rosenhahn et al. 2010). In another study, the increase of *Enteromorpha* zoospore adhesion with rising contact angle (hydrophobicity) was dependent on the surface composition of the mixed –OH/–CH₃-terminated alkane thiol SAM (Callow et al. 2000). Similar results were found by Finlay and colleagues who examined the effect of wettability on the adhesion characteristics of the species *Enteromorpha* and the diatom *Amphora coffeaeformis*. Results showed that there was only slight influence of wettability on the primary adhesion of *Amphora*. However,

motility was subdued at contact angles over 60°, and cells were more adhered to the hydrophobic surface, and less adhered to the hydrophilic surface. This strong adhesion strength was linked to decreased diatom motility on the hydrophobic surface (Wigglesworth-Cooksey et al. 1999). *Enteromorpha* spores showed strong preference, but weak attachment on hydrophobic surfaces (Finlay et al. 2002).

Finlay and colleagues explained the non-significant effect of wettability on adhesion could be attributed to the presence of EPS. Research looking at EPS production and attachment on substrata with varying surface tensions determined that EPS production is greatest on substrata with surface tensions above 30 mN m⁻¹. However, adhesion of *Amphora coffeaeformis* on both low polytetrafluoroethylene and high (glass) surface tension substrata was equally strong, although EPS production was much greater on glass compared to PFA. Therefore, on surfaces that are hydrophobic, factors other than AOM become more important for attachment and biofilm formation (Becker, 1996).

Overall, research suggests that interfacial energetics are complex and are heavily influenced by algal species and the chemical composition of the specific substrate. Shen and colleagues assessed the adhesion of six species of freshwater algae. The species with the greatest adhesion biomass productivity (ABP) *Chlorococcum sp.* was then tested on nine different support materials. Glass fibre-reinforced plastic was found to be the optimum surface. In addition, the study found that initial total nitrogen concentration, pH, culture volume and culture period are the most significant factors determining ABP (Shen et al. 2013).

2.3 Cell to Substrata and Cell to Cell Interactions

There are three physico-chemical approaches available to describe microbial adhesive interactions; the thermodynamic approach, the classical DLVO (Derjaguin, Landau, Verwey, Overbeek) approach, and the extended DLVO approach. The thermodynamic

approach assumes that when interacting surfaces physically contact each other, this occurs under conditions of reversible adhesion (thermodynamic equilibrium). The approach does not incorporate a role for electrostatic interactions, and is instead centred on the free energies of the interacting surfaces. In contrast, the DLVO approach incorporates van der Waals along with electrostatic interactions and their decay with regards to separation distance to describe the interaction energies between two surfaces (Bos et al. 1999). Research suggests that both approaches have use for describing microbial adhesion for some species, but have thus far unsuccessfully accounted for all aspects of microbial adhesion (Bos et al. 1999). The extended DLVO approach further incorporates acid-base interactions to seek to explain some of these discrepancies.

2.3.1 The thermodynamic approach

The thermodynamic approach views attachment as a spontaneous change accompanied by reduced free energy of the system. The approach uses the Dupré equation to compare the surface free energies between interacting surfaces:

$$\Delta G_{adh} = \gamma_{sm} - \gamma_{sl} - \gamma_{ml}$$

γ_{sm} , γ_{sl} and γ_{ml} refer to the solid-microorganism, solid-liquid and microorganism-liquid interfacial free energies. Microbial adhesion is favourable when ΔG_{adh} is negative, that is if γ_{sm} is smaller than the sum γ_{sl} and γ_{ml} . This represents a state of minimal free energy. Adhesion is therefore energetically unfavourable when ΔG_{adh} is more than 0 (Cui & Yuan, 2013).

In order to determine the values for surface interfacial free energies, the contact angles of liquids on test substrata can be utilised as an indirect estimate. Contact angles are related to the work of adhesion via the Young-Dupré equation:

$$\gamma_{lv} \cos \theta = \gamma_{sv} - \gamma_{sl}$$

The subscripts refer to the surface free energy between the vapour (v), solid (s), and liquid (l).

In summary, the model predicts that adhesion will rise as the surface tension of the substratum rises, as long as the surface tension of the liquid medium is lower than the surface tension of the cells (Absolom et al. 1979). If on the other hand the liquid medium surface tension is greater than that of the cellular surface tension; then cell adhesion will decrease as the surface tension of the substratum increases (Absolom et al. 1979). This thermodynamic model of adhesion has been shown to be useful in understanding the adhesion of other microbes. For example, by varying the surface tension of the liquid medium with the use of dimethyl sulfoxide (DMSO), granulocyte and platelet adhesion was shown to match the thermodynamic model (Absolom et al. 1979). In addition, different strains of bacteria show varying attachment depending on cell surface composition, which in turn results in varying surface free energy (Fletcher & Pringle, 1985).

Cui & Yuan (2013) simulated microalgal attachment to solid-carrier surfaces using the thermodynamic model. Results indicated that if the polar surface energy of the cell is lower compared to water, attachment is more favourable on surfaces with greater dispersive surface energy and lower polar surface energy. Experimental data using freshwater algae *S. dimorphus* and marine algae *N. oculata* on five materials (nylon, stainless steel, polycarbonate, polypropylene, and glass) qualitative matched the findings of the modelling data. Overall, findings support data that algal cell attachment is determined by the surface energies of cells and their substrata (Cui & Yuan, 2013).

Research has shown that although the thermodynamic model can explain some microbial attachment patterns, there are limitations with the model. Firstly, it assumes

an equilibrium situation. This fails to account for microbial contributions to the initiation or stabilisation of attachment, for example by the production of adhesive polymers. In addition, microbial surface attachment mechanisms are more chemically complex and the thermodynamic model does not account for conformational changes in polymers and other entropy-gaining processes (Katsikogianni & Missirlis, 2004). Algal surfaces can be extremely complex with long-chain polymers, flagella and fimbriae extending into the medium, and are therefore difficult to incorporate into a reductionist approach (Cui & Yuan, 2013).

2.3.2 The classical DLVO Approach

The DLVO approach describes microbial adhesion as an equilibrium between attractive Lifshitz-van der Waals forces, and either repulsive or attractive electrostatic forces (Van Oss et al. 1989; Ozkan & Berberoglu, 2013a). The inclusion of electrostatic interactions here requires that the zeta potentials of the interacting surfaces are measured, along with contact angle measurement. The interaction energy between two surfaces can be seen as:

$$(1) G^{\text{tot}}(d) = G^{\text{LW}}(d) + G^{\text{EL}}(d)$$

$$(2) G_{\text{LW}}(d) = -AR/12d$$

$$(3) G_{\text{EL}}(d) = 2\pi\epsilon R\psi^2 \ln[1 + \exp(-\kappa d)]$$

G^{tot} refers to the total, G^{LW} denotes the Lifshitz-van der Waals forces, and G^{el} denotes electrostatic interaction energy. Decay with distance (d) of the interaction energies is dependent on the geometry of interacting surfaces. A is the Hamaker constant. The van der Waals force is responsible for attraction therefore the corresponding interaction energy, G_{LW} , is usually negative. The interaction energy, G_{EL} , of the electrostatic repulsive force is positive (Van Oss et al. 1989; Ozkan & Berberoglu, 2013a).

In equation (2), G_{LW} decreases as an inverse power of the distance between the cells. G_{EL} in equation (3) is an exponential function of the distance between two cells with a range of the order of the thickness of the double layer (κ^{-1}). Therefore, van der Waals attractions are prominent at small intercellular distances, while electrostatic repulsion is most prominent at intermediate distances (Van Oss et al. 1989; Ozkan & Berberoglu, 2013a).

Based on the classical DLVO theory, only the electrostatic double layer force can be modified to a significant extent, and repulsion can be greatly affected by changing the ionic strength of the suspension medium or by modifying the surface charge of the cells through pH adjustment or addition of positively charged flocculants. DLVO models have been used to quantify the adhesion energy in bacterial adhesion and aggregation as a function of the separation distance between surfaces for *Escherichia coli* (Redman et al. 2004), *Pseudomonas* (Rijnaarts et al. 1995) plus *Streptococci* and *Staphylococci* species (Truesdail et al. 1998).

Another study assessed two bacteria species as biocoagulants to harvest *Chlorella zofingiensis* and *Scenedesmus dimorphus*, and assessed the influence of UV-irradiation and a polyethylenimine (PEI)-coating on harvesting efficiency. The authors used the soft-particle DLVO theory to determine that an energy barrier formed between uncoated *E.coli* cells and algal cells, and this explained the reduced harvesting efficiency when compared to PEI-coated *E.coli* cells (Agbakpe et al. 2014). The DLVO model has been used to predict flocculation characteristics of *Scenedesmus dimorphus* and *Nannochloropsis oculata*; algal cells with a lower total DLVO interaction energy had greater flocculation efficiency (Cui et al. 2014).

However, the theory has limitations in it generally assumes that the substratum and the particle surfaces are chemically inert. Interacting bacteria and algae are essentially

assumed to be molecularly smooth. This does not account for the various hydrogen and chemical bonds that are present when bacteria or algae interact with substratum surfaces. Furthermore, surface structure and surface roughness are not considered to impact the energies of interaction by the classical DLVO model (Agbakpe et al. 2014).

2.3.3 The extended DLVO approach

This approach developed by Van Oss and colleagues focuses on the four non-covalent interactions: these are Lifshitz-van der Waals, electrostatic, Lewis acid-base and Brownian motion forces (Van Oss et al. 1989; Park & Kim, 2015). The addition of Lewis acid-base interactions is based on the electron-donating and –accepting properties that occur between polar groups in aqueous solutions, and therefore theoretically account for hydrogen bonding which occurs on close approach of bacteria and substratum (Bayouhd et al. 2009). The free energy balance of acid-base (ΔG_{adh}^{AB}) is integrated into the extended DLVO approach by the attribution of a decay function. Van Oss and colleagues proposed that these attractive or repulsive polar interactions may be up to 10-100 times greater than electrostatic and Lifshitz-van der Waals forces (Van Oss et al. 1989). These forces are only prominent when the interacting surfaces are less than 5mm apart (Bos et al. 2006).

The total interaction energy is given as (Van Oss et al. 1989):

$$G^{TOT}(d) = G^{AB}(d) + G^{LW}(d) + G^{EL}(d)$$

The free energy balance of acid-base is given as (Ozkan and Berberoglu, 2013a):

$$G^{AB}(d) = 2\pi a \lambda \Delta G_{adh}^{AB} e^{[(d_0-d)/\lambda]}$$

In this equation, ΔG_{adh}^{AB} refers to the polar free energy change of the overall system. λ is the gyration radius of water molecules in a solution, which is greater around

hydrophobic surfaces and less around hydrophilic surfaces (Ozkan and Berberoglu, 2013a).

These acid-base interactions may account for differences between DLVO predictions and experimental findings (Bayouhd et al. 2009). A comparison between the DLVO and extended DLVO approaches with regards to the adhesion of two bacterial strains to glass and indium tin oxide (ITO)-coated glass found that the extended DLVO approach was more accurate (Bayouhd et al. 2009). The extended DLVO model was more accurate in predicting the density of algal cells and their strength of adhesion when *Chlorella vulgaris* and *Botryococcus sudeticus* were tested with hydrophilic and hydrophobic surfaces (Ozkan and Berberoglu, 2013a). The authors compared the extended DLVO model with the thermodynamic and the DLVO models. It was found that the thermodynamic model was unsuccessful in predicting the adhesion of *C. vulgaris* to a hydrophilic surface. The DLVO model did predict the density of cells adhered to both surfaces, but failed to account for the weaker interaction of *C. vulgaris* to glass (Ozkan and Berberoglu, 2013a).

Ozkan and Berberoglu (2013b) found that acid-base interactions were the predominant mechanism for the adhesion characteristics of 10 different strains of freshwater and saltwater microalgae. The authors identified that *Botryococcus braunii* and *Cerithiopsis fusiformis* as promising species for bioflocculation and biofilm formation in freshwater and saltwater aquatic systems, respectively.

2.4 Methods for harvesting algae

Following the cultivation of algae in suspended or non-suspended systems, algae is then harvested. As previously stated, algal biomass harvesting comprises up to 20-30% of the total biomass production cost. Therefore, optimal harvesting methods are crucial to make large-scale production viable.

Algae cultivation uses high volumes of growth medium, and separation of microalgae from this growth medium comprises the harvesting process. In addition, high biomass concentration results in mutual shading of microalgae, thus decreasing productivity. Overall, this results in relatively low biomass concentrations: ranging from approximately 0.5 g/l in open pond reactors to about 5 g/l in photobioreactors (Vandamme et al. 2013). Therefore, the correct balance between biomass production and efficient harvesting techniques is imperative for large-scale production.

Very large volumes of water must be removed to harvest the biomass. Two factors which prevent the sedimentation or simple screening of growth medium to harvest algae are the small size of the microalgal cells (2-20 μm) and the colloidal stability of microalgal suspensions. When particles are suspended in water, this results in the formation of an electric double layer of ions and counter ions which maintain electrical neutrality: This is composed of a dense layer close to the particle surface termed the Stern layer, and a diffuse layer further away (Vandamme et al. 2013).

As the particle moves through solution, the ions surrounding the particle move with it up to a certain boundary; this is termed the slipping plane. The potential difference between the bulk fluid and the layer of counter ions which move with the charged particle is named the ζ potential (measured in mV). Therefore, electrostatic repulsion between particles depends on the value of the ζ potential; the greater the ζ potential (>25 mV), the stronger the repulsion, and the more stable the suspension becomes. If the ζ potential approaches 0, particles can approach each to a point where attraction via Van der Waals forces occurs, resulting in the aggregation and flocculation or coagulation of particles (Vandamme et al. 2013).

With regards to microalgae, surface charge is predominantly determined by cell surface carboxylic (-COOH) and amine (-NH₂) groups. Above pH 4-5, carboxylic groups are negatively charged while amine groups are uncharged, resulting in a net negative surface charge. AOM has also been found to influence charge density, flotation and coagulation. AOM composition can also vary between different species of algae (Henderson et al.,2010).

Contemporary algae harvesting generally uses centrifugation, however the high cost and high energy use of this technique makes it suitable for only high-value algae products. A suitable alternative harvesting method for low-value products (i.e. biofuels) is required to scale-up microalgal biomass production, and is one of the main barriers to large scale economically viable microalgae cultivation (Schlesinger et al. 2012; Vandamme et al. 2013).

Flocculation, where single cells form large aggregates, is considered to be an encouraging method compared with other aforementioned techniques. It allows for the rapid treatment of large quantities of microalgal culture. It can be also be used with a variety of species (Uduman et al. 2010). The flocculants or aggregates of cells can be subsequently filtered from the growth medium by simple gravity sedimentation. A two-step harvesting process for microalgae would first use flocculation to concentrate a dilute suspension 0.5-5 g/l dry matter into a slurry of 10-50 g/l (Shen, 2014). Subsequent dewatering using mechanical centrifugation is then performed, finally resulting in an algal paste with 25% dry matter content (Vandamme et al. 2013; Shen, 2014). Centrifugation is more economically viable for this second step because the primary flocculation step equals aggregates of particles and a lower volume of water.

Flocculation has a range of industry applications which include brewing, water treatment and mining (Vandamme et al. 2013). In contrast to algal cultivation, flocculation is utilised to separate impurities from a large volume of liquid, with the liquid being the final product. Flocculation can be induced in a number of ways: Chemical flocculation uses metal salts which form metal hydroxide precipitates. These can induce flocculation through charge neutralisation which negates electrostatic repulsion and thus causes particles to coagulate. Chemical flocculation can also cause flocculation by bridging particles together, or by entrapping particles in mineral precipitates (termed sweeping flocculation) (Schlesinger et al. 2012). A significant drawback is that metal salts accumulate in the harvested biomass. Chemical flocculation can also occur with synthetic polyacrylamide polymers, or with biopolymers like chitosan and poly- γ glutamic acid. Biopolymers are safer than synthetic polymers, however Chitosan is only effective at unsuitable pH levels conducive to microalgae growth, and other biopolymers are ineffective at cultivating microalgae in saltwater (Uduman et al. 2010).

Flocculation can occur spontaneously in lakes or rivers containing natural blooms of algae. This is attributed to extracellular polymer substances and occurs via an unclear mechanism, possible due to species-dependent production of infochemicals. Bioflocculation is used in wastewater treatment using microalgae. Bacteria and fungi can also induce the bioflocculation of algae, however this results in microbiological contamination which is an issue where biomass is used for food or feed applications (Vandamme et al. 2013).

Autoflocculation can occur spontaneously when pH is increased above 9 via the production of calcium or magnesium precipitates, however this can also result in high concentrations of minerals in the harvested biomass. Physical flocculation would avoid

contamination of biomass. Proposed methods are via standing ultrasound waves, electrocoagulation, or magnetic nanoparticles. Studies have used nanoparticles composed of single (Cerff et al. 2012) or composite (Lee et al. 2013) structures. Iron oxide (Fe_3O_4) nanoparticles adsorb directly onto microalgal cells, and cells are then separated by applying a magnetic field. Aminoclay and Chitosan composite nanoparticles result in fast harvesting and enhanced biomass recovery respectively (Lee et al. 2014), however high manufacturing costs remain a bottleneck. Recent advances in efficiency and processing time of microalgal harvesting with nanoparticles are promising, however methods for cost-effective recycling as well as efficient and stable nanoparticles are required (Lee et al. 2014).

Overall, development of an efficient and cost-effective flocculation technology is imperative in making large scale algae cultivation viable. Promising areas of research are physical flocculation using nanoparticles and the genetic modification of algae which facilitate flocculation (Wijffels & Barbosa, 2010). Research into the influence of algal species and growth medium on flocculation, as well as the infochemicals that induce flocculation is also required. Bioflocculation using this method would allow harvesting without the addition of contaminants that occurs with chemical and microbiological flocculation.

2.5 Algae as a potential Biofuel

Overall energy consumption of the world is expected to continue to rise concurrently with the increase in population. Data from 2010 shows that the world's primary energy consumption increased by 5.6%, which was the largest percent growth for a single year in just under 40 years (BP, 2011). Much of this growth included increased usage of the major fossil fuels; coal, natural gas and oil. The finite supply of fossil fuels combined with the environmental repercussions of their continued usage has highlighted the need

for alternative and renewable sources of energy (Jones and Mayfield, 2012). A recent review in 2010 by researchers from Oxford University concluded that conventional production of oil will likely decline (Owen et al. 2010), which supports the notion in the Hirsch report that the ‘era of plentiful, low-cost petroleum is approaching an end’ (Hirsch, 2005). The study also highlights the negative repercussions that changes in oil price can exert on the macro-economy. Therefore, investing in alternative fuels carries financial benefits in addition to improving energy security and reducing emissions (Owen et al. 2010).

Diversification of available liquid fuels is necessary to meet the rising demand. Government policies focused on reducing emissions of greenhouse gases and improving energy security have led to a renewed interest in biofuels over the last few decades. The first generation biofuels are derived from starches, sugars, animal fats and vegetable fats produced in food crops such as corn, sugar cane, soy, and plant or nut oils. Two of the most commonly produced biofuels are bioethanol derived from corn or sugarcane, and biodiesel produced from a variety of oil-seed crops such as palm, rapeseed and soybean (Jones and Mayfield, 2012). These crops can be cultivated on arable land and are relatively easy to extract. However, many of these products are vital for global food supply and feedstock worldwide. For example, the cultivation of corn crops specifically for biodiesel production rather than food production leads to raised food prices worldwide (Moore, 2008). A further criticism is that the large-scale deforestation necessary to clear land for growth of these crops can in fact lead to the release of carbon stocks, overall reducing carbon savings (Mohr and Raman, 2013).

Second generation biofuels are also termed advanced biofuels, and refer to fuels manufactured from more sustainable types of biomass, namely landfill, plant and oil material. Polysaccharide-rich lignocellulosic material derived from plant crops and

waste vegetable oil are two examples. As these products are more sustainable, the second generation biofuels have a greater carbon benefit per hectare when compared to first generation biofuels (Greenergy, 2010). However, virgin lignocellulosic material in particular requires a great deal of processing before it can be fermented into ethanol. This can be done by thermochemical conversion via gasification (which produces syngas), pyrolysis or torrefaction; or biochemical conversion which mainly extracts polysaccharides (Naik et. al 2010). The requirement for this extensive processing means that capital and logistics costs are high, while energy yields are generally lower than that of first generation biofuels (Greenergy, 2010).

The Renewable Fuel Standard 2 (RFS2) mandates by the US Federal Government state that by 2020, 30 billion gallons (bgals) of fuel production should be from renewable fuel sources (Schnepf, 2013). To achieve this using corn ethanol as the sole source, utilisation of total US corn crops would have to rise from 30% to 100%, which would have subsequent drastic effects on food availability (Jones and Mayfield, 2012). The first-and second-generation biofuels have shown use, especially in Brazil where sugarcane ethanol accounts for almost 20% of total energy consumption by the transport sector (Martinelli & Filoso, 2008). However the significant disadvantages of deforestation, processing costs (Huang et al. 2009), and effects on food prices (Jones and Mayfield, 2012) has led to governments pursuing alternative sources of biofuel. Furthermore, the limited environmental savings from corn ethanol has mandated that 21 of the 30 bgals should be from non-corn starch products. Therefore, there is a clear need for alternative sources of biofuels.

Algae have been identified as a viable source for biomass and bio-oil for almost 5 decades: in 1978 the US Department of Energy's Office of Fuels Development funded

an Aquatic Species Program (ASP) aimed at using algae to produce renewable fuel for transportation (Sheehan et al. 1998). At present, algae is still termed the ‘third-generation’ biofuel (Lee and Lavoie, 2013). Microalgae comprise unicellular and simple multicellular microorganisms, while macroalgae include larger species such as seaweeds. The photosynthetic process results in the production of a variety of organic carbohydrates and lipids, which can subsequently be utilised to generate biomass or be extracted directly as biofuels (Fig.2.4) (Jones and Mayfield, 2012; Razeghifard, 2013). Other advantages are the ability to cultivate algae in salt and wastewater and on non-arable land, and the potential for greater productivity over smaller areas of land compared to the aforementioned conventional terrestrial crops (Gendy and El-Temtamy, 2013). Algae cultivation can additionally result in the production of a range of valuable non-fuel products such as omega-3 fatty acids, carotenoids, anti-oxidants and vitamins.

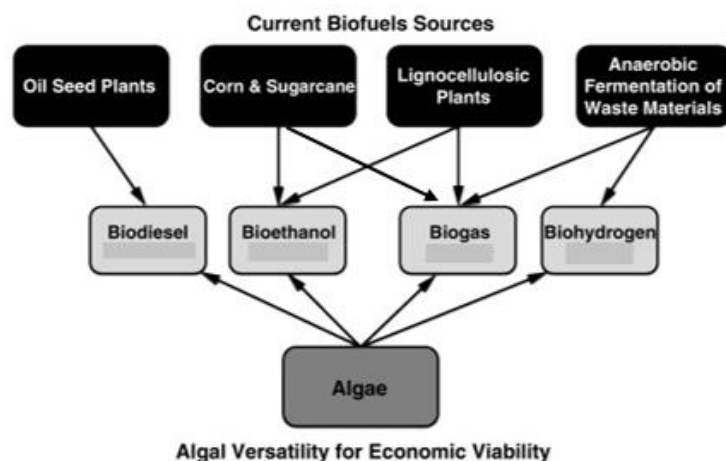


Figure 2.4 - Proposed versatility of algae as biofuels compared to current sources (Adapted from Jones and Mayfield, 2012 & Bondesson et al., 2013).

Biodiesel is produced by the trans-esterification of methanol with biologically derived oils with results in the production of fatty acids methyl esters (FAMES). These ideally

show high stability; low water and volatiles content; and a low amount of sulphur and nitrogen-containing polymers. FAME content is dependent on the fatty acid structure of the biomass feedstock. The high lipid content (20-60%) of certain species of algae makes them an attractive source of biodiesel. However, algae-based biodiesel remains much more costly when compared to petroleum-based diesel, with prices of US\$1.25/lb and US\$0.43/lb, respectively (Li et al. 2011). If productivity were able to be increased to 10,000 gal acre⁻¹, this would reduce the price of algal oil from \$25 to \$2.5 gal⁻¹ (Pienkos and Darzins, 2009). Current research is aimed at finding high-lipid and fast growing algae strains, and optimisation of the transesterification process. At present, it remains a solid candidate as a source of commercially viable biodiesel (Jones and Mayfield, 2012).

Algae can also be used for ethanol production via saccharification (hydrolysis of the algae cell wall), fermentation, and finally distillation (Razeghifard, 2013). Research using yeast to ferment the algae *Chlorococum sp.* resulted in an ethanol concentration of 3.83 g L⁻¹, derived from 10 g L⁻¹ of lipid-extracted microalgae. This amounts to a productivity level of 38% w/w. This is similar to current production methods, and so consequently highlights the potential role of producing bioethanol from algae (Harun et al. 2010).

Macroalgae may be a suitable substrate for biohydrogen production, which can be used for fuel or electricity generation. Park and colleagues determined that the red algae *Gelidium amansii* cultivated by sunlight without fertiliser is viable as a substrate for biohydrogen (Park et al. 2011). Microalgae and cyanobacteria are also able to produce biohydrogen via anaerobic photofermentation, which is a current area of interest for research. Biohydrogen production from algae is many years from commercial applications, however the potential is promising (Jones and Mayfield, 2012).

The commercialisation and scaling-up of algae cultivation for biofuel production is currently reduced by government funding opportunities and tax breaks in the area of renewable energy. These investments may result in reductions in the significant cost barrier for algae production: the Taiwanese TAIGEM-EB model approximates total production cost for 0.6 tons of microalgae biodiesel in a 5-ton photobioreactor is around \$100,000 (~\$19 gal⁻¹) for the first year of operation (Lee, 2011). In comparison, Gallagher estimated the cost of algal oil in an open pond system is \$4.75 gal⁻¹, and is especially feasible with moderate-high lipid yields combined with crude oil prices above \$100 a barrel (Gallagher, 2011).

A widespread criticism of research looking at potential microalgae production is that growth models using small-scale experimental or pilot-study data frequently overestimate potential lipid yields (Moody et al. 2014). To remedy this, a recent study combined meteorological data from over 4,000 global locations with a large-scale growth model to approximate the prospective lipid and biomass productivity of current photobioreactor architecture. The authors determined that maximum lipid yields between 24 and 27 m³ ha⁻¹ y⁻¹ on average are feasible in South America (Brazil and Colombia), Africa (Egypt, Ethiopia, Kenya) as well as in Australia, India, and Saudi Arabia. This is consistent with biomass productivity of 13 to 15 g m⁻² d⁻¹. This falls into the lower third of modelling estimates quoted in research, which shows that productivity is frequently overestimated. However, the authors concluded that with these results, the aforementioned countries could supplement 30% of their fuel consumption from microalgae cultivation (Moody et al. 2014).

Overall, there are still remaining limitations that must be addressed to harness the potential of algae as biofuels. These are the high cost of infrastructure, the difficulties in scaling-up production, and the energy requirements for growth and harvesting.

Promising avenues to address costs and the difficulties in biofuel production are genetic engineering of algae strains to alter lipid chain length, novel extraction systems to facilitate harvesting, and the co-production of valuable non-fuel products to ensure biofuel production is economically viable (Jones and Mayfield, 2012; Gendy and El-Temtamy, 2013).

2.6 Algae and Biofuel Production

The interest in using algae for biofuel production is partly due to greater lipid content per land area when compared to food and plant-oil based crops (Rodolfi et al. 2009; Wijffels & Barbosa, 2010). Furthermore, the chemical content of algae can be manipulated by altering growth conditions; many species store triglycerides and lipids as an energy reserve when faced with nutrient deprivation (Wijffels & Barbosa, 2010). As mentioned, algae can also be cultivated in areas unsuitable for conventional crops. Therefore, in order to optimise microalgae-based oil production, there are a range of factors that must be accounted for. As previously mentioned, an economically viable high lipid yield per area is imperative, and as existing research shows difficult to attain. A suitable microalgal strain which contains a high lipid content and can additionally produce more lipids in response to nutrient deficiency is desirable. However, much research has shown that lipid-rich strains can overall show lower biomass productivity (Rodolfi et al. 2009). Species selection poses other challenges, as the metabolism and molecular makeup of many species varies widely depending on environmental conditions.

Candidates for biodiesel production must have an optimum fatty acid profile that meets strict requirements (EN 14214): Specifically, the cetane number (CN), oxidative stability, cold flow properties, iodine value, and overall viscosity are all crucial

parameters of quality fuel. The CN is a surrogate for the ignition properties of a fuel, and is therefore crucial for engine performance and minimising exhaust emissions (Ramos, 2009). Oxidative stability measures how long a fuel can resist oxidative degeneration, and decreases as the number of double bonds in fatty acid methyl esters (FAMES) increases. Fatty acids with more than one double bond are relatively common place, which therefore is one of the primary reasons that make biodiesel production difficult (Ramos, 2009). The iodine value refers to the total unsaturation of a mixture of fatty acids. Poor cold flow properties lead to obstruction of fuel lines, pumps and filters. Fuel quality control uses the cold filter plugging point (CFPP) which is the temperature at which a fuel can no longer pass through a filter in a given time (Stansell et al. 2012). It is noteworthy that fatty acids with a favourable CN generally result in below-optimum cold flow properties; suggesting that a combination of unsaturated and saturated fatty acids are necessary (Stansell et al. 2012).

Stansell and colleagues assessed the fuel properties of a number of microalgae strains and determined that the majority of microalgae species tested contained very high concentrations of fatty acids with over four double-bonds, therefore conferring poor oxidative stability. Most species additionally showed below-optimum cold-flow properties. However, microalgae lipids showed acceptable viscosity and concluded that if the content of polyunsaturated fatty acids (PUFAs) could be decreased this would then confer improved CN and oxidative stability. The authors also suggested that strains rich in monounsaturated fatty acids (MUFAs) such as the *Mediophyceae* and *Xanthophyceae* are promising (Stansell et al. 2012). Manipulation of fatty acid composition via genetic/environmental factors is likely to be the most promising route (Wijffels & Barbosa, 2010).

Research has shown that temperature, irradiance and nutrient availability can all affect composition and content. For example, increasing light intensity typically results in increased triacylglycerol (TAG) levels (Roessler, 1990), while low light levels result in the production of polar lipids (phospholipids and glycol-lipid) which are important components of the cell membrane (Rodolfi et al. 2009). Salinity has variable effects depending on species (Rodolfi et al. 2009). It has long been demonstrated that nitrogen starved algae species show increased lipid content as a percentage of total cellular mass (Roessler, 1990). More recent research shows that this is a species-specific phenomenon as some algae strains accumulate starch in response to nitrogen starvation. However, The Aquatic Species Program by the US Department of Energy found that lipid accumulation through nitrogen deprivation does not necessarily equal higher overall productivity; as the restricted growth conditions result in lower biomass production (Sheehan et al. 1998). Therefore, species selection is imperative.

Griffiths and colleagues (2011) screened eleven microalgal species and concluded that lipid yields and overall productivity were greater at 150 mg L⁻¹ nitrate compared to 1,500 mg L⁻¹ in ten out of the eleven species, with the Chlorophyta (e.g. *Chlorella vulgaris*) exhibiting the greatest increase in lipid content. Culture conditions still need to be optimised or the fuel blended to attain the European standards for biodiesel production (EN 14214). Rodolfi and colleagues (2009) screened thirty microalgal strains for productivity and lipid content, which resulted in the selection of four strains. Of the four, two marine microalgae species accumulated lipids under nitrogen deprivation. The most promising was *Nannochloropsis* sp.; the authors extrapolated that cultivation of this species had the potential for over 30 tons of lipid production per hectare per year in tropical climates.

In strains that show an increase in lipid production in response to nitrogen starvation, the majority of these lipids are non-polar TAGs. Qualitative analysis of microalgal lipids shows that TAGs are primarily composed of saturated and monounsaturated fatty acids, which provide more energy upon oxidation in comparison to polyunsaturated fatty acids (PUFA), and can be stored in the cell for use as an energy and carbon source. Therefore, the accumulation of TAGs in response to nitrogen deprivation confers a reserve for rebuilding the cell (Rodolfi et al. 2009).

2.7 Surface modification via polyelectrolyte layer-by-layer coatings.

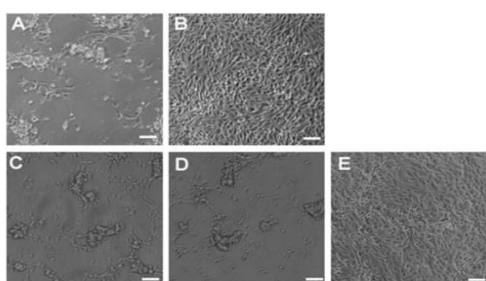


Figure 2.5: Microscopic images of BAEC growth and adhesion on different

There are many ways to modify the properties of a surface, but most of these methods are not appropriate for commercial applications (Gold.,2009). Example of methods that are used to modify surfaces include gas plasma treatments, plasma spraying, physical vapor deposition, self-assembled coatings, chemical etching, laser micromaching and different lithographic techniques. Surface modifications via coatings are often made to functionalise surfaces. In biological applications, this can include cell adhesion, protein adsorption, cell proliferation, and inflammatory response. Layer-by-Layer (LbL) polyelectrolyte (PE) coatings can provide these functions and can self-organise into thin films (approx.1 um) onto surfaces (Hossfeld et al.,2013). Surface properties on a micro or nano scale can affect the cell's structure, function and behaviour at biointerfaces (Gold., 2005).

Previous studies have shown how PE coatings can influence cell attachment. Figure 2.5 are microscopy images taken from Guillaume-Gentil and colleagues study which illustrates how cell adhesion differs on a variety of polyelectrolyte coatings. It was

found that none of the PE films were cytotoxic and that most of them served as a cell adhesive (Guillaume-Gentil et al.,2008).

An alternative study focussed on antifouling functions for their nanofiltration (NF) membrane. They used polyacrylic acid (PAA), polyvinyl alcohol (PVA) and polyvinyl sulfate (PVS) to form a protective layer on their NF membrane via electrostatic force and hydrogen bonding. These strong interactions caused the coating layers to remain stable through acid cleaning. The PE coatings resulted in a reduction of pore size, permeation flux and rejection of neutral sugars and an increase in charge salts. They also found hydrophilicity and smoothness was enhanced. Overall they found that surface charge played a significant role in foulant adsorption. As the uncoated membrane was positively charged, foulants such as sodium alginate and humic acid attached rapidly and strongly. This was also the case for their PVA coated membrane due to also having a positive charge. After further optimisation, the NF membrane developed in this study will be used in a membrane bioreactor (MBR). This study illustrated the potential of modifying membranes in order to cater to different industrial demands (Ba et al.,2010).

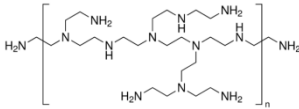
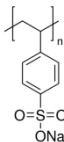
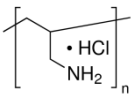
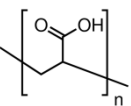
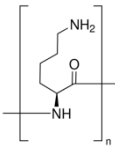
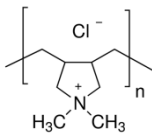
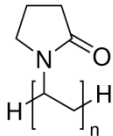
Like the previous study mentioned, hydrophilicity is a surface property reported by others after the layering of PE's. Park and others found coating their titanium implants with PEs increased surface wettability without changing the surface roughness. These PE coated implants were found to enhance osteoblast differentiation (Park et al.,2011). Haselberg and others illustrated the use of atomic force microscopy (AFM) to characterize polyelectrolyte coatings. The study showed the coating procedure resulted in nm-thick layers on silica substrates. They also concluded that individual polymer lay flat on the surface due to intramolecular electrostatic interactions. It was additionally

found via AFM imaging that a single PE layer did not cover the surface completely and that at least a tri-layer was needed for complete coverage (Haselberg et al.,2013).

Nehme's and Perrin's protocol on developing highly charged polyelectrolyte coatings to prevent protein adsorption stated that compared to the use of non-covalent coatings; using charged PE's instead is more efficient and simple. Very stable coatings were obtained when optimal conditions were followed. The coatings were able to withstand a large pH range (2 – 10) and in the presence of organic solvents. In addition the study stated that hundreds of analyses could be carried out without the need for coating regeneration (Nehme's and Perrin's.,2013).

Table 2.1 includes a list of polyelectrolytes tested in the present study along with their known applications.

Table 2.1: List of properties and known applications for PEs selected.

Name	Chemical structure	Applications
Poly(ethylenimine) (PEI)		Used as a transfection reagent and to increase attachment of weakly anchoring cells (Vancha et al. 2004).
Poly(styrene sulfonate) (PSS)		Used for novel macroporous amphoteric gels for drug delivering applications (Oh et al., 2008; Kudaibergenov et al. 2012).
Poly(allylamine hydrochloride) (PAH)		Cationic electrolyte used for multilayer capsules (Antipov et al. 2001).
Poly(acrylic acid) (PAA)		Used for adhesives and ion exchange resins (Orwoll et al. 1999).
Poly-L-lysine (PLL)		Used as an attachment factor to improve cell adherence (Mazia, et al. 1975).
Polydiallyldimethylammonium chloride (PDADMAC)		Used to produce ultrathin films (Moriguchi & Fendler, 1998), water purification (John et al. 2002) and waste water treatment (Edzwald et al. 2011).
Polyvinylpyrrolidone (PVP)		Film forming and binding agents. (Haaf et al. 1985).

2.8 Conclusion

Over the past few decades, the utilisation of algae to develop a range of industrial and agricultural compounds along, with its numerous advantages over first- and second-generation biofuels has highlighted its potential promise. In order to fully realise this

promise, there are a number of important factors that need to be addressed in future work.

Firstly, there are issues with cost and scaling-up existing reactor designs. The suggested price for economic fuel production is approximately US\$ 0.25 kg⁻¹ (Darzins et al. 2010) and algal biofuel production costs based on existing technologies are noted to be anywhere from 3 to 10 times greater than this (Darzins et al. 2010; Acien et al. 2012). With significant improvements to existing technologies along with optimum site and strain selection, algae do have the potential to provide a significant proportion of fuel along with a number of other high-value compounds (Darzins et al. 2010).

While there are significant savings with regards to the use of industrial carbon dioxide and wastewater for cultivation (Acien et al. 2012), a remaining bottleneck to large-scale production is energy-intensive harvesting. Future work focusing on biofilm-based reactors should focus on perfecting the simple, automated harvesting via scraping of biofilm-based reactors (Blanken et al. 2014). With regards to PBRs, promising avenues to facilitate flocculation are by inducing physical flocculation with nanoparticles (Lee et al. 2014), or by the genetic modification of algae which facilitate flocculation (Wijffels & Barbosa, 2010).

With regards to large-scale algae cultivation, the most promising avenue may be to follow the biorefinery concept, where multiple fuels and products are derived from algae cultivation in an integrated facility (Markou & Nerantzis, 2013). The harvesting of lipids as well as carbohydrates means that feedstock for biodiesel and bioethanol is available. Furthermore, proteins, pigments and high-value cosmetic and supplemental compounds would make the biorefinery concept cost-effective: the global market value of commercially-used carotenoids and β -carotene for example is expected to reach \$1.4 billion and \$334 million by 2018, respectively (Borowitzka, 2013). An area for future

work is the development of effective co-extraction and separation of multiple metabolites from the biomass (Serive et al. 2012; Markou & Nerantzis, 2013; Behera et al. 2015).

The promising surface and footprint biomass productivity figures of biofilm-based reactors make these a viable prospect. These reactors may minimise harvesting costs, which as stated are a significant barrier to large-scale production. However, biofilm-based reactors are a relatively novel technology, and key areas for future work are again identifying optimal strains and ensuring the best surface material to facilitate adhesion and biofilm formation (Gross et al. 2015). As with PBRs, the potential of algal biofuels has been technically and experimentally confirmed with laboratory- and pilot-scale studies, but the most important factor now is to confirm that algal cultivation for biofuels and other end-products is economically feasible on the large, commercial scale (Darzins et al. 2010; Acien et al. 2012; Gross et al. 2015).

Chapter 3

Encouraging algae biofilm formation using polyelectrolyte coated polymers

Abstract

Electrostatic and hydrogen bonds are the major forces involved in the interaction between microalgae and the surface. The mucilage layer secreted by algae allows settled cells to glide easily across the surfaces aiding in the rapid colonisation of the surface. Polyelectrolyte coatings that contain charged groups which can aid in the interactions of extracellular polymeric substances (EPS) and microalgae were tested. Polyelectrolytes were assembled onto commercially available substrates via manual dip coating. It was found that layers of polyvinylpyrrolidone and poly (acrylic) acid labelled as coating 1 (C1) performed the best in terms of growth of *Chlorella Sorokiniana*. In addition to the substrate polyethylene terephthalate glycol-modified (PETG) was also found to be the best performing substrate. Contact angle measurements revealed all polyelectrolyte coatings lowered the contact angle of all substrates significantly, but did not necessarily correlate with high growth.

3.1 Introduction

Due to limitations with suspended algae reactors, there is now a growing interest in using surface attached algae biofilm systems. Ozkan and others (2013b) reported that their developed biofilm photo bioreactor substantially reduced water requirements by 45% and reduced energy costs considerably. These results highlight the potential of further development and innovation in algal biofilm reactors.

The ALGADISK project aims to produce high value organic algal products while maintaining low production costs. The ALGADISK system utilises rotating disks which facilitate algae biofilm formation. Consequently, this study aims to provide these biocompatible surfaces that encourage and enhance algal attachment and biofilm yield. Previous studies have shown increased microbial attraction onto oppositely charged surfaces (Busscher et al. 1990). Thus, the initial strategy explored was developing a coating that can aid in electrostatic attraction of algal cells onto low-cost polymer substrates. Surface coatings that can aid in these interactions were therefore proposed. Coatings comprising of charged polyelectrolyte multilayers (PEM) via layer-by-layer (LbL) deposition were explored.

Polyelectrolyte (PE) polymers are flexible and can form super lattice structures. Polymers can bridge over any defects and after as little as three layers can completely cover a charged surface (Krol et al. 2006). Adsorption of polymers with more than one layer causes a charge reversal. This, therefore, acts as a regulating system which allows only a monolayer to form, thus allowing the oppositely charged polymer to be adsorbed in further stages (Decher et al. 1997). Research in PE coatings is valuable due to its many applications in the biomedical and electronics fields (Stewart et al.2006; Thierry et al.2003; Kommireddy et al. 2005).

This chapter is primarily concerned with exploring the potential of using PEM coatings to encourage algae attachment. Chapter 4 is concerned with optimising the final selected coating from this chapter for the ALGADISK prototype.

3.2 Materials and Methods

3.2.1 Algae culture

Chlorella vulgaris (211/BK), *Scenedesmus obliquus* (276/50), *Dunaliella salina* (19/12), *Arthrospira maxima* (1475/9) were obtained from Culture Collection for Algae and Protozoa (Oban, UK). *Chlorella sorokiniana* (Sorokin and Myers, 1953) was received by Wageningen University (Netherlands). Cell-hi F/2 + Si (Guillard's) media was used for marine algal species and Cell-HI NC was used for freshwater species. Both media concentrates were purchased from Varicon aqua and diluted to recommended specifications (1 ml per 1000 L of water). Glass tanks were cleaned prior to inoculating with algae and filled with distilled water. For marine species (*D. salina*) tanks were supplemented with water conditioner and a sea salt mix (Aquarium Systems). *C. sorokiniana* and *D. salina* were grown in 1 L flasks before being transferred into glass tanks (50 L) with one fluorescent tube (15 W) at $20 \pm 2^\circ\text{C}$ on a 16/8 hours light and dark cycle. Air was bubbled through an air stone via an air pump which also provided mixing. The remaining algae species were cultivated in flasks under two fluorescent light tubes (1500 Lux) at $20 \pm 2^\circ\text{C}$ at a 16/8 hours light/dark cycle and shaken manually daily.

3.2.2 Adhesion assays

3.2.2.1 Testing initial attachment

Substrates (area: 3.5 cm^2) were placed into petri dishes with 15 mls of algae suspension with cell concentrations at 5.0×10^4 cells/ml (± 0.5) and left on a BlotBoy™ 3D platform rocker, AC input 115 V (12 rpm) (Sigma Aldrich, UK) for 2 hours. After 2 hours of

incubation the substrates were rinsed gently with water and the number of cells found on the surface of the substrates were counted using a microscope (GXML 320 1 LED, GX Optical UK) and a hemacyter kit.

3.2.2.2 Testing strength of attachment

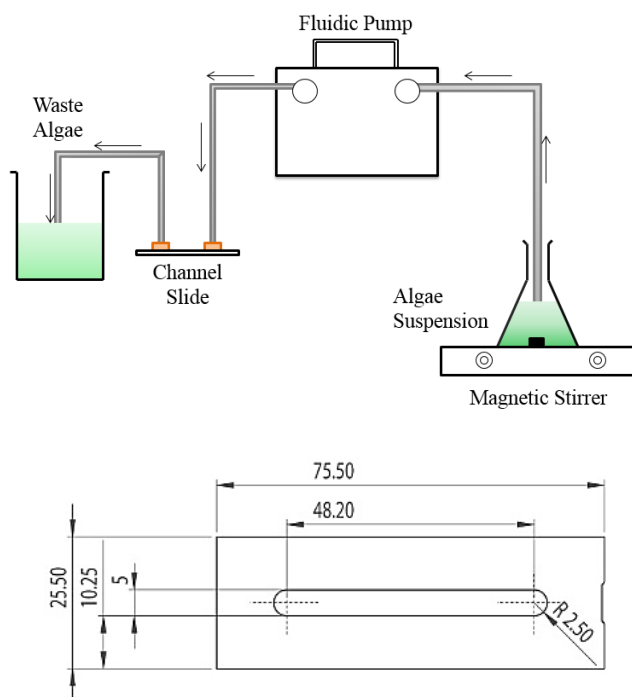


Figure 3.2.1: (A) Schematic diagram showing algae adhesion assay set up for absorption and desorption tests. (B) Schematic drawing of Ibidi 0.2 Luer Sticky-slides.

Substrates were mounted onto Ibidi 0.2 Luer Sticky-slides (Fig.3.2.1 B) with 2.5 cm² growth area and a channel volume of 50 µl. The slides were then connected to a fluidic pump (KNF VP Series, UK) and fixed with fluidic adaptors with a flow rate of (5mls/min) (Fig.3.2.1 A). Cell concentrations were kept at a range of $\times 10^4$ cells/ml and flowed through for 20 minutes and then left to settle for 72 hours. Number of cells and cell viability was calculated immediately after 72 hours. Water was then rinsed through

(5mls/min) for 15 minutes and the remaining cells were counted using a microscope. Strength of adhesion was determined by calculating the number of remaining adhered cells as a percentage of the number of cells counted before the flushing process.

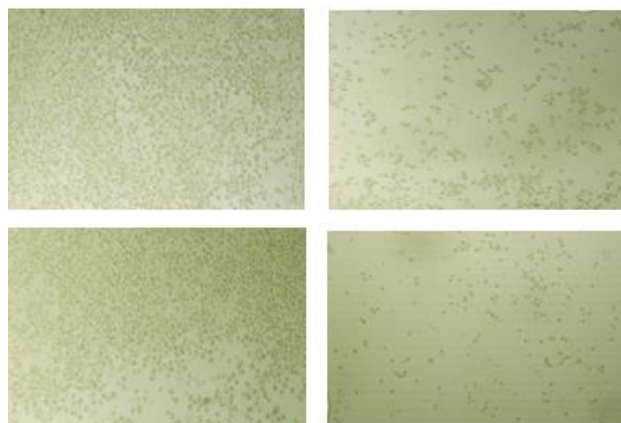


Figure 3.2.2: Microscopic images taken of *C. sorokiniana* before (left) and after flushing with water (right).

3.2.3 Cell viability assays

Cell viability was determined without sample preparation. Using already described method of using autofluorescence of chlorophyll from viable cells and green autofluorescence from non-viable cells using the blue excitation setting (Schulze et al. 2011). This was undertaken after 72 hours of incubation with algae.

3.1.4 Long term growth studies and harvesting

To measure biofilm density between harvests, long term growth studies were set up in petri dishes under two fluorescent light tubes (1500 Lux) at $20 \pm 2^\circ$ C at a 16 hours light cycle at 12 rpm on a platform rocker. Seven days were left between each harvesting cycle. Algae were harvested from substrates via manual scraping with a plastic scraper ensuring all substrates were harvested in the same manner each time. The harvested algae were dried in the oven for 12 h at 105° C onto glass-fiber paper and then weighed and recorded.



Figure.3.2.3: Long-term growth experiment set-up. Image shows example of static and non-static (rotating table) growth tests. All samples are placed directly beneath two fluorescent light tubes (15 W).

3.2.5 Substrate selection and preparation

The following polymer substrates were tested in conjunction with polyelectrolyte coatings: Polypropylene (PP), Polyethylene terephthalate (PETG) Polycarbonate sheets (PC) and were all purchased from Plastic store Ltd, UK. Polystyrene film (PS) was purchased from Goodfellow, UK. These substrates were all selected on the basis that they all have low scratch-resistance, are low cost and very durable. Substrates were cleaned with 70 % ethanol before being rubbed with acrylic fibers approximately 15 times on each side.

3.2.6 Fabrication of polyelectrolyte coatings

Polyelectrolytes used were all purchased from Sigma Aldrich, UK: Polyvinylpyrrolidone (PVP, 10 000 Mw), Poly(allylamine hydrochloride)(PAH, 15 000 Mw) , poly(sodium 4-styrenesulfonate) (PSS, 70 000 Mw), Poly(acrylic acid) (PAA, 1800 Mw), Polyethylenimine (PEI, 10 000 Mw), Poly(diallyldimethylammonium chloride) (PDADMAC, 20 wt. % in H₂O) and Poly-L-lysine (PLL 0.1% (w/v) in H₂O). Polyelectrolytes solutions for dip coating were made into working solutions of 1mg/ml of the polymer dissolved in PBS buffer. Substrates were previously cut into a typical size of 25mm x 25mm and cleaned with 70% ethanol, deionised water (DI) and left to

dry. The substrate was then rubbed with acrylic fibres for 1 minute to induce surface charging. The substrate selected was then dipped into the polyelectrolyte solution (polyanion) so that its surface was completely covered in a solution for 15 minutes. The substrate was then rinsed twice with DI water and dried with nitrogen gas at room temperature. The substrate was then dipped in an oppositely charged polyelectrolyte (polycation) for 15 minutes followed by rinsing the substrate twice with DI water and dried with nitrogen gas at room temperature. This was repeated till the desired number of layers, and outer charge was achieved. An overall schematic of the process is shown in Figure 3.2.4. Table 3.2.1 lists the PE layers in different coatings tested. Table.3.2.2 lists all the PEs used in this study and their known applications in research.

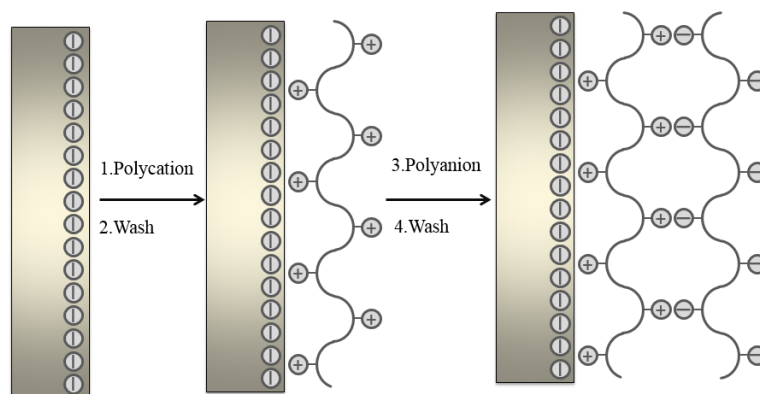


Figure 3.2.4: Schematic diagram showing steps in PEM formation onto a substrate.

Table 3.2.1: Coating labels used and their PE layer composition

Coating label	PEs used in coating
C1	PVP/PAA/PVP/PAA/PVP
C2	PAH/PSS/PAH/PSS/PAH
C3	PLL/PAA/PLL/PAA/PLL
C4	PEI/PSS/PEI/PSS/PEI
C5	PEI/PAA/PEI/PAA/PEI
C6	PDADMAC/PSS/PDADMAC/PSS/PDADMAC
C7	PDADMAC/PAA/PDADMAC/PAA/PDADMAC
C8	PAH/PAA/PAH/PAA/PAH
C9	PVP/PAA/PVP/PAA/PVP/PAA
C10	PAH/PSS/PAH/PSS/PAH/PSS
C11	PLL/PAA/PLL/PAA/PLL/PAA
C12	PEI/PSS/PEI/PSS/PEI/PSS
C13	PEI/PAA/PEI/PAA/PEI/PAA
C14	PDADMAC/PAA/PDADMAC/PAA/PDADMAC/PAA
C15	PDADMAC/PSS/PDADMAC/PSS/PDADMAC/PSS
C16	PAH/PAA/PAH/PAA/PAH/PAA

3.2.7 Contact angle measurements

A static sessile drop method was used using the Attension Theta Tensiometer to measure the contact angle of water on the surface (water drop size of approximately 1.5mm, at room temperature approximately 22°C). Measurements were taken at 6 different locations of the tested surfaces and then averaged.

3.2.8 Zeta potential measurements and charge density

Zeta potential of algae was measured at different pH ranges by firstly removing algae from its media and washing three times with distilled water (dH₂O) followed by re-suspension in a solution of NaCl. The pH was altered using HCL or NaOH. The concentration was determined by a hemocytometer kit and was adjusted to a density of approximately $2 (\pm 0.5) \times 10^7$ cells/ μ L. Samples were then analysed by a Zetasizer3000 (Malvern Instrument 2000HAS) and tested 5 times per sample. Charge density was measured using Sharp et al., 2006's method using the zetasizer with PDADMAC (Sigma Aldrich) (charge density: 6.2 mEq g⁻¹).

3.2.9 Determining cell wall functional groups

A previously detailed method (Ivanova et al. 2012) was used to quantify the functional groups in the cell walls of algae. This method uses potentiometric titrations where dried biomass is mixed in 50 cm³ of dH₂O. HCL was used to adjust the initial pH to 1 and was then titrated with 0.1M of NaOH up to a pH of 12. A control was also carried out with no algae. The Gran's method (GRAN, 1952) was then used as detailed again by Ivanova and colleagues (2012) to determine the total organic acidity (A_{TO}) consisting of strong acidities (A_S) at pH <4, weak acidities (A_w) at 4 <pH>7, and very weak acidities (A_{vw}) at pH>7.

3.2.10 Data analysis and Statistics

Pearson's Correlation coefficients were calculated to test correlation. Two tailed Student's t-tests were used to compare contact angles and weighted dry biomass with and without coatings; values that were $p < 0.05$ were considered significant.

3.3 Results and Discussion

3.3.1 Testing PEM coatings adsorbed onto polymers on different algae species

All three algae species tested showed coatings with a positive outer layer frequently found higher weighted growth in contrast to uncoated (C0) and to surfaces with an outer negative charge (C9 – C16) after a growth period of 7 days. Attachment assays also found a higher number of attached cells on positive coated surfaces followed by negatively charged coated surfaces and lastly non-coated substrates (refer to Fig 3.3.1-3.3.3). The use of a high positive surface charge in attracting algae cells to the surface has been observed previously; Ederth and colleagues (2008) explained that the high surface charge of their self-assembled monolayers may have been responsible for retaining their spores on to the surface. They also found that *Ulva* spores preferred

uncharged or positively charged rather than negatively charged surfaces (Ederth et al. 2008).

All 18 coatings lowered the contact angles of the hydrophobic polymer substrates significantly ($p < 0.05$) (refer to table.3.3.1). Static and non- static conditions were tested to examine the effect of hydrodynamic action on the performance of the coated substrates. In most cases higher biofilm densities resulted when hydrodynamic action was introduced (Fig 3.3.1 b - 3.3.3 b). This is most likely due to the increased opportunities for the algal cells to make contact with the surface.

When plotting average biofilm density for all three algae species against contact angles, there was a general trend of higher yields on substrates with contact angles below 34 (Fig.3.3.5). However, it cannot be assumed that contact angle influenced adhesion as some coated surfaces with lowered contact angles did not perform any better than the uncoated hydrophobic polymers (refer to Fig 3.3.1- 3.3.3). Previous studies have also indicated that contact angle did not necessarily correlate with degree of colonisation (Irving et al. 2011; Barberousse et al. 2007). Therefore, the coating charge and chemical properties in combination with the substrate polymer selected have had a more considerable influence on algae biofilm formation.

Each algae species had its own preferences in terms of substrate and coating. Table 3.3.2 summarizes the highest recorded weights for each species.

C1 performed the best for *C. sorokiniana* in terms of biofilm density harvested (Fig.3.3.1A). Coating 3 performed well with both *S. obliquus* and *C.vulgaris* (Fig.3.3.2 A & 3.3.3 A). Testing the strength of adhesion on initial attachment via adhesion assays revealed C3, C6 and C7 performed well generally for all three algae species tested (Fig.3.3.1C, 3.3.2C, & 3.3.3C). It should be noted that high percentage adhesion after flushing did not always correlate with high biofilm density after 7 days. It was also

apparent non-coated and negatively charged surfaces had substantially weaker adhesion with all algae. This generally low performance on negatively charged surfaces is understandable as these coatings produce electrostatic repulsion and so algal cells would have weaker adhesion.

Substrate PETG performed generally well for all three algae strains with C1 and C3 and cell viability tests showed low toxicity. Therefore, PETG was selected as the primary substrate selected for further experiments.

Table 3.3.1 Contact angle measurements (°) taken with water of all coated substrates.

Substrate	C0	C1	C2	C3	C4	C5	C6	C7	C8
PETG	83±2.1	46±1.3	32±2.3	38±2.5	26±2.1	32±1.1	52±1.7	47±2.3	34±1.6
PS	98±1.6	42±2.1	35±1.4	36±3.6	28±1.8	29±2.4	52±3.2	51±1.8	37±2.5
PP	75±3.2	46±0.8	28±1.6	33±4.2	24±2.0	26±2.2	47±2.5	45±2.3	32±2.7
PC	92±2.8	49±1.4	34±3.1	31±3.1	27±3.3	31±1.1	53±1.9	49±2.5	36±2.3

Substrate	C9	C10	C11	C12	C13	C14	C15	C16
PETG	39±1.8	41±2.8	36±2.8	46±3.2	29±2.4	49±1.2	31±2.6	24±1.7
PS	37±2.6	45±2.7	35±1.9	45±2.5	26±2.3	48±2.5	26±2.2	27±1.6
PP	34±1.2	41±2.2	32±1.6	47±3.1	27±3.7	44±1.8	24±2.4	23±1.3
PC	36±1.5	44±2.3	37±2.2	48±1.7	29±2.5	47±3.2	22±3.1	26±2.2

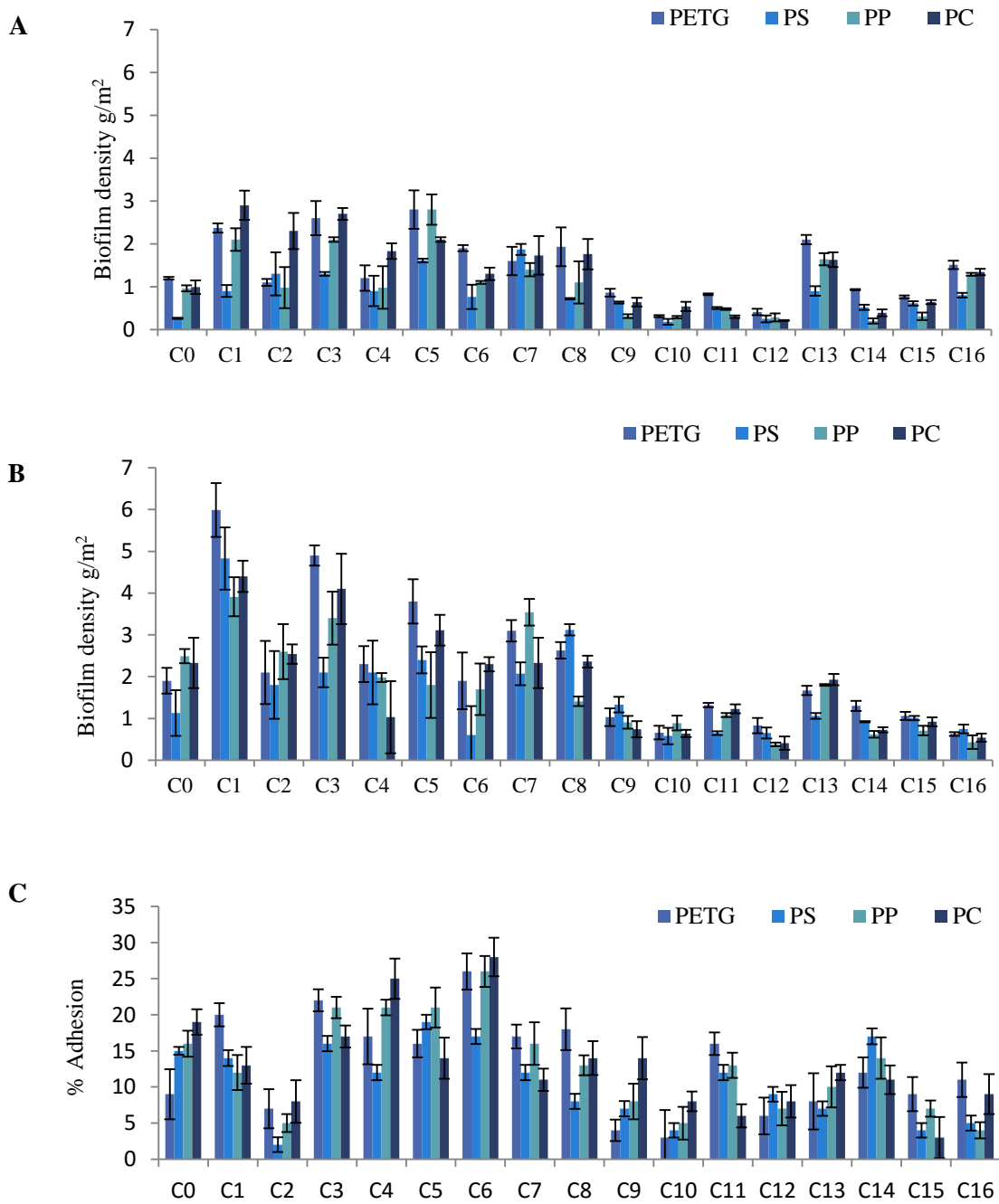


Figure 3.3.1. (A) Static growth results of *C.sorokiniana*.(B) non-static growth results of *C. sorokiniana*. A & B show algae dry weight harvested at day 7 on surfaces tested. (C) Adhesion of *C. sorokiniana* found on surfaces after wash-out, calculated as a percentage. Error bars represent standard deviation of the mean (n=3).

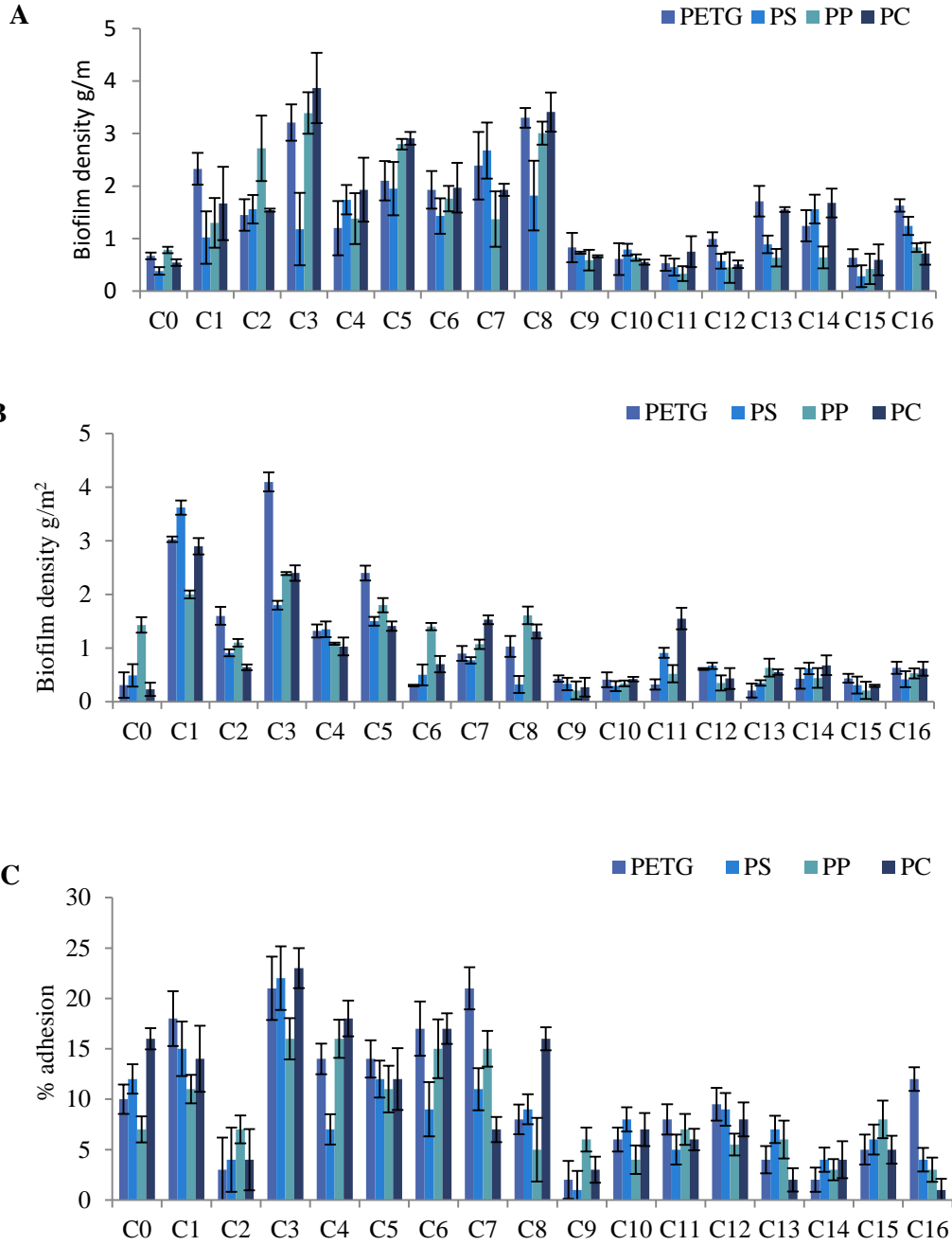


Figure 3.3.2. (A) Static growth results of *S. obliquus*. (B) Non-static growth results of *S. obliquus*. A & B show algae dry weight harvested at day 7 on surfaces tested. (C) Adhesion (%) of *S. obliquus* found on surfaces after wash-out, calculated as a percentage. Error bars represent standard deviation of the mean (n=3).

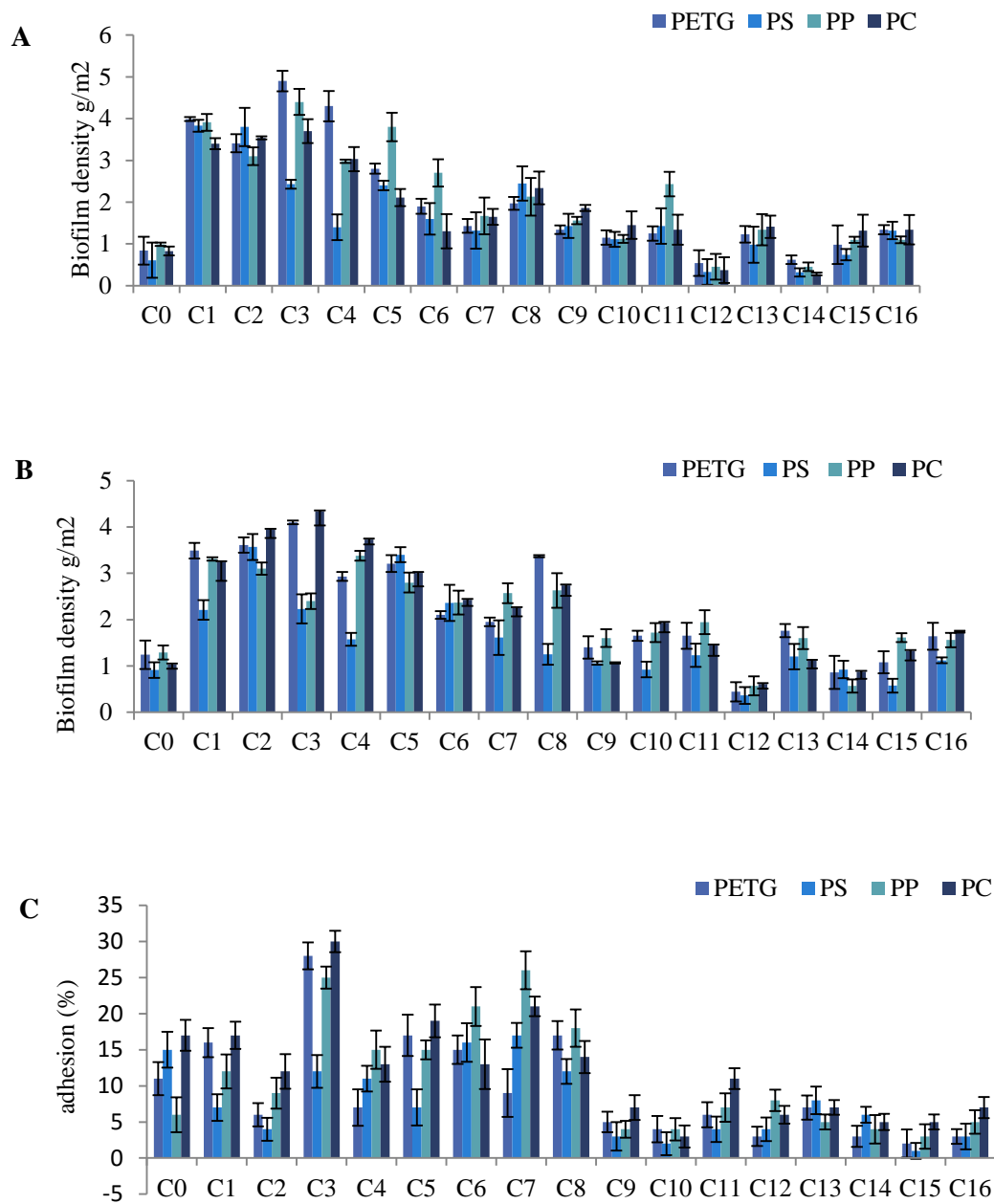


Figure 3.3.3. (A) Static growth results of *C. vulgaris*. (B) Non-static growth results of *C. vulgaris*. A & B show algae dry weight harvested at day 7 on surfaces tested. (C) Adhesion (%) of *C. vulgaris* found on surfaces after wash-out, calculated as a percentage. Error bars represent standard deviation of the mean (n=3).

3.3.3 Cell viability assays

Figure 3.3.4 displays the % of viable cells found on all surfaces after 72 hours for all 3 algal species. C4 and C6 for *C. sorokiniana* had the lowest observable viable algal cells.

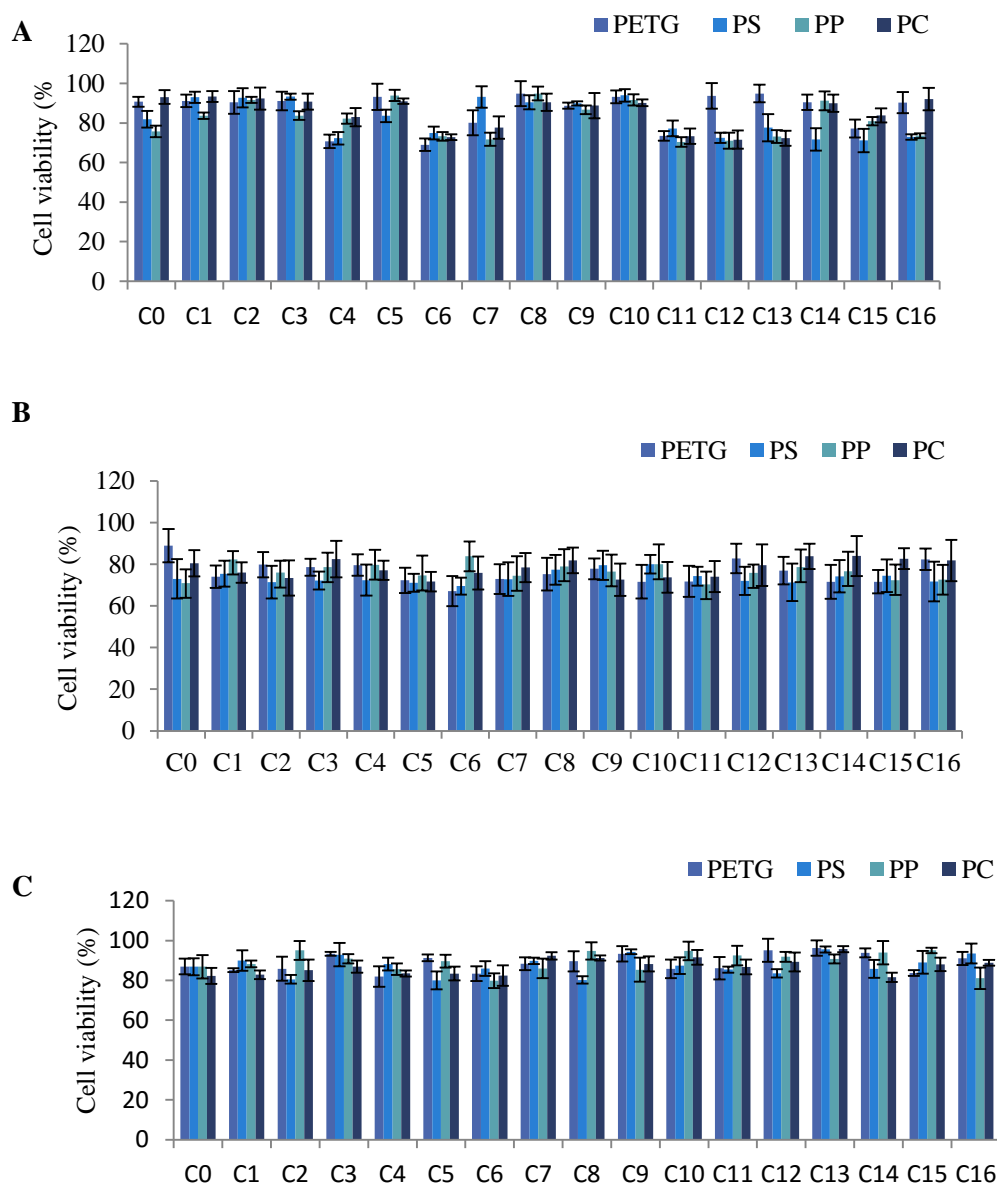


Figure 3.3.4. (A) Cell viability (%) of *C. sorokiniana*. (B) Cell viability (%) of *S. obliquus*. (C) Cell viability (%). Cell viability was determined via fluorescent microscopy. *C. vulgaris*. Error bars represent standard deviation of the mean (n=3).

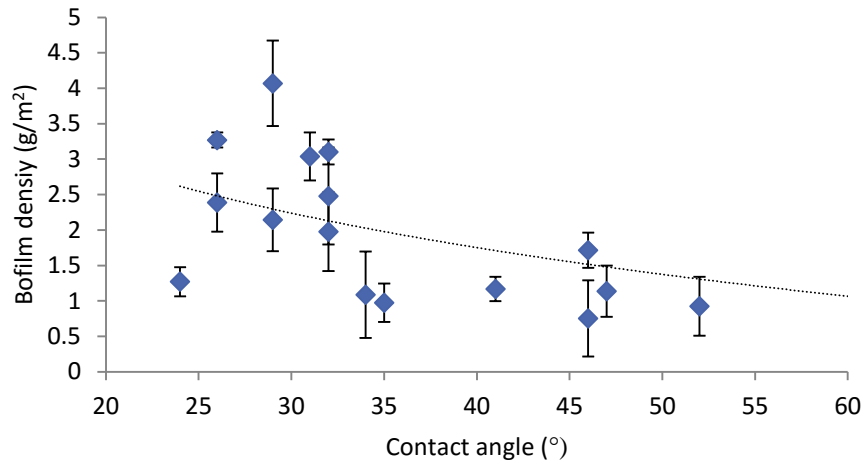


Figure 3.3.5: Graph shows average biofilm growth for *C.sorokiniana*, *S.obliquus* and *C.vulgari* plotted against contact angle of the substrate. Error bars represent standard deviation of the mean (n=9).

The natural zeta potential of algae did not have an apparent influence on the amount of attached cells found on positively charged PETG C3 (Fig.3.3.6 B). Although, *S. obliquus* had overall the most negative zeta potential (refer to Fig.3.3.6 A), and the highest average number of cells attached was for *C. vulgari* followed by *C. sorokiniana*. Therefore, the charge density of algae was investigated and additional species of algae were tested to examine the role of charge density on attachment to C3 PETG (refer to Fig.3.3.6 C). Results indicated a correlation coefficient of 0.76 with positively charged coating (C3) and a negative correlation coefficient of -0.71 with negatively charged coating (C11). This indicates that charge density of the algae can influence attachment onto charged substrates. This was not the case for C1, which had a moderate correlation coefficient of -0.58. This confirms other factors also need to be considered other than degree of electrostatic attraction/repulsion when it comes to explaining why C1 aids in biofilm formation.

Interestingly, the negatively coated substrates in several cases still had a higher amount of biofilm growth when compared to uncoated substrates, especially in non-static

conditions (refer to Fig.3.3.1- 3 A). *C. sorokiniana* had a notably higher amount of growth found on negatively charged coated surfaces (C13 & C16) when compared to non-coated (Fig.3.3.1 A). A possible explanation proposed could be due to the positively charged domains on the algal cell surface. These domains facilitate in adhesion by local electrostatic attraction and acid- base interactions regardless of the overall acting repulsion (Bos et al. 1999). This is further confirmed when looking at the functional groups found in the cell walls of all three algae (refer to table 3.3.4). *C. sorokiniana* was found to have a higher percentage of amine functions (positively charged) when compared to *C. vulgaris* and *S. obliquus*. Although the number of negatively charged functional groups (carboxylic, phosphoric and sulfonate groups) in the cell walls made up 48.9 % of all binding sites, the high presence of weak acidities (amine groups) may have influenced adhesion onto negatively charged coated substrates. Zita and Hermansson (1997) observed this behavior strongly with *E. coli* attachment to sludge flocs. They found the number of positively charged surface structures correlated with adhesion to sludge flocs, in contrast to the number of negative surface structures which showed no correlation. The results presented in this study however, indicate that although microscopic interactions of positive cell wall entities facilitate the attachment of algae onto negatively charged surfaces, macroscopic attraction is more influential in algal surface attachment. This is shown in the higher biofilm densities found on positive surfaces rather than negative surfaces.

It is also evidently shown in the zeta potential and algal adhesion assay experiments when increasing the negative charge of algae via pH (refer to Fig.3.3.6 B). The initial attachment of algae onto positive coated surfaces (C3) increases with the increase of the cells negative charge. This observed increase in attachment is most likely due to the increase in macroscopic attractive forces between the algae and coated substratum

allowing the two to interact. It has been suggested that once microbial species are at a few nanometers away, complementary stereochemical groups can then attract each other. This interaction energy is higher than the macroscopic interactions for microbial species (Van Oss, 1995). When looking at the reacting charged groups of the polyelectrolytes, a possible link to their performance can be suggested. PVP as the outer layer generally performed well in all three algae species tested in growth tests but mainly in non-static conditions (refer to Fig. 3.3.1- 3 B). PVP has the ability to interact with both carboxylic and amino groups via ion dipole interactions and hydrogen bonding. In addition to this, when looking at the attachment assay results, the amount of cells found after 6 hours on the surface was lower than that of coatings that consisted of strong positively charged polyelectrolytes (C3)(Fig.3.3.6 B). However, it should be noted that the size of the cells varied between species and so would therefore influence the number of cells found on the surface.

These results suggest that Coating 1 provides favorable highly localised molecular groups for specific interactions with complementary groups found on the cell surface of algae. However, in contrast to C3, C1 is thought to provide little long range macroscopic interaction and is mainly operative over small distances with algal cells. This further explains why once hydrodynamics were introduced, the amount of algal adhesion increased more drastically than any other coating (Fig.3.3.1-3). The increased frequency of algal-substratum contact meant the lower electrostatic attraction offered by C1 was no longer a limiting factor. C1 therefore should be used in non-static conditions for optimum biofilm yields. C1 also showed good attachment despite the zeta potential of algae and charge density relative to other coatings (Fig.3.3.6 C). C3 also performed well with all algae species tested, and again when looking at the chemical structure of its outer layer (Table 3.2.1), PLL is also capable of hydrogen bonding and ion dipole

interactions, which none of the other remaining polycations are able to do. Unlike C1, C3 also performed well in initial adhesion tests. This is most likely due to the fact that PLL is positively charged in contrast to PVP (neutral) and so adhesion is enhanced by electrostatic attraction. Thus, C3 would be a good candidate for biofilm-based photo bioreactors with no hydrodynamics offered and requires high initial attachment to stimulate growth on the surface.

Conversely, it should be highlighted that high electrostatic attraction did not always coincide with high overall yield. PDADMAC is a strong polycation and was used as an outer coating in C6 and C7. Adhesion assay results showed although the strength of attachment on C6 had high values for all three algae species tested (refer to 3.3.1 - 3 C), it had very low biofilm densities in the long term growth tests (refer to 3.3.1 - 3 A & B). C6 is composed of both strongly charged polycation and polyanion layers and so although it may have attracted a high number of algae to the surface with strong adhesion, it may have in actual fact inhibited the proliferation of algal cells. Autofluorescence assays were conducted to determine cell viability at 72 hours and revealed C6 had slightly higher number of non-viable algal cells for all three algae species tested. PEI found in C6, is typically used to increase attachment of weakly adhering cells in biotechnology. However, it has also been shown to be toxic along with PSS and PDADMAC by inducing surface modifications on the membrane of microbial cells (Vancha et al.2004). Cell viability was good for those grown on C1 and C3 as shown in Figure 3.3.1C – 3.3.3C on all three algae species.

Table 3.3.2: Summary of coatings and substrates with the highest biofilm growth

	Coatings	Substrates
<i>C. sorokiniana</i>	C1 & C3	PETG
<i>C. vulgaris</i>	C3 & C4	PETG & PC
<i>S. obliquus</i>	C1, C3 & C8	PETG & PC

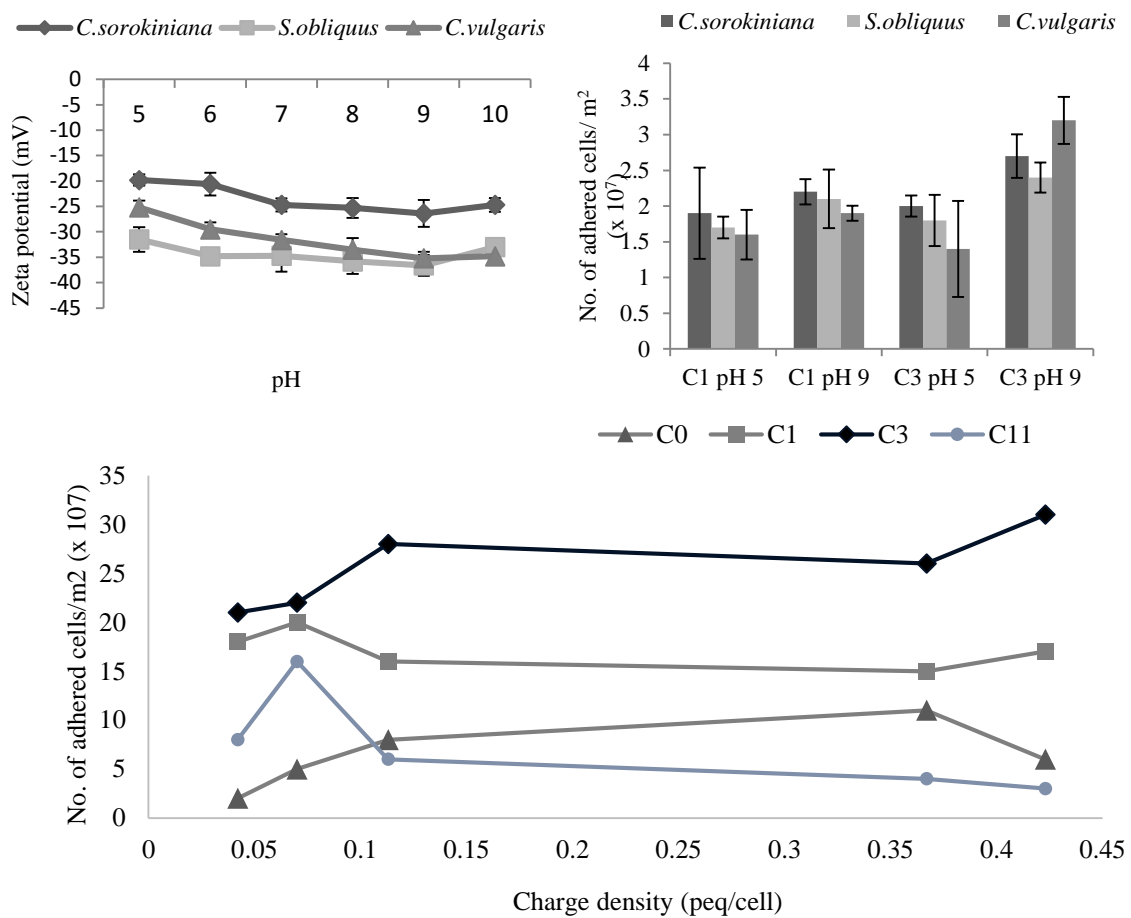


Figure 3.3.6. (A) Effect of pH on zeta potential of all three algae species. (B) Effect of pH and corresponding zeta potential on algal adhesion on C1 PETG and C3 PETG. (C) Effect of charge density on 5 different algal species on C3 PETG. Error bars represent standard deviation of the mean (n=3).

Table 3.3.3 Charge density of algae

Algae	Charge density (peq/cell)
<i>S. obliquus</i>	0.042
<i>C. sorokiniana</i>	0.07
<i>C. vulgaris</i>	0.113
<i>D. salina</i>	0.367
<i>A. maxima</i>	0.423

Table 3.3.4 Amount of acidic sites found in the cell walls of *C. sorokiniana*, *C.vulgaris* and *S.obliquus*.

Algae species	A _s	A _w	A _{vw}	A _{TO}
<i>C. sorokiniana</i>	0.21	0.98	1.24	2.43
<i>S. obliquus</i>	0.82	0.34	0.87	2.03
<i>C. vulgaris</i>	0.21	0.15	0.13	0.49

(mmol g⁻¹)

The aim of this study was to produce a versatile, low cost coating that can be used with the ALGADISK system, primarily for *C. sorokiniana*. *C. sorokiniana* was chosen as the main algae for the ALGADISK project by the consortium due to its high specific growth rate, (0.27 h⁻¹) and its tolerance to high irradiance, temperature and CO₂ concentrations (Sorokin, 1959; Matsukawa et al. 2000). Therefore C1 was selected as the main candidate for further optimisation and testing due to its promising results with *C. sorokiniana*. C3 was also further tested due to the high growth values and cell viability observed with *C. vulgaris* and *S. obliquus*.

3. 4 Conclusion

The following can be concluded from this chapter about using PE coatings for the role of encouraging and enhancing biofilm formation:

- Positively charged outer PE layers can increase initial attachment, biofilm density and strength of adhesion via electrostatic attraction onto commercially available polymer substrates.

- A neutral polymer such as PVP used in conjunction with a polyanion such as PAA in C1 can enhance biofilm yield. This is thought to be due to microscopic rather than macroscopic interactions with algae.
- C3 consisting of PLL as a polycation outer layer can enhance biofilm growth and is thought to aid in better macroscopic attraction of algae to the surface. Charge density of algae influenced initial attachment to C3 substrates.

This study showed the potential of using PE coatings to enhance initial attachment, strength of attachment and biofilm density. However, further optimisation and research into modifying substrates for maximised growth was needed. The remaining chapters address these objectives.

Chapter 4

Cost-effective methods to improve regrowth between harvests

Abstract

C1 was imaged via environmental scanning electron microscope (ESEM) and characterised using atomic force microscopy (AFM) and confocal laser scanning microscopy (CLSM). Harvesting growth results showed inconsistencies, thus surfaces were etched manually to help inoculate algae cells for the following growth period. Tests carried out in lab-scale ALGADISK photobioreactors also showed a similar issue of inconsistent regrowth. Comprehensive growth studies were undertaken in order to investigate the effects of surface roughness induced by sandpapering. Surface roughness (Ra) was quantified using DekTak surface profiler. Results indicated that while initial attachment and strength of attachment was not affected by surface roughness, long-term growth showed a strong positive correlation.

4.1 Introduction

The surfaces selected (PETG C1 & PETG C3) based on results presented in chapter 3 have relatively smooth surfaces with minimal surface roughness. The substrates physical properties, in particular degree of roughness has been associated with increased number of attached cells in previous studies.

Ulva zoospore settlement have been shown to depend on a variety of factors, from biological to topographic features (Callow & Callow, 2000). Surface roughness and topography can be significantly influential for the attachment of different organisms (Fletcher & Callow, 1992). Hassan and others (2012) found increasing the degree of roughness increased the number of algal strands attached onto coupons. They also found increasing the shear flow reduced attachment. Cui and others (2013) used texturised solid surfaces and found that algal cells preferred surfaces that had feature sizes closer to the algal cells dimensions. Larger or smaller features had in fact reduced attachment. An alternative study investigated spore settlement on polydimethylsiloxane elastomer (PDMSE) which consisted of microtopographic structures at a range of 1.5 – 20 mm intervals. Results showed spores preferred valleys, with a large portion settled in an angle against the base of pillars (Callow et al., 2002). It is thought that rough surfaces provide protection from hydrodynamic actions (Vadas et al., 1990).

Granhag and others investigated the adhesion of *Ulva linza* on Plexiglas (medical grade PMMA) with differing surface topographies made from impressed plankton nets (Rz: 25 – 100 mm). The strongest adhesion was found on the the smallest topographic structure (Rz: 25 mm). Furthermore it was found zoospores that found in depressions were less likely to be removed compared to ridges (Granhag et al., 2007).

However an alternative study found the substrates topography had a non-significant effect on periphyton biomass but algae were sensitive to micro-topographical changes (Lima de Souza & Ferragut, 2012).

This chapter therefore investigates the effects of surface roughness and texture on initial attachment, strength of attachment, biofilm density and re-growth after harvesting. Labscale ALGADISK reactor results are also presented, in which problem-solving/optimising methods were based on.

4.2 Methodology

4.2.1 Algae culture and growth studies

Cell culture conditions, adhesion assays, cell viability tests and long term growth studies were carried out in the same fashion as detailed in sections 3.2.1 and 3.2.2 respectively.

4.2.2 Substrate preparation and PE deposition

Polypropylene meshes (PPM) with 100 um and 200 um aperture diameters were purchased from Industrial Netting Inc, USA.

Substrates were cleaned with 70% ethanol. Dip coated substrates (DC) were prepared and coated in the same fashion as described in section 3.2.6.

4.2.3 Surface characterization using microscopy

Confocal laser scanning microscope (CLSM) (LSM510 Meta, Zeiss) and atomic force microscopy (AFM) were used to analyse the surface topography of the coated substrates. Environmental scanning electron microscopy (ESEM) (LX30, FEI) was used to examine the coatings structure. Energy-dispersive X-ray spectroscopy (EDX) was used for elemental analysis of PETG with C1 after harvesting.

4.2.4 Dektak surface profiler

Dektak stylus profiler (Dektak³ST, Veeco) was used to measure surface roughness (Ra) and film thickness. Force selected: 30 mg. Scan length: 2000um. Film thickness was obtained using step measurements by comparing uncoated regions to coated regions.

4.2.5 Surface roughness studies

PETG substrates were cleaned with ethanol (70%) before roughening of the surface. Grit blasted (GB) surface was carried out using a Grit blaster (F1600, Guyson) with a general purpose 120 mesh grit. For Sandpapered (SP) substrates, sandpaper of differing grit sizes were used and rubbed against both sides of the substrate for 3 minutes each. Substrates were then rinsed with water and cleaned again with ethanol. Etched grids were made onto PETG manually via a diamond tip. Lines were etched with equal pressure approximately every 2 mm vertically and horizontally.

4.2.6 Data analysis and Statistics

Pearson's Correlation coefficients were calculated to test correlation. Two tailed Student's t-tests were used to compare contact angles and weighted dry biomass with and without coatings. Values that were $p < 0.05$ were considered significant.

4.3 Results and discussion

4.3.1 Examining use of C1 and C3 in long term growth studies

Durability and longevity are vital requirements of any coating selected to aid in continuous production, remain cost-effective and allow harvesting of algae in any commercial reactor. The ALGADISK system uses an automated harvesting system which utilises suction at the surface with a plastic vacuum head.

Harvesting in this investigation was carried out via manual scraping. The effect of harvesting on the surface and growth of algae was investigated in long term experiments. Table 4.2 shows contact angle measurements of surfaces taken after each harvest. Results generally indicate that the coated substrates still had contact angles of less than 90°. However, it cannot be assumed that the coating still remained on the substrate just because the contact angle still remained low. Other reasons for low observed contact angles could be salt residue, remaining AOM or a resulting conditioning film left on the surface. ESEM images taken after harvesting (Fig.4.3.1) of algae did not reveal the same coating structure as taken prior to inoculation with algae (Fig. 4.3.2 B & C). This may be due to a conditioning layer left on the surface of organic matter and EPS. The uncoated substrates did still have high contact angles when compared to coated substrates but were notably lower after 5 harvests (Table.4.3.2). Coated and uncoated surfaces showed initial growth was lower than subsequent harvested biomass. Figure 4.4.3 shows the average biofilm harvests over 10 harvesting cycles. It was found that the amount of biofilm found on the surface increased slightly in most cases over time (Fig.4.3.3). Barberousse and others proposed that the age of culture had an influence on adhesion strength due to more AOM associated with longer contact time (Barberousse et al. 2006a; Barberousse et al. 2007). Bacterial adhesion studies suggest due to cellular degradation associated with age, weaker adhesion occurs

which stimulates the release of EPS as facilitators of adhesion (Lind et al. 1997; Tsuneda et al. 2003). This agrees with the results presented in Figure 4.3.3, as over time the amount of biomass harvested increased for both uncoated and coated.

Interestingly, C1 revealed distinctive particle features attached to the surface in the ESEM images taken after harvesting (Fig. 4.3.2 B). Further EDX analysis found a high elemental presence of calcium, carbon and oxygen (table 4.3.1). The ESEM image is also reminiscent of SEM micrographs seen in Jada and Jradi's (2006) study of the role of polyelectrolytes in the crystallogenesis of calcium carbonate. They proposed that the role of the polyelectrolyte's they tested (including PAA) was to stabilise high surface energy crystal planes and as a result of the adsorption process, aggregated nanocrystal morphology resulted. This could be a similar phenomenon observed in this study as the media used for *C. sorokiniana* has calcium-containing salts.

Some species of algae have been found to secrete calcium carbonate but are mainly limited to Coralline algae (Guiry, 2007), and so is unlikely that the calcium carbonate nanocrystals observed here are due to *C. sorokiniana*. Moreover, the amount of growth after the sixth harvest (when CaCO_3 was first observed) was still comparable to the first 6 harvesting cycles (Fig.4.3.3). Endolithic algae are able to solubilise calcium carbonate as a carbon source and have also been found to photosynthesize within the crystals themselves. *C. sorokiniana* is an endolithic species, and so could explain why the calcium carbonate nanocrystals observed on the surfaces did not affect growth negatively (Horath & Bachofen, 2009). The biomass harvested between each cycle was inconsistent and this could be due to the harvesting method. As harvesting was conducted by manual scraping, the amount of algae left on the surface to stimulate biofilm for the next period varied greatly. This was also found to be the case in the

ALGADISK lab scale experiments conducted in WU using a polycarbonate disk coated at Cranfield University (refer to Fig.4.3.4 B).

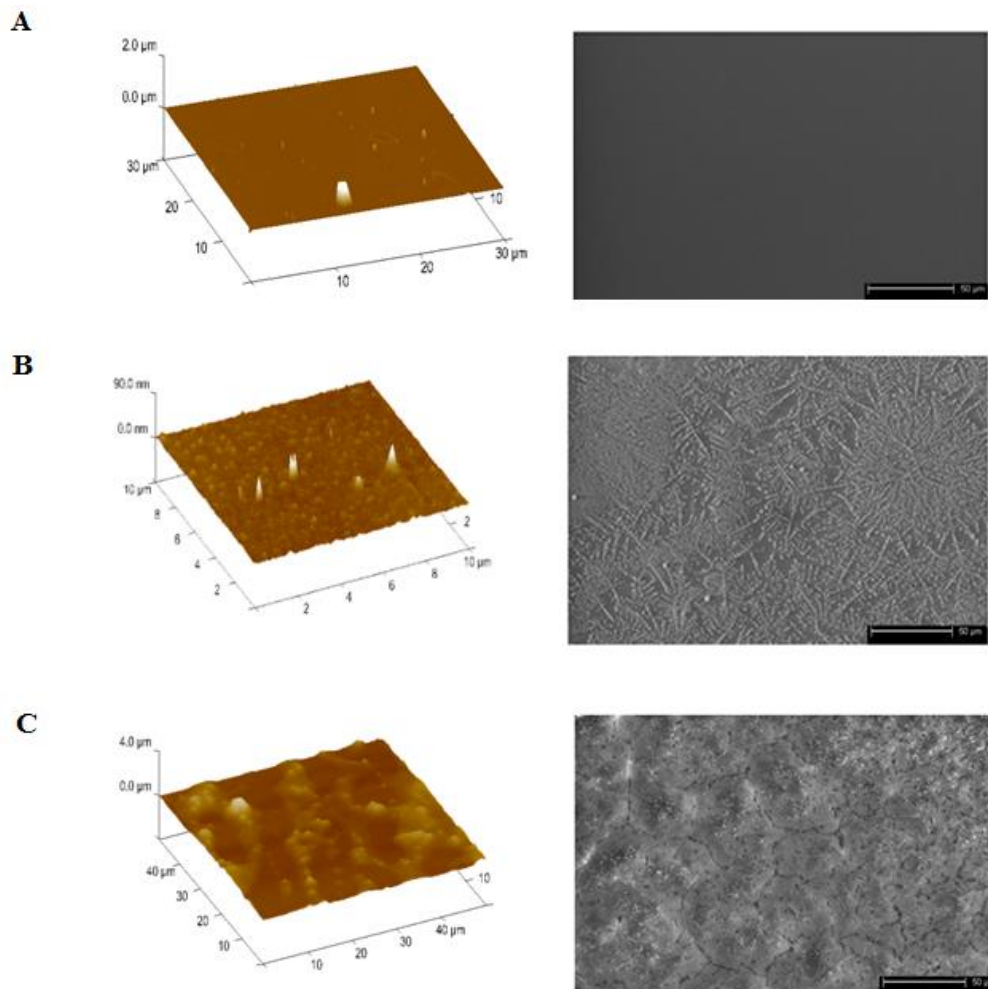


Figure 4.3.1. AFM (left) and ESEM images (right). (A) PETG C0. (B) PETG C1 (C) PETG C3.

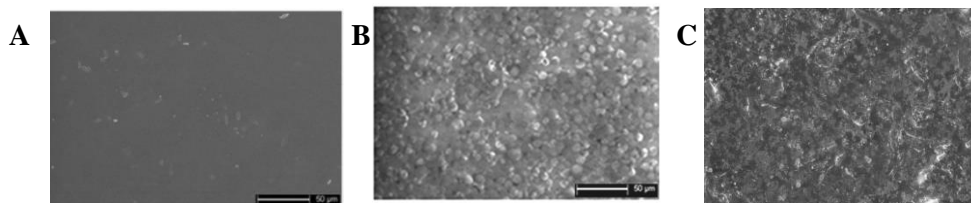


Figure 4.3.2. ESEM images taken after harvest 6 (A) PETG C0. (B) PETG C1 (C) PETG C3.

Table 4.3.1: Elemental analysis of C1 PETG after harvest 6 via EDX.

	Apparent Concentration	k Ratio	Wt%	Wt% Sigma	Atomic %
C	18.94	0.18938	37.55	0.43	50.57
O	16.2	0.0545	39.63	0.47	40.07
Na	0.16	0.00068	0.21	0.07	0.15
Mg	0.22	0.00145	0.3	0.05	0.2
Cl	0.31	0.00273	0.31	0.04	0.14
Ca	22.62	0.20208	22.01	0.24	8.88
Total			100		100

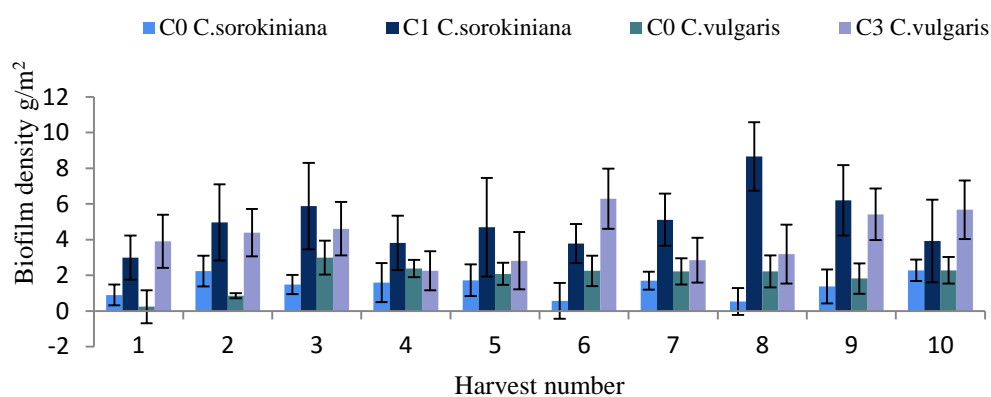


Figure 4.3.3: Harvest growth results. Harvesting took place every 7 days for up to 10 harvests for *C. sorokiniana* and *C. vulgaris*. Error bars represent standard deviation of the mean (n=3).

Table 4.3.2: Contact angle (°) measurements taken before and after harvesting.

	C0	C1	C3
Before harvest	83±2.1	46 ±1.3	38 ±2.5
After harvest 10	64±6.6	27 ± 4.5	33 ±7.1

Polycarbonate (PC) disks sent by WU were coated with C1 and tested in WU's lab scale reactor (Fig.4.3.4 A & C). The standard deviation of the average productivities were shown to be high for PC C1 when compared to the steel meshes tested (Fig. 4.3.4B). The inconsistent growth between each harvest was most likely due to the lack of structure PC has. The amount of algae left on the surface after each harvest varied as there were no gaps in the surface to allow algae to remain. The steel mesh tested performed well and was most likely due to it being able to retain algae because of its structure, aiding in rapid re-colonisation. However, due to its high costs it was deemed unsuitable for the aims of the ALGADISK project. It was reported that PC C1 had the fastest initial attachment highlighting its potential (Blanken et al., 2014). Therefore the steel mesh used in this study was characterised so that its dimensions could be mimicked, and a low cost alternative could be introduced. CLSM analysis found the average width of the gaps for steel fine mesh was 76.86 µm and for rough steel mesh to be 162.85 µm. The pore depths were also measured at 78.46 µm and 110.45 µm for fine and rough mesh respectively.

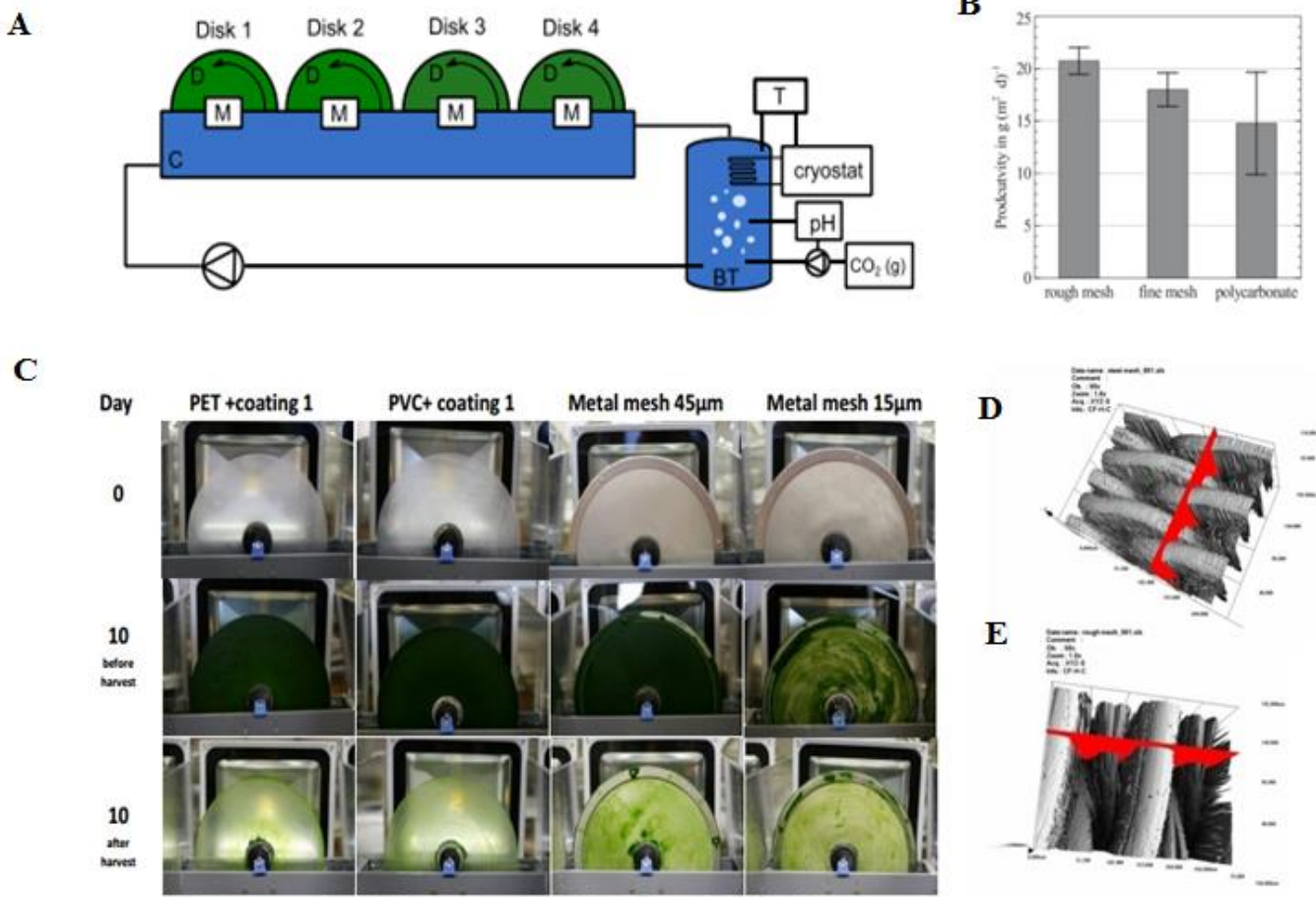


Figure 4.3.4: (A) Schematic representation of the ALGADISK lab scale reactor. D= disk, M= motor, C- container, T= temperature control system, BT= buffer tank. (B) Average productivities of four growth harvest cycles at 11 rpm. Due to technical issues with disk one (PET), productivity results were not presented. (C) Biofilm progression of lab scale experiment before and after harvest on day 10. Error bars represent standard deviation of the mean (n=3). The following surfaces were tested: Rough mesh (45 μm) (steel), fine mesh (15 μm) (steel) and Polycarbonate with coating 1, on *C.sorokiniana*. Error bars show standard deviation of the mean. (Blanken et al. 2014). (D) CLSM characterization of rough and (E) fine steel mesh, both obtained from WU.

4.3.2 Optimizing regrowth on coated substrates between harvests

4.3.2.1 Testing polymer meshes and etched grids

In order to improve on stable regrowth of polymer substrates with C1, different textures and roughness was investigated. Polymer woven meshes were tested with varying aperture sizes in order to emulate the stable productivity and re-growth shown using rough steel mesh. Growth experiments surprisingly revealed very low productivity and regrowth despite having similar dimensions to the steel mesh (Fig. 4.3.5 A i). Upon inspection with an optical microscope, it was revealed that the steel mesh is made up of two layers whereas the plastic meshes are made of one. Having only one layer meant the algae could not be sufficiently harvested as the gaps were too large and had a smaller surface area for algae to adhere to. The layers in the steel mesh facilitated in the entrapment of algae and provided a robust structure for harvesting. Specially manufacturing polymer meshes with layers would incur higher costs which the ALGADISK system aims to reduce. Therefore, other cost-effective avenues were explored in order to improve regrowth.

One method involved etching a grid pattern with a diamond tip into the substrate (Fig.4.3.5 A iii), in order to help trap and leave algae behind in the grooves made. Average productivity taken from 5 harvests from etched grid substrates (EG) were comparable to non- etched substrates, but had lower standard deviations for both algae strains testes and coatings (Fig.4.3.5 B & C). With these promising results, lab scale polyethylene (PE) (diameter: 24 cm) disks received from BAYBIO were etched and coated with C3. They were then tested at BAYBIO with an alternative ALGADISK lab scale reactor (Figure 4.6 D) and tested with an unknown isolated *Chlorella* strain. Results show generally higher productivity, biofilm thickness and lipid production on

C3 PE compared to without C3 (Fig. 4.3.6 A –C). Due to technical failures of the ALGADISK lab scale reactor, evaluation of algae regrowth could not be determined. In addition, etched grids made the automated harvesting procedure difficult as the grooves made would slow down the harvesting head and exhibit friction. Therefore alternative methods to improve regrowth and consistent harvesting was investigated further with sandpapering (SP) and grit blasting.

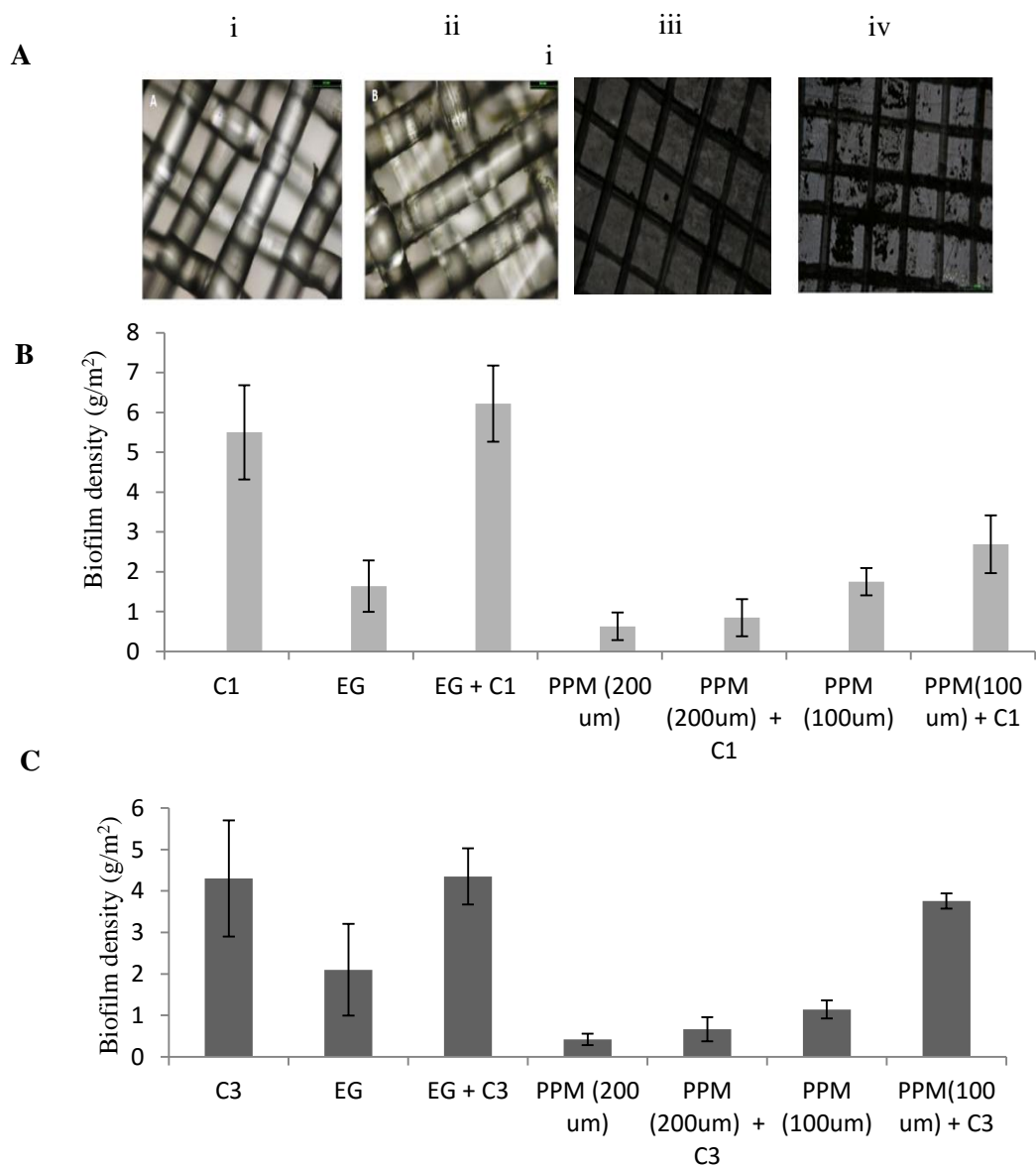


Figure 4.3.5: (A) Optical microscopy images of polypropylene mesh (PPM) with 200 um sized gaps (I & ii) and 100 um sized gaps (iii & iv) Etched grids (EG) before and after harvest (B) Average harvest weight from 5 harvest cycles for *C. sorokiniana*. (C) Average harvest weight from 5 harvest cycles for *C. vulgaris*.

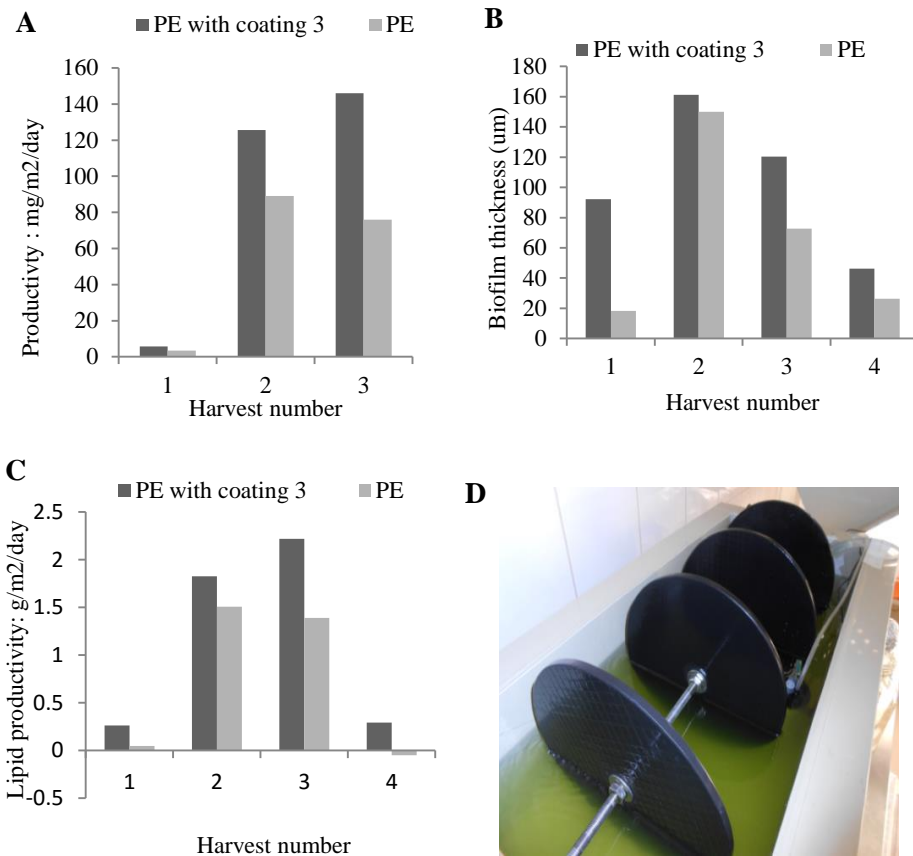


Figure 4.3.6: (A) Dry *Chlorella* strain weight found on polyethylene with and without coating 3. (B) Biofilm thickness (µm). (C) Lipid productivity found on coated and uncoated disk material. (D) Image of lab scale ALGADISK reactor at BAYBIO.

4.3.2.2 Testing sandpapered and grit blasted surfaces

Sandpapering (SP) and grit blasting (GB) substrates were investigated with the main aim of improved regrowth between harvests. SP with grade P90 inferred a Ra value of $2.8 \times 10^5 \text{ \AA}$ with the highest deviation detected at 21.5 \mu m via CLSM. GB had a Ra value of $0.2 \times 10^5 \text{ \AA}$ and the highest deviation detected at 4.75 \mu m via CLSM. Figure 3.12 (A& B) shows for both algae species tested SP surfaces performed better than GB surfaces. The standard deviation of the average biofilm densities of 8 harvest cycles was

the lowest for C1 SP surfaces when compared to the other surfaces tested (refer to Fig.4.3.7 G). CLSM analysis shows GB surface topography consists of small pits rather than scratches and so although can increase surface area, entrapment of algae is not possible (Fig.4.3.7 C). When looking at microscopic images of SP PETG after harvesting, it is apparent that algae are able to remain in the scratches made to help promote rapid re-colonisation in the next growth cycle. Therefore, sandpapering as a cost effective method of increasing biofilm density and consistent regrowth was further investigated to find the optimal degree of surface roughness (Ra).

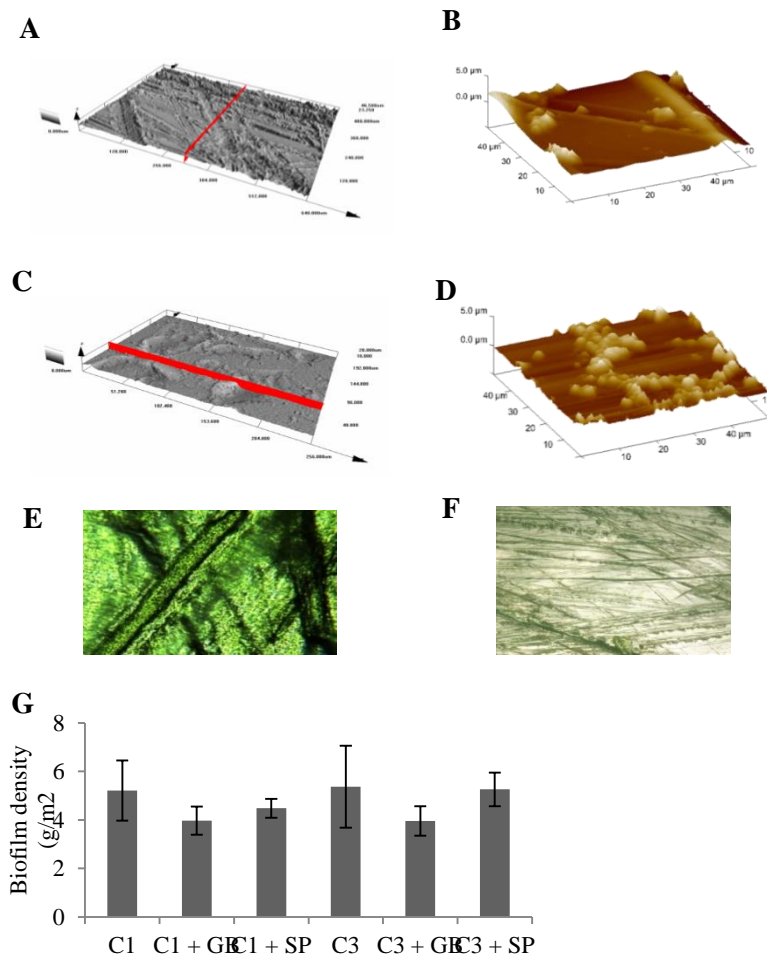


Figure 4.3.7: Topographical analysis using CLSM (A & C) and AFM (B & D). (A & B) PETG Grit blasted. (C & D) PETG sandpapered with grade p90. (E & F) Microscopic images of sandpapered PETG C1 after harvest (Objective: X 20 & X 5 respectively). (G) Average harvested weight for 8 harvest cycles. Harvesting was undertaken every 7 days. Error bars show standard deviation of the mean.

4.3.2.3 Finding optimal degree of surface roughness and its effect on algae attachment

It has been reported that algae growth is more active on rougher surfaces than on flat planar surfaces. This is thought to be due to an increase in surface area and a decrease in shear forces (Characklis et al. 1990; Cao et al. 2009). However, Irving's and others (2011) study concluded surface roughness showed only a small increase in cell density and that species selection was more important.

In order to examine the significance of surface roughness, species selection and optimum Ra value; growth and attachment assays were conducted to test varying degrees of surface roughness.

Figure 4.3.8 displays the effect of surface roughness on initial adhesion (A), strength of adhesion (B) and long term growth (C). Adhesion assays revealed that surface roughness did not strongly affect initial attachment for strains *C. vulgaris* ($r = -0.35$) and *S. obliquus* ($r = -0.22$) and showed very weak correlation for *C. sorokiniana* ($r = 0.69$) (Fig.4.3.8 A). Testing the correlation between surface roughness and strength of adhesion found a correlation coefficient of 0.69 for *C.vulgaris* and no correlation for *C. sorokiniana* ($r = 0.01$) and *S. obliquus* ($r = -0.20$) (Fig.4.3.8 B). This was in contrast to the results presented for long-term growth studies, where surface roughness and average biofilm density for 4 harvest cycles showed strong correlation to increasing Ra values (refer to Fig.4.3.8 C).*C.sorokiniana*, *C.vulgaris* and *S. obliquus* had correlation coefficients of 0.79, 0.92 and 0.72 respectively. In addition, it seemed that surface roughness was also species sensitive, with *C. vulgaris* having the highest correlation for both the adhesion assay testing attachment strength and the long term growth tests. Sandpaper grade p20 had the highest amount of biofilm growth for *C. sorokiniana* and so was selected for future tests.

Surface roughness can therefore aid in increased long term growth and may be due to the topography inferred by sandpapering. The scratches made are able to keep algae cells after the harvesting procedure and therefore aid in better re-colonisation. Understandably, the deeper and wider the scratches made the more algae trapped and kept at the surface for the next growth period.

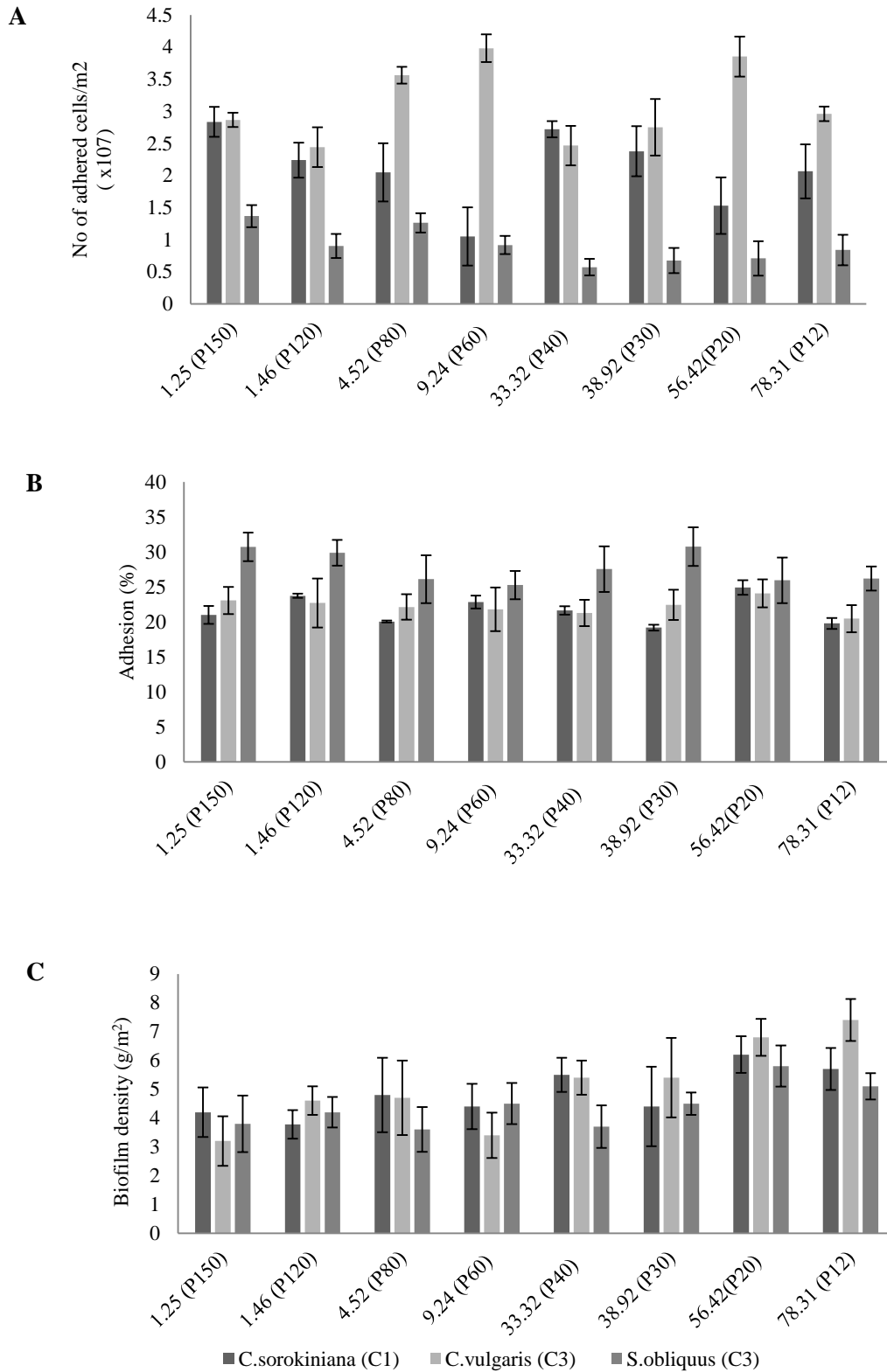


Figure 4.3.8: (A) Number of algal cells measured in initial attachment adhesion test. (B) % of remaining cells measured after wash-out via adhesion assays (C) Average growth results taken for 4 harvest cycles. Harvesting was undertaken every 7 days.

4.3 Conclusions

The following can be concluded after investigating cost-effective methods to increase attachment and improve consistent regrowth.

- Lab scale tests of the ALGADISK reactor showed promising results using C1 and C3 coated disks, but further optimisation on re-growth was needed.
- Roughening PETG with sandpaper was found to be an economical and practical method for improving and enhancing consistent re-growth.
- The effects of surface roughness were species-dependent and the optimum Ra value for each species was found using growth tests.
- Surface roughness did not influence initial adhesion of algae but did however increase re- growth between harvest

Scratches made by sandpaper was sufficient for trapping algae cells after harvesting, and therefore providing seed cells for the next cycle. However, the longevity of the coating was not confirmed. In addition, methods for improving coating adsorption, strength and cost of coating would be beneficial. These methods are investigated in chapter 5.

Chapter 5

Optimisation of coating and application for large scale production for the ALGADISK system

Abstract

The previous method of fabricating polyelectrolyte multilayers (PEM) onto polymer substrates detailed in Chapter 3 and 4 was using a traditional dip coating method. Large-scale production however would prove costly and time-consuming. Issues associated with the Layer-by-Layer (LbL) dip-coating techniques have been addressed previously in research by modifying ionic strength, deposition temperature and concentration of the polyelectrolyte solution. However the method of application in itself is limited and so research into investigating a method appropriate for large-scale production would be most valuable. In order to improve PE adsorption, substrate prepping prior to deposition of PE was investigated. Hydrolysis and plasma etching were compared to the cost-effective method of substrate polarisation via friction. Scratch and wear data revealed hydrolysis provided better C1 strength but did not improve coverage. Therefore alternative methods to improve coating strength were investigated. Photo-cross linking was found to improve coating strength and surface energy. Airbrushing as a method of coating application reduced the amount of polyelectrolyte solution needed and deleted the need for in-between wash steps. The optimum ionic strength for PE solutions was determined via AFM imaging, scratch and wear data, hysteresis values and growth tests. The newly devised method was employed in the ALGADISK pilot-scale prototype.

5.1 Introduction

Polyelectrolyte multilayered coatings have a wide variety of possible applications, from use in electronic devices to the biomedical field where implants are coated (Ladam et al. 2001; Advincula et al. 1999). Most research to date has focused primarily on using substrates that are glass, silicon or quartz and so their use in the biotechnology field is limited (Kostler et al. 2005). Research in this chapter therefore focuses on examining the effect of the underlying substrate, the ionic strength, and different pre-treatment methods on the resulting multilayer formation and cost.

Results shown in Chapter 3 concluded the best performing coating was C1 for *C. sorokiniana* and thus this chapter focuses on optimising C1 production and application for prototype construction. The first large scale prototype was installed in Almazan, Spain at the BFC Biogass Plant in May 2014. The method of coating production and application utilised for the prototype disks was devised using the experimental results presented in this chapter.

The previous method of fabricating polyelectrolyte multilayers onto polymer substrates detailed in Chapter 3 was using a traditional dip coating method. Although this method worked well, the potential for large scale production was limited and alternatives were vital for optimisation. The LbL method has been deemed as time consuming and requires too much repetition for industrial purposes. Methods suggested to counteract these issues include changing the ionic strength, deposition temperature and concentration of the polyelectrolyte solution (Hilal et al. 2015). Commercially feasible approaches are still under investigation but dynamic deposition methods have shown great potential. This method typically uses a cross flow or vacuum unit that controls the movement of polyelectrolytes across the substrate. One layer is often only needed as the performance of the polyelectrolyte is still sufficient (Ba et al. 2010; Baowei et al. 2012).

However, this method would not be suitable for the ALGADISK reactor as it would be economically unviable. UV initiated grafting of polyelectrolytes onto substrates has also been suggested to reduce cost and can be applied to already existing membrane surfaces (Hilal et al. 2015). The number of polyelectrolyte layers as well as the molecular weight used can also make changes to the hydrophilic properties and porosity of the coatings (Meier-Haack et al. 2001).

Plasma etching uses ionised gas which is discharged against the substrates surface, thereby increasing chemical functional groups. Any selected gas in a plasma state contains electrons that can promote graft copolymerisation as well as initiate cleavage of chemical bonds and form macromolecule radicals (Tsuji et al. 2006). Plasma surface treatment is said to offer more stable, uniform and longer-lasting surface energy enhancement (Zia et al. 2015). Andersen and others had illustrated in their study the compatibility of Argon plasma treated substrates and PVP (Anderson et al. 2011). In general, plasma treatment can promote adhesion of a coating and so maybe beneficial in terms of improved absorption and longevity. Due to potential high costs associated with atmospheric plasma, an additional pre-treatment method was also investigated in the present study (Nady et al. 2011).

Substrate hydrolysis with aqueous sodium hydroxide as a pre-treatment step on polymer substrates was also tested. The aim of this pre-treatment step was to promote polyelectrolyte adsorption by providing free carboxylic groups induced by chemical hydrolysis (Chen & McCarthy et al. 1996).

This chapter is concerned with improving on the quality of C1 by modifying the method used in chapter 3. The new method was implemented in the prototype pilot test detailed later in this chapter.

5.2 Materials and methods

5.2.1 Algae culture and growth studies

This chapter focused only on *C. sorokiniana*, which was kept in the same culture conditions as detailed in 3.2.1. Adhesion assays, cell viability tests and long term growth studies were also carried out in the same fashion as detailed in sections 3.2.2, 3.2.3 and 3.2.4 respectively.

5.2.2 Substrate preparation and PE deposition

Substrates were not sandpapered in this chapter in order to examine the coating morphology accurately. Dip coated substrates (DC) were prepared and coated in the same fashion as described in section 3.2.6.

5.2.3 Contact angle measurements, Hysteresis and Surface energy measurements

The static contact angle was measured using the same technique as detailed in section 3.2.7. Hysteresis values were obtained by subtracting advancing contact angle by the receding angle. The advancing angle was measured by gently increasing the volume of the water droplet before the base line begins to advance. The receding angle was obtained by decreasing the droplet size before the baseline starts to recede. Six measurements were taken for each coated substrates at different locations and then averaged (Fig 5.2.1).

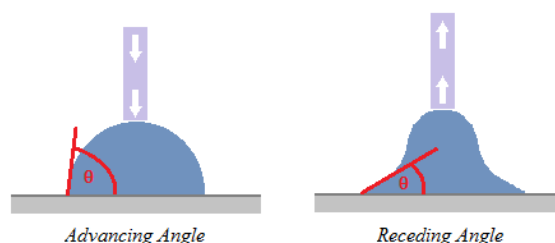


Figure 5.2.1. Diagram showing how advancing and receding contact angles are measured.

Surface energy was obtained using Owens/Wendts theory of surface energy, where by the sum of dispersive and polar energy equates to surface energy (mJ/m^2) (Owens & Wendt., 1969). Diiodomethane was used to determine the dispersive forces and deionised water was used to determine the polar components.

5.2.4 Scratch and wear testing

The Teer ST-3001 was used to assess the mechanical strength, adhesion and wear properties of the coated surfaces. Single scratch test under a progressive load (starting loading 5 N) was used to determine the homogeneity of the coating along the surface of a sample and its strength of attachment. The acoustic emission (dB) emitted when a material undergoes stress as a result of an external force was analysed. This external force was a 5 mm carbide ball which increased its force against the surface from 5 N to 30 N. Therefore, the frequency of acoustic emission fluctuations is an indication of coating uniformity. Any large sudden increase or decrease as the load increases could signify failure in the coating. Generally smooth surfaces with no coating will have a consistent acoustic emission range with minimal fluctuation. Thus also serves as a reference point for surfaces with coatings.

5.2.5 Hydrolysis of PETG

To produce free carboxylic acid groups, substrates were exposed to NaOH (1mol/l) at 60 ° for 1 hour followed by HCL solution (0.1 mol/l) for 10 minutes at room temperature (21 °C). To stop the hydrolysis process, the substrates were then placed in dH_2O for 10 minutes and dried at room temperature. This hydrolysis process is described in more detail in a previous study (Kostler et al. 2005).

5.2.6 Plasma treatment

Polaron Plasma Barrel Etcher was used to apply a conditioning layer of argon (80%) /oxygen (20 %) onto the substrate. Substrates were cleaned with isopropanol beforehand. Surfaces were exposed to plasma etching for 3 minutes (20 V).

5.2.7 Coating application via spraying

The polyelectrolyte solution (polyanion) of choice is placed in the airbrush chamber and then sprayed onto the substrate so that its surface is completely covered. The substrate is then left to either air dry at room temperature or dried with nitrogen. The substrate is then airbrushed with an oppositely charged polyelectrolyte (polycation) followed by drying. This is repeated till the desired number of layers, and outer charge is achieved. Airbrush guns mentioned in this study are as follows: Fine mist - Badger Spray Gun Model 250.4. Medium mist - Metabo Spray gun Model FB 150. Heavy mist - RS spray gun Model 672-071

5.2.8 Ultraviolet (UV) treatment

Photo-cross linking in lab experiments were carried out using a 40 W, 290 nm UVC lamp capable of emitting 5.71×10^{33} /s of photons. Varying time lengths were tested on C1 PETG and a minimum of 120 minutes was needed for maximum benefit. For induced photo-cross linking on large scale disks (area: 1m^2), UV-C 400W Flood Lamp (UV Light technology, UK) capable of emitting 5.71×10^{32} /s of photons was used to illuminate the whole disk. According to lab tests conducted, a total of 12 minutes of exposure times was needed with this UV lamp.

5.2.9 Determining optimal number of AB layers in C1

To determine the optimal number of layers in C1 using the fine mist airbrush gun, 5, 7, 9 and 11 layers were tested and then characterised. The PE deposition method was kept the same as detailed in section 4.2.7.

5.2.10 Determining optimal polymer concentration for AB application

PE deposition solutions were made with varying PE concentrations (0.5 – 2.5 mg/ml) and applied in the same fashion as described in section 4.2.7 with the fine mist airbrush gun.

5.2.11 Determining optimum ionic strength

PE deposition solutions were supplemented with varying concentrations of NaCl (0M – 2M) before being applied onto PETG forming C1 with 9 layers. The effects of differing ionic strengths was tested and characterised.

5.2.12 Disk coating method for ALGADISK prototype

The following method was used for the prototype pilot installed at the BFC biogas plant in Almazan, Spain May 2014. Disks (area: 1 m²) were cleaned with 70% ethanol followed by sandpapering. The fine mist gun was attached to a 196 Twin Cylinder with Air Tank Airbrush Compressor and PE deposition solutions were made at a concentration of 1 mg/ml with distilled water with an ionic strength 1M NaCl. Two airbrush guns were used to apply the alternating PE layers of C1 with a total of 9 layers, followed by UV- C exposure for 12 minutes (UV-C 400W Flood Lamp, UV Light technology, UK). Disks were then rinsed with distilled water before inoculations in the ALGADISK reactor.

5.3 Results and Discussion

5.3.1 Investigating alternative substrate pre-treatments

A significant problem identified previously is that loss of coating and poor repeatability can occur when PVP is weakly bonded to the substrate (Nady et al. 2011; Norhan et al. 2011). To improve and optimise polyelectrolyte absorption, methods to prime the substrates prior to coating were investigated. Chapter 3 involved the pre-treatment step of inducing electrostatic static charge onto the surface via frictional contact with a material containing a different dielectric constant as a pre-treatment step (Cross, 1987; Wildhaber et al. 1996). Prepping the substrate using this method is not a common practice but was investigated due to its low-cost and large-scale potential. Although contact angle measurements and ESEM images provided evidence of successful polyelectrolyte adsorption; coverage was not always consistent (Fig.5.3.2 Ai). Scratch and wear data found that C1 could only resist forces of up to 10 N (Fig.5.3.2 B). Therefore, investigating alternative pre-treatment methods to enhance the strength of PE adsorption could prove beneficial. Atmospheric plasma was investigated along with substrate hydrolysis.

Table 5.3.1 shows contact angles of untreated and pre-treated substrates. The contact angle for both substrates that were treated with plasma or aqueous NaOH had lowered contact angles than substrates that were statically charged with acrylic fibres. This was also the case with resulting contact angles measured after C1 application; proving the nature of the underlying substrate has an influence on coating properties. PETG pretreated with ionised oxygen/argon notably decreased contact angles followed by hydrolysis of PETG. To examine the extent of coating coverage and heterogeneity, hysteresis values were obtained (Fig.5.3.1). Hysteresis is a term used for advancing

(maximal) contact angle, and (minimal) contact angle, of the droplet immediately after being placed onto the surface. Figure 5.3.1 shows the pre-treatment of surface charging experienced slightly higher values of hysteresis than the other pre-treatment steps. This could signify incomplete coating coverage as the hydrophobic nature of the underlying substrate could be exposed. However, a one way ANOVA test revealed no significant difference was apparent for all three treatment steps ($P>0.05$).

Table 5.3.1: Contact angle and surface tension measurements of substrate PET

Substrate treatment	Contact angle with water	Surface energy (mJ/m ²)
Hydrolysatation	53.3 ± 2.5	58.01± 1.3
Hydrolysatation/C1	27.6 ± 1.8	74.61± 1.6
Surface charging	83 ± 2.1	50.3 ± 2.4
Surface charging/C1	46 ± 1.3	69.3 ± 3.1
Plasma etching	46.6± 2.6	43.1 ± 1.3
Plasma etching/ C1	26.8± 3.1	74.2 ± 2.2

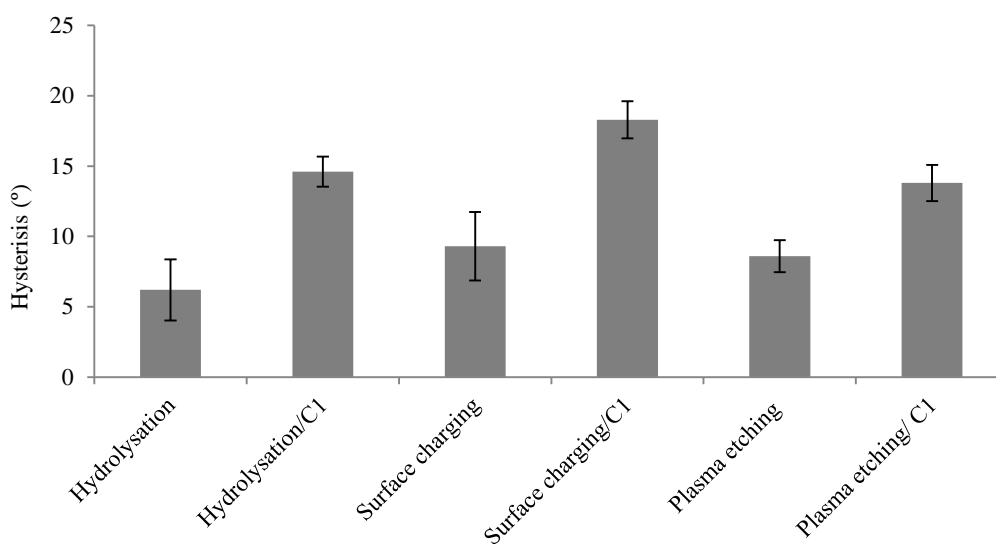


Figure 5.3.1. Hysteresis values calculated for differing pre-treated PETG with and without C1. Error bars represent standard deviation of the mean.

Table 5.3.2: Pretreatment and resulting coating thickness

Pre-treatment	Coating thickness (nm)
Hydrolysis/C1	43.4± 3.2
Surface charging/C1	31.7 ±2.7
Plasma etching/C1	46 ±1.3

ESEM images show differences in coating structures between the different pre-treatments methods, but still all resemble a crystalline layout. It is also apparent that despite the different pre-treatments, full coverage of the substrate was still not achieved (Fig 5.3.2 A).

When examining the effect of the pre-treatments on the strength of coating adhesion via scratch and wear testing, it was confirmed that the hydrolysed substrates had the highest resistant to coating failure (Fig 5.3.2 C). The plasma treated substrates experienced a possible coating failure at 10 N. Statically charged substrates performed similarly with observable failure just above 10 N.

Using these results, it can be said that the pre-treatment of static charging does not provide the optimal conditions for strong PVP binding. Hydrolysis of the substrate prior to coating via NaOH showed overall better adsorption of PVP when looking at ESEM and hysteresis data, followed by atmospheric plasma treatment with Oxygen/Argon.

One-way Anova revealed there was no significant difference between the three pre-treatment methods tested when comparing strength of algae attachment, initial attachment and long-term average growth studies ($p < 0.05$) (refer to Fig.5.3.3).

Static charging of the substrate before coating application does have better potential in large-scale application in terms of ease and costs when compared to hydrolysis and atmospheric plasma. The resulting coating durability is questionable and thus would require further optimisation to confirm long-term use. Exploring alternative avenues to

enhance C1 adsorption and mechanical strength was vital. Therefore, method of coating application and static charging in conjunction with photo-cross-linking was investigated in the following sections.

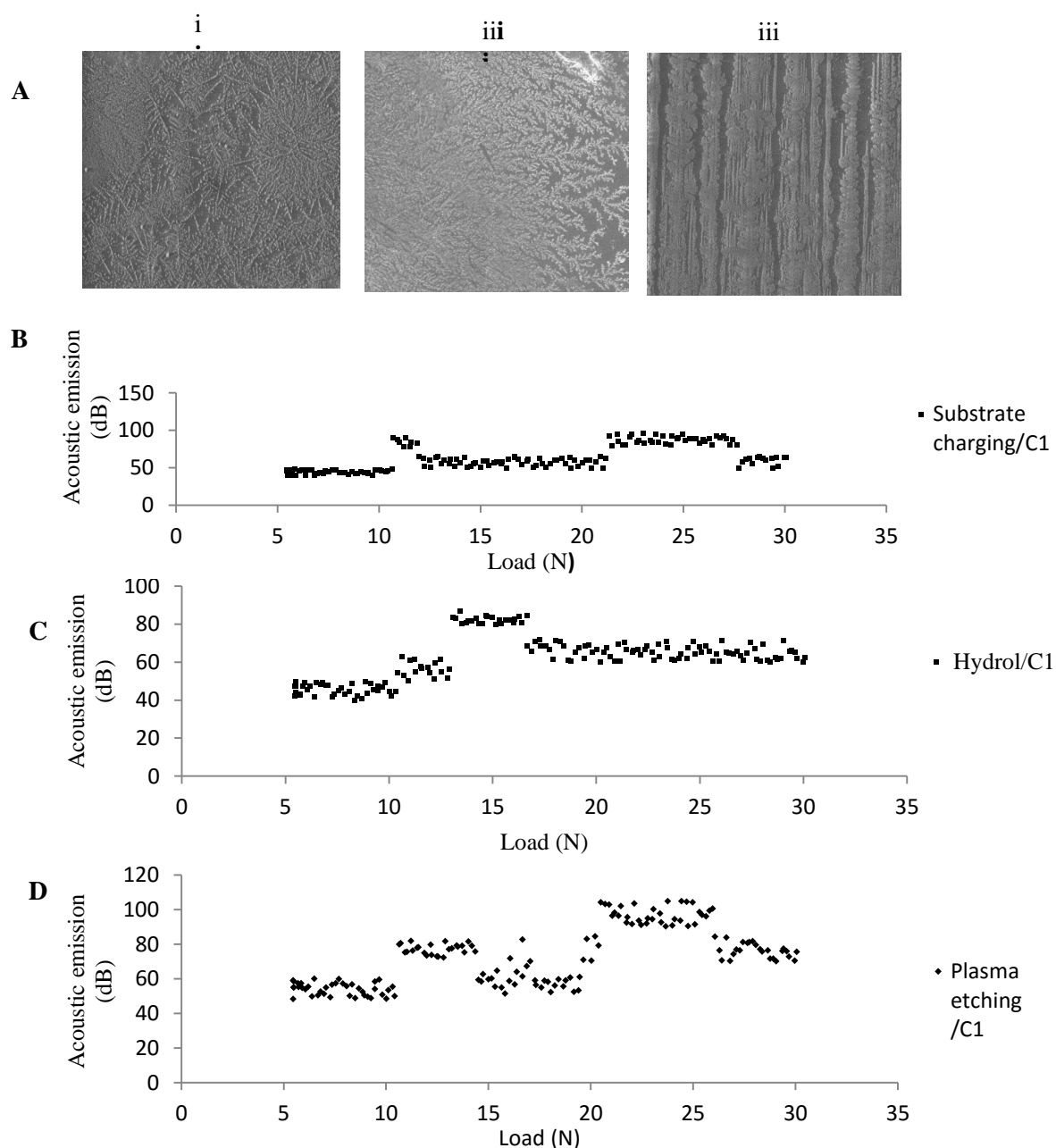


Figure 5.3.2. (A) ESEM images (1000 x) of C1 on different pre-treated substrates. (I) Substrate charging. (II) Hydrolysis. (III) Plasma etching. (B – D) Scratch and wear testing on differently pre-treated substrates followed by C1.

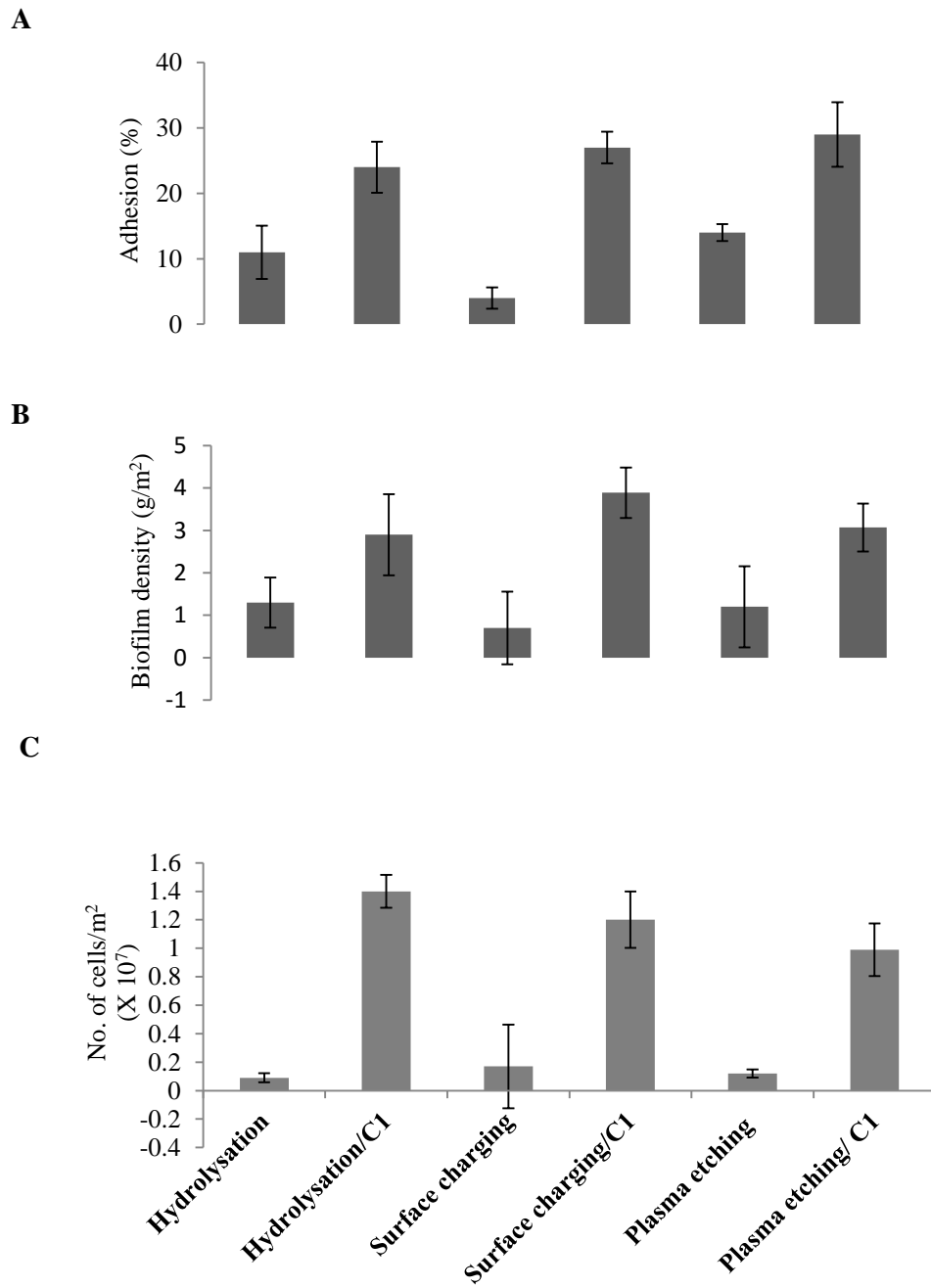


Figure 5.3.3. (A) Adhesion of *C. sorokiniana* found on surfaces with C1 with different pre-treatments after flushing. (B) Number of cells counted after 6 hours of incubation followed by washing. (C) Biofilm density harvested after 7 days. Error bars represent standard deviation of the mean (n=3).

5.3.2 Investigating spraying as method of coating application

A considerable contributing cost factor is the volumes of polyelectrolyte solutions needed for large scale production. The ALGADISK disks for the prototype have an area of 1 m², with multiple disks in 1 unit. This would require large filled containers for dipping resulting in high waste and costs. Manual dip coating in large scale applications would be costly and time strenuous with the multiple washing steps required. The use of automated robotic dip coating would require the purchase and design of very expensive equipment. Therefore, this area required a much needed solution and optimisation to reduce costs without compromising the efficacy of the coating.

Spraying of PE was investigated by Schlenoff and colleagues where they were able to show the fabrication of PEM was up to 40 times faster than dip coating. After two alternative sprayed layers the substrates were rinsed by spraying deionised water. They also found that without the rinsing step the films were thicker (Schlenoff et al. 2000). Airbrushing was consequently investigated, with several air brush guns tested (refer to Fig.5.3.4). The airbrush guns were labelled fine, medium and large mist according to the resulting droplet size seen in ESEM images in Figure 5.3.4.

Figure 5.3.4 A-B showed the deposition of 5 layers via AB did not offer uniform coverage as found in DC substrates (Fig.5.3.3 A). When comparing degree of hysteresis between DC and AB, it was apparent that AB substrates had relatively higher heterogeneity in coating structure and coverage (Fig.5.3.5). This is most likely due the nature of the application method. Rather than forming a monolayer, airbrushing applies in a depositing fashion and does not always cover the surface completely. Therefore AB substrates had higher amount of surface defects which was represented by high hysteresis values.

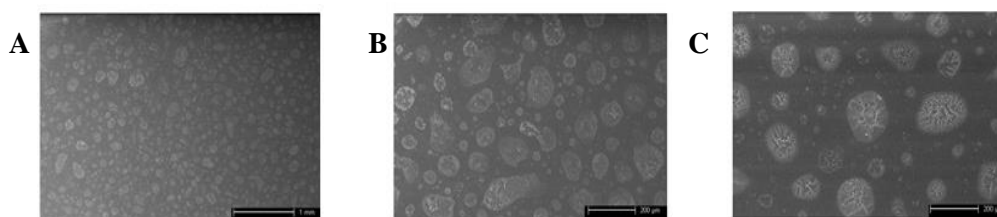


Figure 5.3.4: ESEM images at 1000x taken of substrates PET with AB C1 (A) Fine mist. (B) Medium mist. (C) Large mist.

Table 5.3.3: Contact angle measurements and film thickness of airbrushed and dip coated methods of C1 application

Method of C1 application	Contact angle with water	Film thickness (nm)
<i>Dip coated</i>	46 ± 1.3	31.7 ± 2.7
<i>Airbrushed (fine)</i>	36.5 ± 2.0	46.5 ± 3.3
<i>Airbrushed (medium)</i>	42.4 ± 3.2	39.4 ± 2.2
<i>Airbrushed (heavy)</i>	38.7 ± 1.5	42.6 ± 3.5

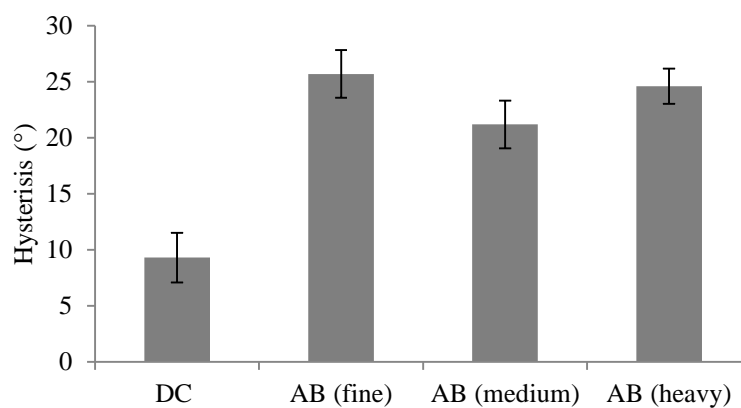


Figure 5.3.5: Hysteresis values calculated for PETG with and without C1. Error bars represent standard deviation of the mean (N =3).

Along with differing CA measurements observed in table 5.3.3, scratch and wear testing found a different profile compared to DC substrates. The acoustic emission varied substantially across the surface, signifying a very heterogeneous uneven topography. An apparent failure was detected at approximately 18 N for the fine mist AB gun used, and the remaining substrates used with the other tested guns had no obvious detected failure (Fig.5.3.6).

The thickness of the C1 measured was higher for AB samples than DC samples (refer to table 5.3.3). This could be due the depositing nature of the AB gun and due to the fact that there was no washing steps introduced in the AB method. The resulting thicker coating could have therefore enhanced the strength of the coating.

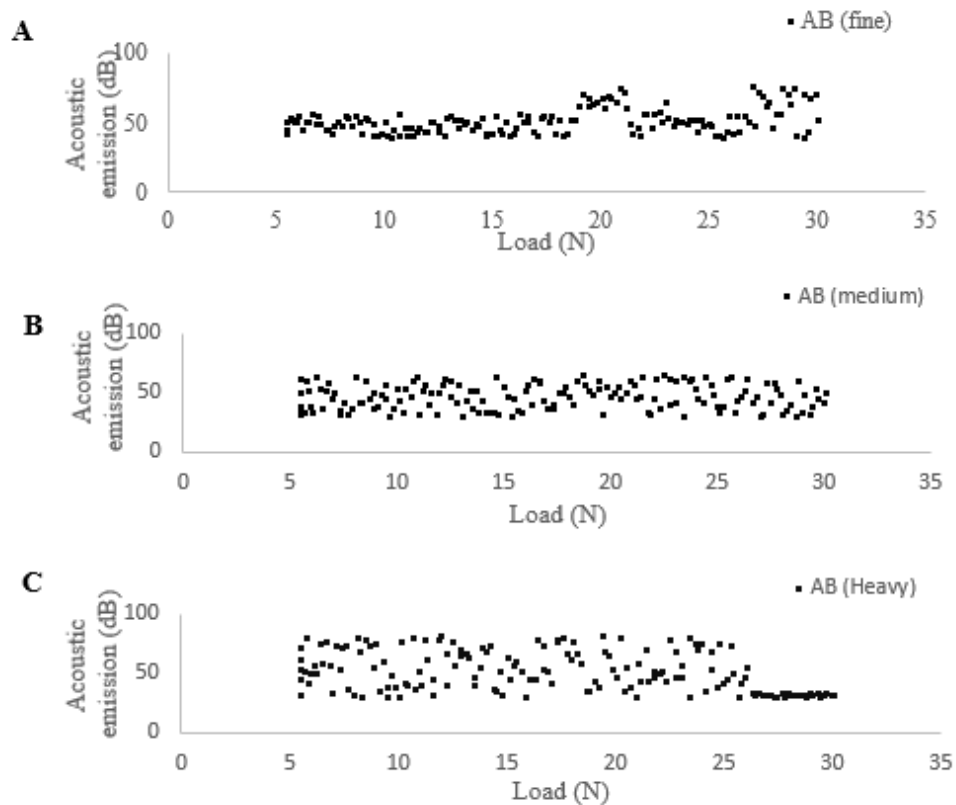


Figure 5.3.6. Comparison of DC and AB methods. (A – C) Scratch and wear testing on different airbrush gun application.

Student-paired T test found the amount of biofilm density weighed after 7 days was not significantly different ($p = 0.46$) between AB and DC samples (Fig.5.3.7 C). The strength of algal adhesion was also not statistically significant between DC and AB surfaces (Fig.5.3.7 B). Initial attachment was still not comparable to DC substrates and was most likely due to the lower coating coverage offered on the substrate (Fig.5.7 A). This is also evident when comparing initial attachment with different airbrush guns themselves. The fine mist airbrush gun had the highest observed algal attachment, which ESEM images (refer to Fig.5.3.4 A) revealed it also offered better substrate C1 coverage.

AB results were comparable to DC and had exhibited better mechanical properties. Using these results the Fine mist airbrush gun was selected for further testing and optimisation. However, further work was needed to improve coating coverage on the substrate and improve coating adhesion to the substrate. Therefore photo-cross linking and increasing the number of layers was investigated in the hopes of improving these properties.

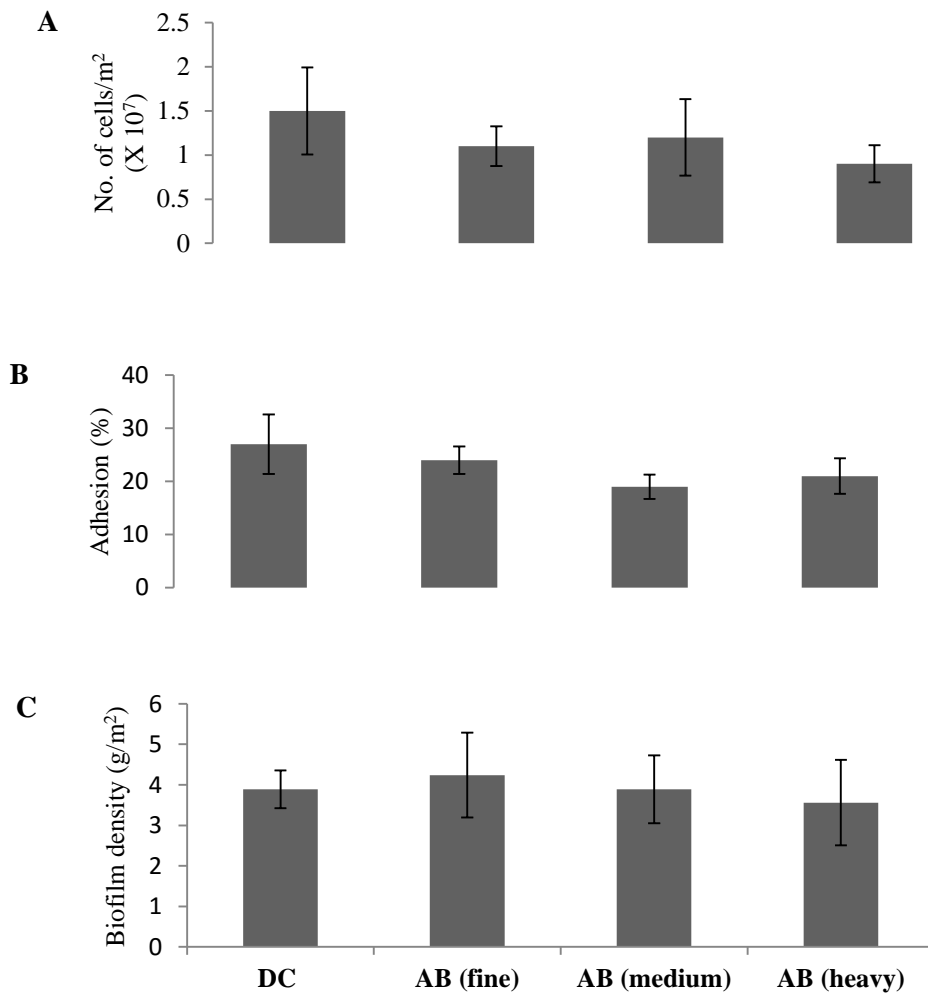


Figure 5.3.7. (A) Number of attached cells counted after incubation with *C. sorokiniana* followed by washing. (B) Adhesion (%) of *C. sorokiniana* found on tested coated surfaces at 72 hrs after flushing. (C) Biofilm density found on tested surfaces. Error bars show standard deviation of the mean (n=3).

5.3.4 Photo-cross linking with Ultraviolet (UV)

UV exposure can form carboxylic groups on the substrate as well as cross link and cleave polymers.

Photochemical grafting of polymers is a common practice and in particular N-vinyl-2-pyrrolidone (NVP) has been reported previously (Pieracci et al. 1999; Luan et al. 2012). Photo-crosslinking with UV light is said to be cost-efficient and can improve substrate properties without adding bulk (Ulbricht, 2006).

Using the pre-treatment of static charging, surfaces were exposed to UV irradiation immediately after coating application. Table 5.3.4 lists contact angle and surface energy (SE) measurements of both airbrushed and dip coated substrates before and after UV exposure. SE measurements can present quantitative analysis, which is beneficial when determining how the underlying substrates and photo-crosslinking can influence the resulting PEM coatings.

SE measurements were increased after UV exposure for both DC and AB substrates. ESEM images show a distinctive mud-flat cracking pattern after UV exposure of 3 hours (Fig.5.3.9 A & B). AFM analysis showed a smoother topographical appearance but ESEM images still showed C1 coverage was still poor with AB surfaces (Fig.5.3.9 C & D).

Contact angle and SE measurements recorded at 20 min intervals, found surface energy increasing for the first 100 minutes and then levelling off for the remaining time (Table.5.3.4). Therefore, 100 minutes would be needed for the minimum amount of induced surface energy enhancement via UV light.

Scratch and wear data revealed increased durability and homogeneity with UV exposure for both DP and AB surfaces (Fig.5.3.10 A & B). This is expected as film rigidity is said to increase due to photo-cross-linking (Vazquez et al. 2009). Hysteresis values did

not significantly change after UV exposure in all cases. This implies that hysteresis is due to the underlying substrate still being exposed. Although UV can strengthen coating adhesion, it cannot however improve coverage of the coating onto the substrate as shown in ESEM images (Fig.5.3.9 A & B).

Vazquez and others showed PE photo-cross-linked onto silica plates actually found an increase in cell proliferation and changed settlement pattern with myoblast cells (Vazquez et al. 2009b). In the present study however, attachment assays found slightly lower initial attachment value on surfaces exposed to UV compared to those that weren't (Fig.5.3.10 C & D). A possible reason for lower strength of attachment and biofilm density (in harvest 1) (Fig.5.3.10 E) could be due to the UV exposure completely sterilising the surface of bacteria. Surfaces developed thus far in this study were only cleaned with ethanol after coating application and before inoculation with algae. It is generally known that although algae biofilms can form in the presence of no bacteria, bacteria are thought to be initial colonisers which help assist algal attachment (Cooksey & Wigglesworth-Cooksey, 1995).

Longer-term growth studies found after harvest 2, growth was very comparable to coated substrates that were not exposed to UV. Therefore, the use of UV irradiation to aid in cross-linking of polymers PVP and PAA onto PETG would be beneficial in terms of improving coating adhesion and strength.

Table 5.3.4: Contact angles and surface energy measurements of surfaces exposed to UVC.

UV C exposure time	Contact angle with water (deg.)	Surface free energy (mJ/m ²)
0	39 ±2.3	72.5± 1.1
20	38 ±1.7	75.3± 2.5
40	36 ±3.4	75.1± 1.5
60	37 ±2.1	76.6± 1.6
80	35 ±3.1	78.9± 1.1
100	36 ±2.2	79.7± 0.8
120	34 ±3.7	79.4± 1.8
140	36 ±3.3	79.5± 1.5
160	36 ±2.6	79.9± 2.1
180	35 ±1.1	78.2± 1.7
200	37 ±3.1	78.9± 1.8
220	35 ±1.6	79.2± 0.9
240	35 ±2.5	78.9± 1.5

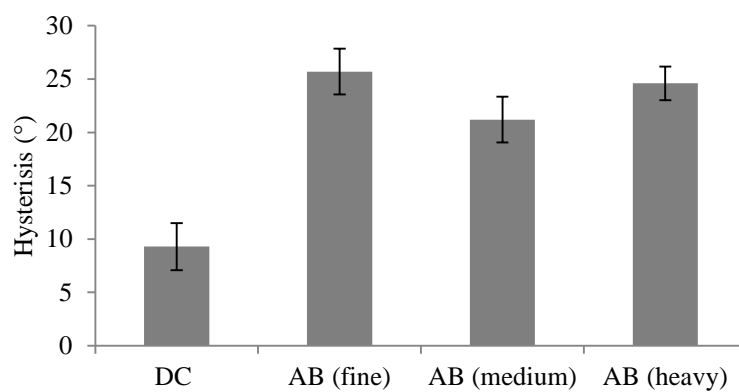


Figure 5.3.8: Hysteresis values calculated for PETG with and without C1. Error bars represent standard deviation of the mean (N =3).

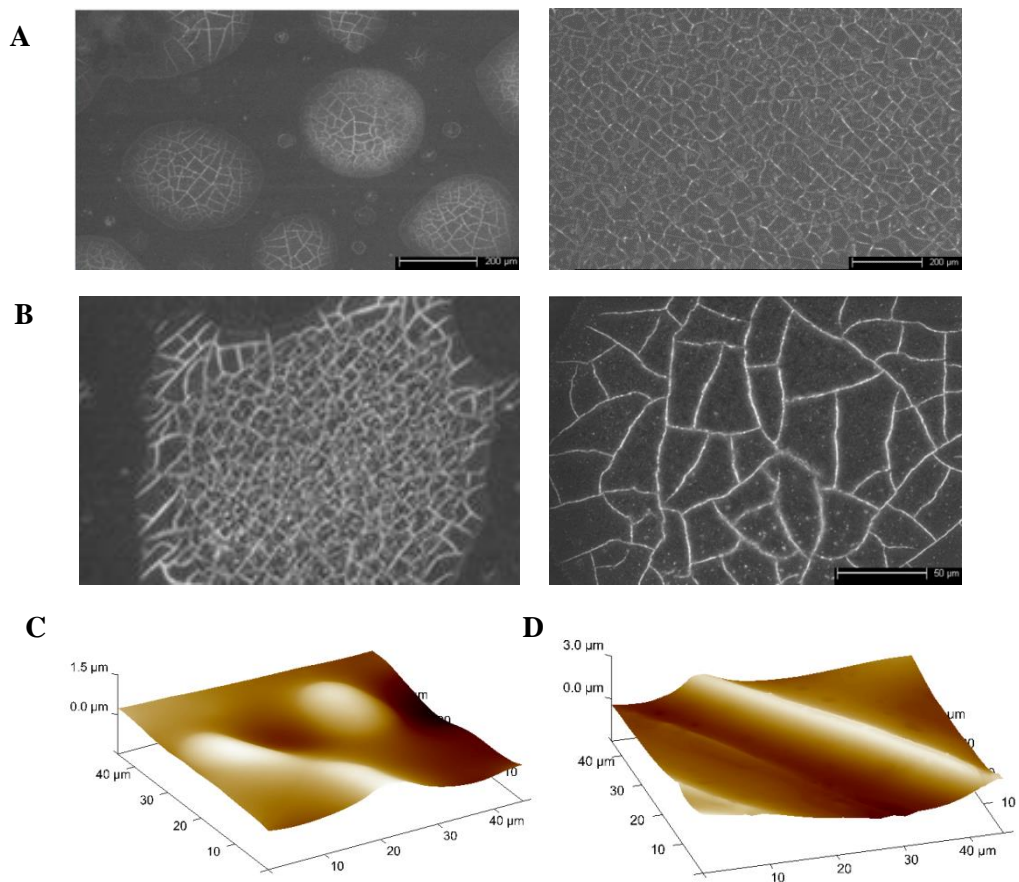


Figure 5.3.9: (A&B) ESEM images at 100x (right) and 1000x (left) taken of substrate PETG with coating 1 after UV exposure. (A) AB PETG C1. (B) DC PETG C1. (C) AFM 3D analysis of AB fine mist (5 layers) of C1 after UV exposure. ((D) AFM 3D analysis of DC of C1(5 layers) UV exposure. UV exposure: 3hours.

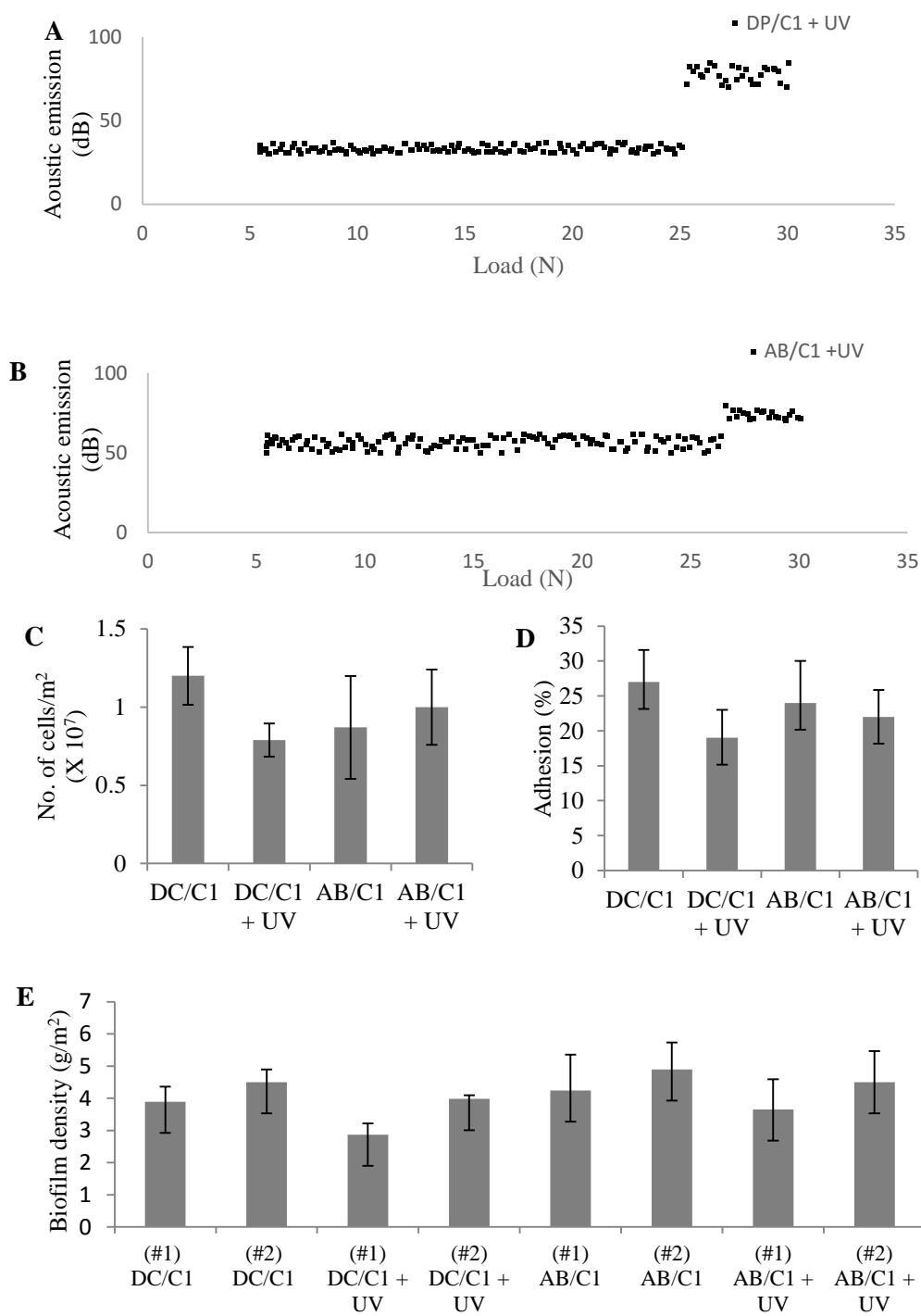


Figure 5.3.10 (A & B) Scratch and wear testing comparing the effect of UV exposure on strength of coating (C) Number of attached cells counted after incubation with *C. sorokiniana* followed by washing. (D) % adhesion found on tested coated surfaces. (E) Biofilm density found on tested surfaces. *C. sorokiniana* algae used. Error bars show standard deviation of the mean (n=3).

5.3.5 Determining optimal polymer concentration

Optimising C1 would require investigating the optimum concentration of polyelectrolyte solutes. Increasing polymer concentration increased resulting film thickness via AB application slightly (Table 5.3.5). Increasing PE concentration did not result in a significant decrease in CA measurements or hysteresis values (Table 5.3.5 & Fig.5.3.11). Scratch and wear data did however show greater heterogeneity and was most likely due to a higher amount of polymer being deposited onto the substrate resulting in further uneven topography (Fig.5.3.13).

When comparing initial attachment assays, it was apparent that C1, with the highest amount of polymer concentration (2 mg/ml), found only a slightly higher proportion of algal attachment. Overall PE concentration did not have a positive correlation on biofilm density ($r = -0.9$) or strength of adhesion ($r = 0.05$) (Fig.5.3.12 B & C). However, there was a moderate positive correlation ($r = 0.62$) between PE concentration and initial attachment (Fig.5.3.12 A). Cell viability assays conducted found no toxic effect of increasing polymer concentrations in C1 (Fig.5.3.12 D).

Table 5.3.5: Contact angle and coating thickness measurements of C1 with different PE concentrations.

<i>Polymer concentration (mg ml⁻¹)</i>	<i>Contact angle with water (°)</i>	<i>Film thickness (nm)</i>
0.5	38.3 ± 1.8	42.8 ± 2.8
1	36.5 ± 2.0	46.5 ± 3.3
1.5	34.6 ± 3.5	56.1 ± 43
2	33.3 ± 2.6	67.2 ± 54
2.5	31.4 ± 3.4	71.3 ± 37

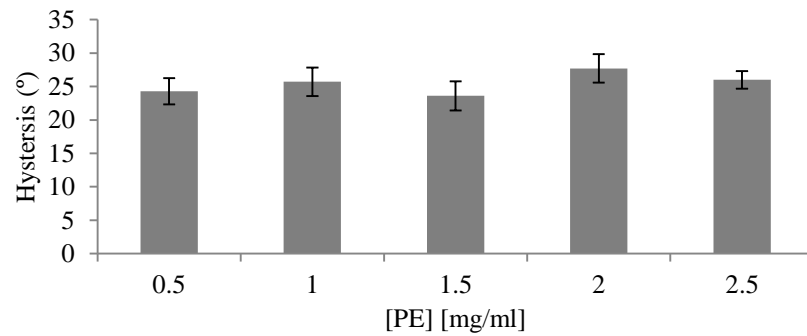


Figure 5.3.11: Hysteresis values calculated for PETG made with varying concentrations of PE in C1. Error bars represent standard deviation of the mean (N =3).

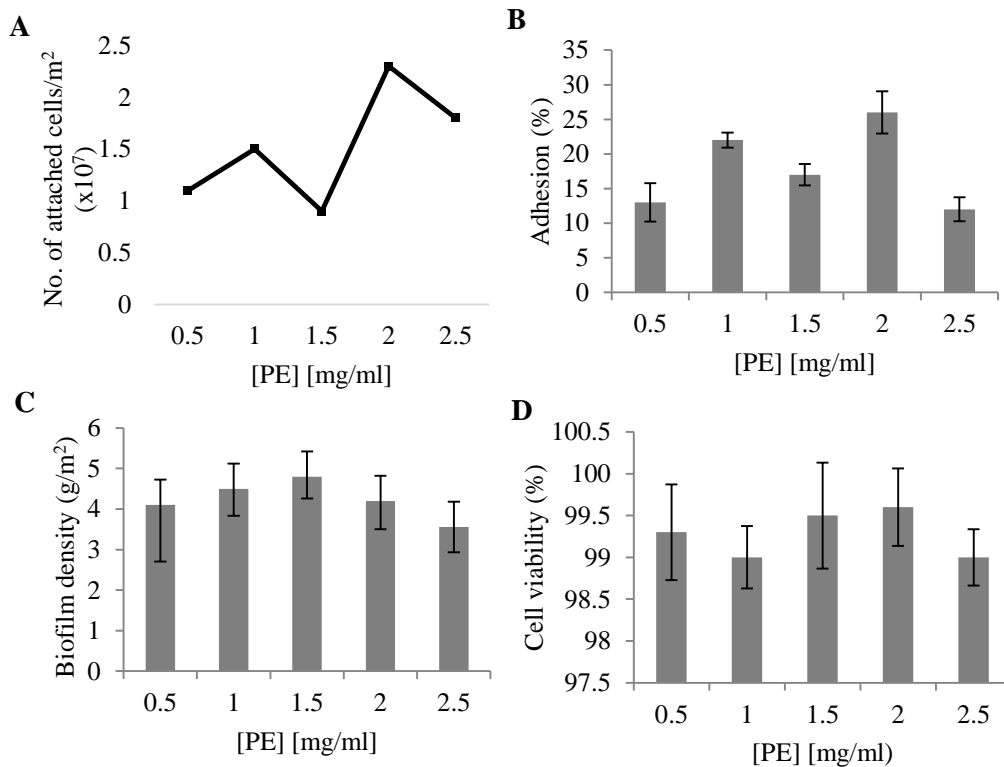


Figure 5.3.12. (A) Number of attached cells counted after incubation with algae followed by washing. (B) Adhesion (%) found on PETG C1 formulated with differing PE concentration after 72 hrs incubation with algae followed by flushing. (B) Biofilm density found on tested surfaces. *C. sorokiniana* algae used. Error bars show standard deviation of the mean (n=3).

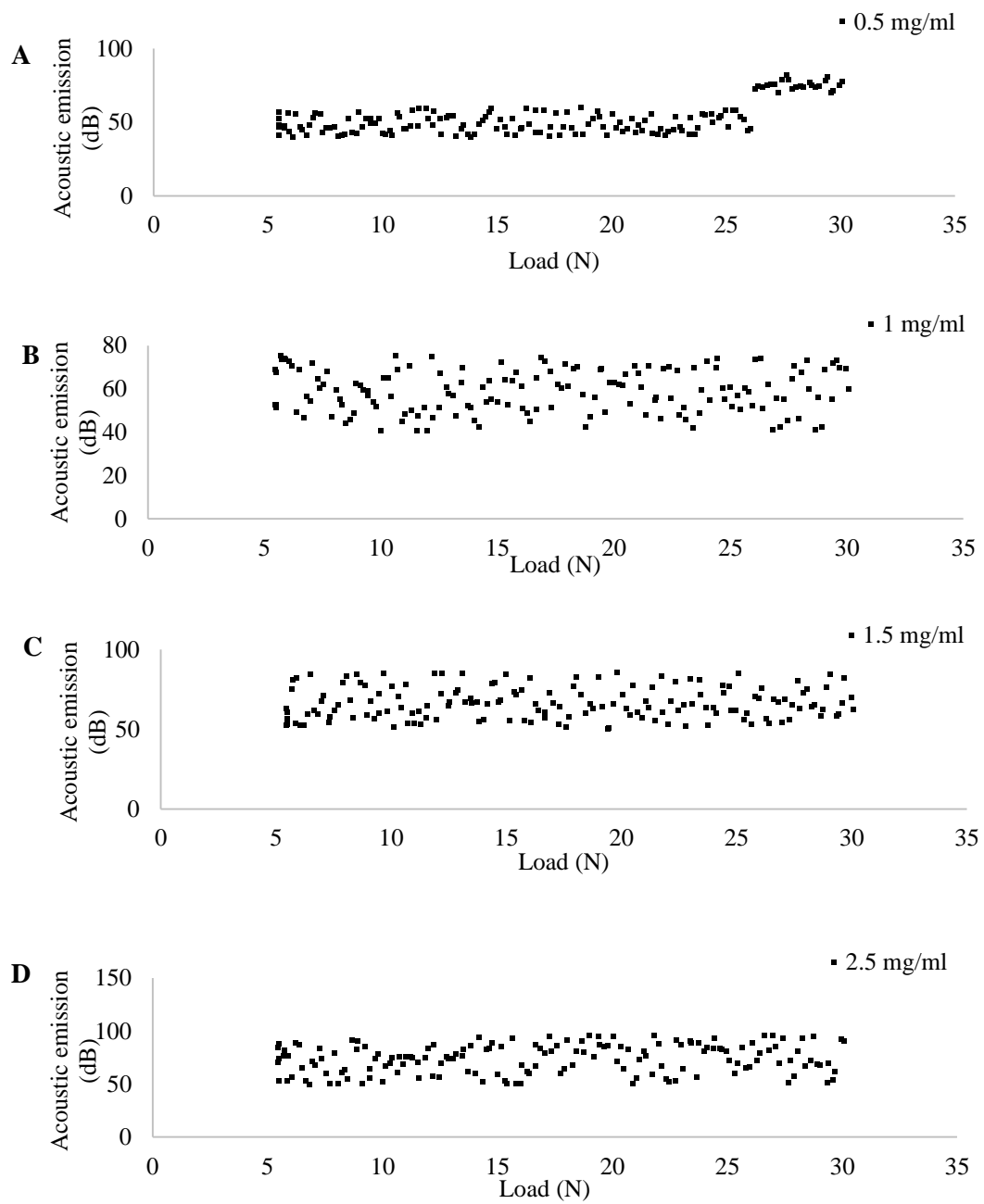


Figure 5.3.13. (A – D) Scratch and wear testing on C1 PETG using different PE concentration (A) 0.5 mg/ml (B) 1.0 mg/ml. (C) 1.5 mg/ml, (D) 2.5 mg/ml.

5.3.6 Determining optimal number of layers

Previous testing with the AB method found poor coating coverage on the substrate, and so was an area that needed to be improved upon. A proposed solution was to apply more layers. Table 5.3.6 shows as the number of layers increase, the CA decreases and film thickness increases as expected.

The degree of hysteresis observed decreased as the number of layers increased (Fig.5.3.16 A). This is in contrast to the observed behavior found in previous research undertaken by others. For example Wang and others stated that as the number of bilayers increased, the amount of hysteresis experienced also increased (Wang et al. 2011). ESEM imaging revealed complete coating coverage after spraying 9 layers and so this decrease in hysteresis could be a reflection of this (Fig.5.3.16 F). As the hydrophobic nature of the underlying substrate is no longer exposed, the heterogeneity of the surface is reduced thereby reducing hysteresis.

Algal adhesion assays conducted found weak correlation between the strength of attachment and number of layers ($r = 0.1$) (Fig.5.3.14 A). Initial attachment tests found a moderate correlation between number of layers and number of cells found on the coated substrate ($r = 0.65$) (Fig.5.3.14 B). There was no correlation between biofilm density measured after 7 days and the number of PE layers ($r = 0.084$) (Fig.5.14 C). Cell viability tests showed no negative influence between number of layers and cell viability of cells attached to the coated surface (Fig.5.3.14 D).

AFM analysis showed a rough and uneven topography which was also reflected in scratch and wear testing (Fig.5.3.16 B).

Scratch and wear data did not confirm whether increasing the number of layers increased the durability of C1 (Fig.5.3.15). Nonetheless, 9 layers was shown to improve coating coverage and initial attachment and so was selected for prototype testing.

Table 5.3.6: Contact angle and film thickness measurements of C1 with differing number of layers

Number of layers	Contact angle with water (°)	Film thickness (nm)
5	39.5 ± 2.0	46.5 ± 3.3
7	32.4 ± 3.2	52.3 ± 2.8
9	34.2 ± 3.5	61.7 ± 4.4
11	33.7 ± 2.6	78.3 ± 3.6

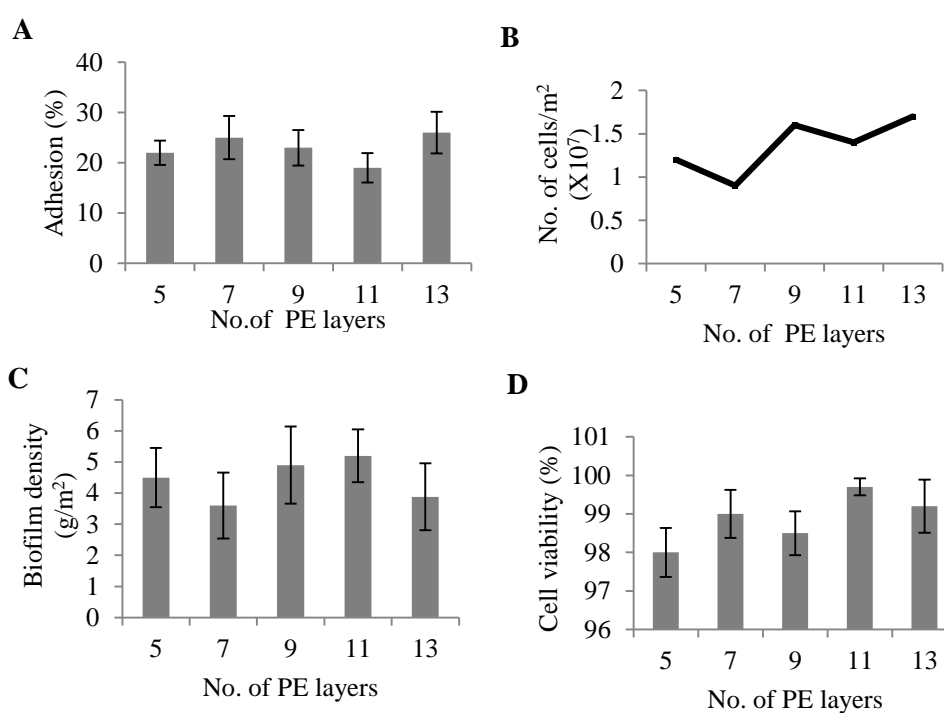


Figure 5.3.14. (A) Adhesion (%) found on C1 PETG with different number of layers. (B) Number of attached cells counted after incubation with algae followed by washing (C) Biofilm density found on tested surfaces. *C. sorokiniana* algae used. Error bars show standard deviation of the mean (n=3).

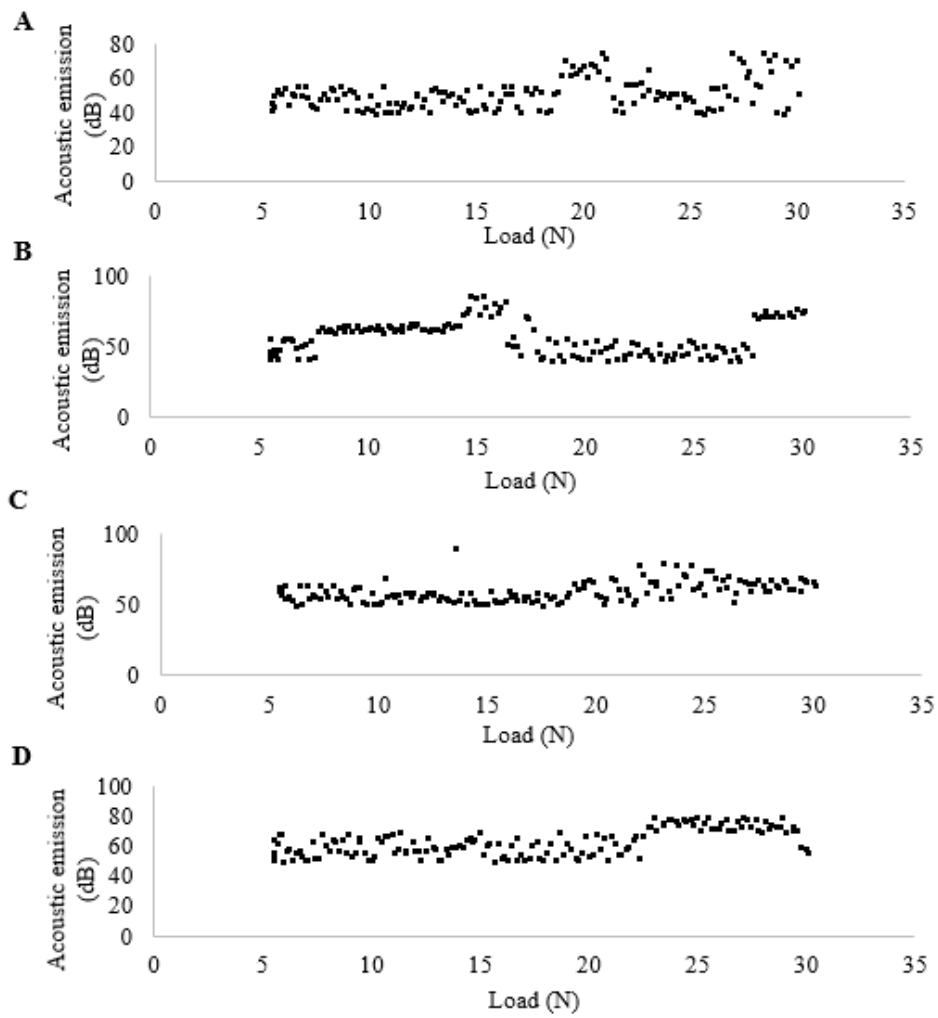


Figure 5.3.15: (A – D) Scratch and wear data investigating effect of number of PE layers on coating strength (PETG C1). (A) 5 layers. (B) 7 layers. (C) 9 layers. (D) 11 layers.

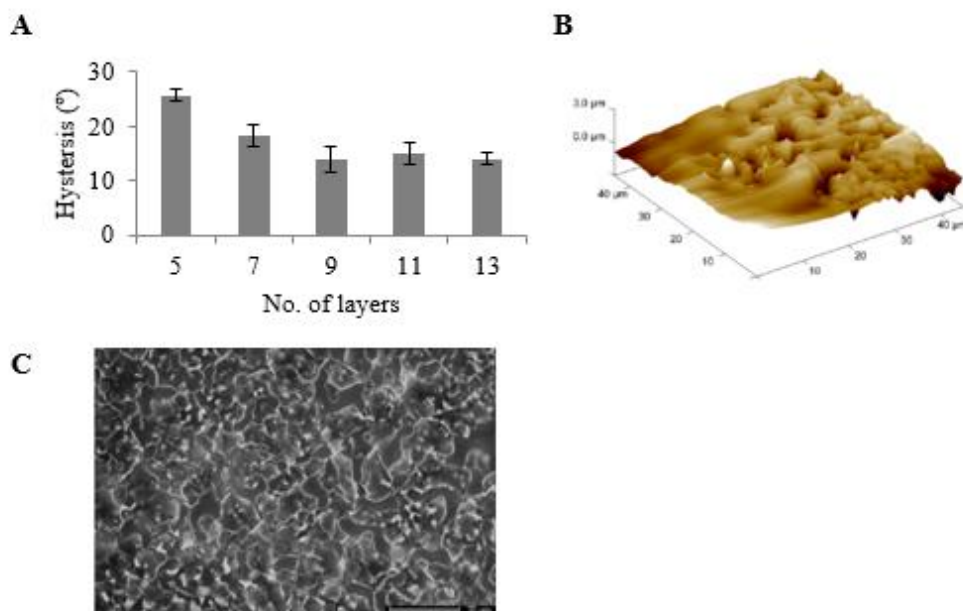


Figure 5.3.16. (A) Hysteresis values observed on different number of PE layers. (B) AFM 3D analysis of 9 layers (C1 PETG). (C) ESEM image (1000 x) of PETG C1 9 layers.

5.3.7 Determining optimum ionic strength

To examine the influence of ionic strength of the PE deposition solution used and its resulting multilayer formations; contact angles, hysteresis values and resulting film thickness were measured. PE solutions were supplemented with varying concentrations of NaCl solution before multilayer fabrications on to substrates were made. Contact angle and film thickness measurements showed increasing salt concentration decreased the contact angle measurements (Table 5.3.7). Previous studies have shown the influence of salt as a growth mechanism due to thicker films resulting from swelling. Swelling occurs as salt ions and water become incorporated into the PEM films. When the ionic strength of the PE solution is higher, the Debye length of an electrical potential is lower, which is thought to be due to the screening effect via salt ions. This screening

effect causes PE to form dense globules due to lower self-repulsion. This coiling therefore causes thicker multilayered films as observed in this study (Ladam et al.1999; Tadmor et al. 2002). Tadmor and others investigated the link between ionic strength and Debye length. They found according to the Debye length (κ^{-1}) equation, the higher the concentration of ions the lower the resulting Debye length (Tadmor et al. 2002).

Debye length equation:

$$\kappa^{-1} = \left(\frac{\epsilon \epsilon_0 k_B T}{\sum_i n_i z_i^2 e^2} \right)^{1/2}$$

where:

- ϵ is the dielectric constant of water
- ϵ_0 is the permittivity of free space
- k_B is the Boltzmann constant
- T is the temperature
- z_i is the valency of ion species
- e is for the electronic charge

Therefore, the behaviour of decreasing contact angles observed here and the increasing film thickness can be explained according to this; as the increase in thickness dilutes the influence of the underlying layers and substrate (Decher, 1997; Lvov et al. 1993; Kostler et al. 2005).

Hysteresis values were the highest for 0M and 2M NaCl concentrations, perhaps signifying surface defects (Wang et al. 2011). Previous research has shown increase in salt content can decrease the amount of surface defects and produce more coherent films (Dubas & Schelenoff, 1999; Wang et al. 2008; Wang et al. 2009). This is reflected when looking at hysteresis values and 3D AFM analysis between 0M and 1M. The degree of hysteresis increased slightly at 2M [NaCl] suggesting an unstable coating (Fig.5.3.18 F) (Wang et al. 2011). AFM analysis showed significant topographical changes with increasing ionic strength of deposition solutions (Fig.5.3.17 A- E). Fery and others

found their PAA/PAH multilayers formed nanopores or vermiculate-like structures which were caused by exposure to water or salt solutions. Zhai and colleagues study produced AFM images of PAA/PAH of PEM films with similar dimpling patterns shown in Fig.5.3.17 D. They found these pores were formed after exposing their heterostructure films to aqueous acidic solutions followed by rinsing with water (Zhai et al. 2004). The changes in morphology induced by ionic strength in the present study is particularly of interest as the method of application was spraying. At 0.1 M [NaCl] the coating structure is uneven and has a high Ra (>1nm) and is in accordance with the nature of the method of AB application used. Airbrushing was found to deposit PEs randomly onto the surface rather than forming a monolayer at each step as with DC. Increasing the salt concentration of the deposition solution showed a smoothing effect after 0.5 M [NaCl] was introduced (Fig.5.3.17 B- E). Reducing roughness is said to be due to the increased mobility of the multilayer (Wang et al. 2011).

Pores started to form at 1M which were not present at 2M [NaCl]. Instead at 2M, less frequent larger micropores were present which also correlated with higher hysteresis values and failures observed in scratch and wear testing. Scratch and wear results showed a very uneven surface at 0.1 M which reduced as the [NaCl] increased. Although higher salt concentrations produced thicker and smoother films, their robustness was not always reflected well in their scratch and wear results (Fig.5.3.18). C1 made with 2 M [NaCl] found coating failure at approximately < 17 N (Fig.5.18 E). The weaker resulting film could be due to the increased PE mobility.

Strength of algae adhesion and biofilm density was the lowest for 0M and 2M [NaCl] and found no correlation (Fig.5.3.17 F & H). Initial attachment however found at 0.1 M and 0.5 M [NaCl] performed the best (Fig.5.3.17 G). Therefore, although the presence of salt in PE solution before deposition is necessary for better PEM film morphology

and algal attachment; the presence of pores induced by high salt levels did not have any advantageous effects on growth. Nonetheless, these nano/micropores have potential applications in other fields such as vapour sensors, monitorable drug delivery systems and tuneable dielectric mirrors (Zhai et al. 2004).

Table 5.3.7: Contact angle and film thickness measurements of C1 made with differing levels of salt

<i>NaCl (M)</i>	<i>Contact angle with water (°)</i>	<i>Film thickness (nm)</i>
0	41.4 ± 1.9	34 ± 1.4
0.1	36.5 ± 2.0	46.5 ± 3.3
0.5	31.2 ± 3.1	103 ± 12.4
1	27.1 ± 2.8	168 ± 16.3
2	22.3 ± 3.2	142 ± 12.2

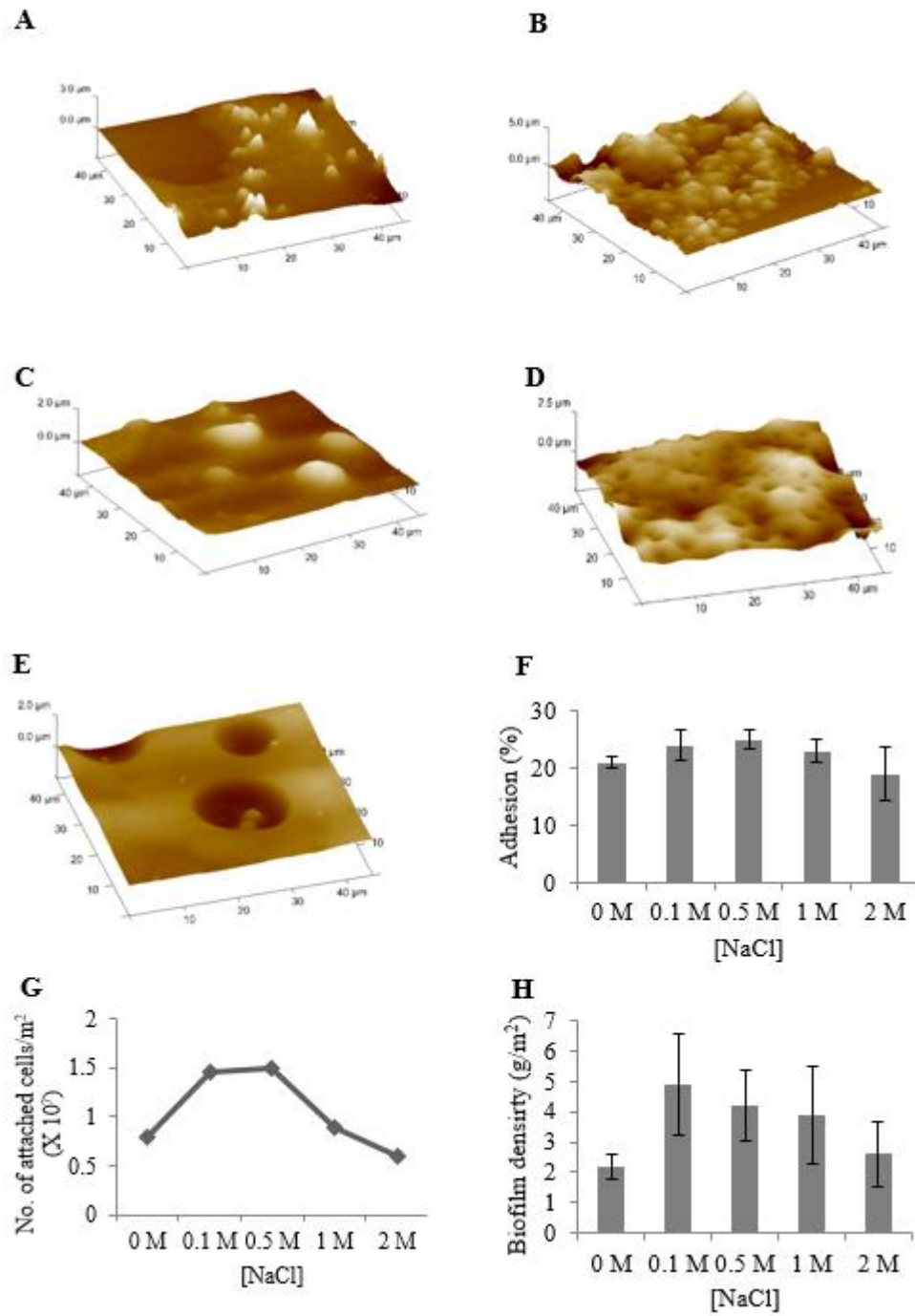


Figure 5.3.17: (A-F) AFM 3D analysis characterising the effect of ionic strength (NaCl conc.) on C1 PETG. (A) 0 M. (B) 0.1 M. (C) 0.5 M. (D) 1 M. (E) 2 M. (F) Adhesion (%) of *C.sorokiniana* (N=3). Error bars show standard deviation of the mean.

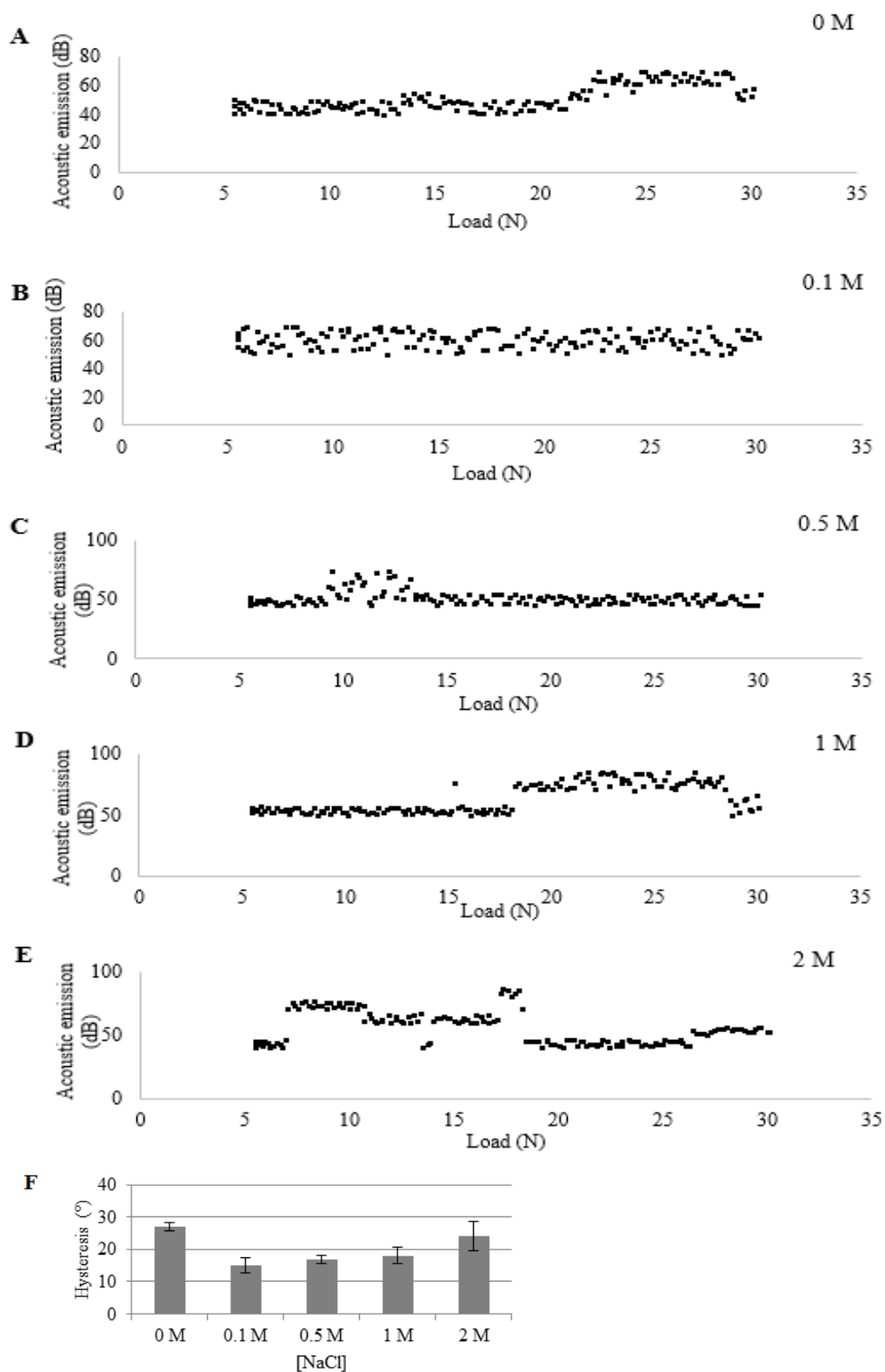


Figure 5.3.18. (A - D) Scratch and wear data investigating effect of ionic strength of PE solution on coating strength (PETG C1). A) 0 M. (B) 0.1 M. (C) 0.5 M. (D) 1 M. (E) 2 M (F) Hysteresis found with varying salt content.

5.3.8 Finalized method for ALGADISK prototype, cost analysis and results

5.3.8.1 Contact angle measurements for on-site characterization

For large scale production of coated disks for the ALGADISK reactor a method for on-site characterisation was proposed. Contact angle (CA) measurements can provide qualitative data to determine polyelectrolyte adsorptions onto substrates. Table 5.3.8 lists the contact angle measurements measured in dry and wet conditions of AB C1 treated with UV. Pre-wetting the surface with algae media M8-a was carried out due to the fact that the coated substrates would be exposed to wetting when in contact with algae in-between harvests. Therefore to examine the effect of this environment on C1, the contact angle along with surface tension measurements were carried out. It was found testing the contact angle with media from dry to wet surface conditions had an apparent influence on its wetting behavior. The CA decreases slightly in all cases when comparing dry surfaces to pre-wetted surfaces (refer to Table.5.3.8). Changes in contact angle measurements were also observed in Kostler and colleagues study, where they observed unusual wetting behavior of PDADMAC. They found when tested with water, the pre-wetted coated substrates had contact angles of up to 10° higher. They proposed the hydrated outer layer of hydrophobic PDADMAC camouflaged the hydrophilic properties of the PSS underneath due to its increase in thickness and slight layer separation (Kostler et al. 2005). C1's outermost layer is PVP, which is hydrophilic and it's beneath layers consist of a less hydrophilic PAA. Therefore, it can be assumed that the strong hydrophobic nature of the PETG substrate and the less hydrophilic PAA was slightly obscured when the coating was observed at a pre-wetted state. These

results can be used as reference data when checking coating adsorptions and life-span on industrial scale reactors with a simple pocket goniometer.

Table 5.3.8: Contact angle measurements taken before and after wetting.

	Contact angle with water (°)
Dry C1/AB/PETG/UV (9 layers)	39 ± 3.1
Pre-wetted C1/AB/PETG/UV (9 layers)	26.6± 2.1

5.2.7.2 Description of coating procedure implemented in the prototype

The scaling up method for coating application was originally to be used with robot dip-coating equipment. However, this method was thought to be potentially very costly and so other methods were explored. Alternatively, using a manual dip coating approach would eradicate the cost of purchasing expensive equipment. This would still require large volumes of polyelectrolyte solutions and a significant amount would end in waste. In addition to this, the previously reported dip coating method itself requires a lot of steps in washing and drying.

Therefore the process of airbrushing was investigated as reported in this chapter. Airbrushing as a method of application was used in the pilot-scale disks (diameter: 1 m). PE solutions were made at a concentration of 1mg/ml with distilled water supplemented with 0.1 M [NaCl] and mixed with a magnetic stirrer. Substrate disks were sandpapered and cleaned with ethanol (70%) before airbrushing on alternating PE layers (9 in total). According the coating application procedure carried out on the pilot, each disk (both sides) required a total of 300 mls of PE solution (£0.12/disk, Sigma Aldrich, UK). This is a large decrease from the amount that would be needed for dip coating disks into large enough containers filled with PE solutions.

A suggested method for on site characterisation was to use a pocket goniometer. The contact angle showing successful coating adsorption onto the substrate is normally within a range of 20– 35 degrees.

5.3.8.2 Summary of results on the performance of the ALGADISK prototype system

The ALGADISK prototype reactor was installed in Almazan, Spain at the Biogas Fuel Cell (BFC) site in May 2012. The prototype consisted of 6 PVC disks (total disk surface area: 15.9 m²) which were coated with C1 and used with mesophilic green microalgae *C. sorokiniana* (CCAP211/8k). PE solutions were made at a concentration of 1mg/ml with distilled water supplemented with 0.1 M [NaCl

The prototype was run until October 2014 with the help of BFC/ALGADISK members. Several technical difficulties occurred affecting the biomass productivity negatively in the first cycle. The productivity of the second cycle improved and was the highest (12 g/m²/day⁻¹ per disk) despite technical difficulties with the CO₂ supply. The automatic harvesting system had no difficulty and was able to harvest 89 g/ L in cycle 2 in total. Using ALGADISK prediction software, it is predicted to increase to 35 g/m²/day⁻¹ without CO₂ limitation. Nevertheless, this field test showed the rapid growth of *C. sorokiniana* when the flue gas was made available and proved to be a good source. It is expected that the biomass concentration will be higher than this when the productivity is enhanced by removing the CO₂ limitation. The prototype will remain at the BFC plant and re-tested again in spring 2015.

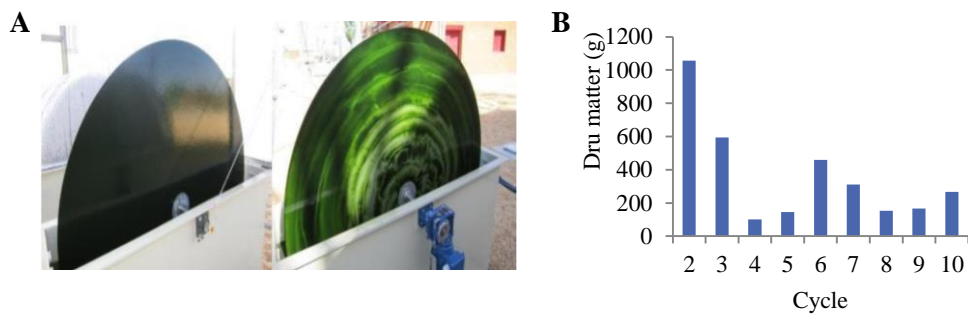


Figure 5.3.19. (A) Image of prototype disk before and after harvest. (B) Prototype reactor growth results for up to 10 harvesting cycles showing total dry matter (g).

5.4 Conclusions

The following can be concluded from the research undertaken in the present chapter on investigating optimal C1 conditions.

- Pre-treatment steps found hydrolysis incurred stronger C1 adhesion on PETG, but did not improve on substrate coverage or algal growth.
- Airbrushing PE layers instead of dip-coating showed large-scale promise and growth results were comparable. However, 5 layers offered poor substrate coverage. Applying 9 layers was later shown to solve this problem.
- Photo-cross linking with UV-C exposure was found to increase coating strength but had lower yield in the first harvest cycle. The second harvest cycle showed growth results were comparable to C1 substrates that weren't exposed to UV-C.
- Varying PE concentrations in PE deposition solutions had little effect on growth results. Varying ionic strength had a far more significant effect on coating morphology and growth results.

- A modified method was proposed for large scale production and used in the pilot test conducted at the biogas plant.
- A method to characterise the coating applied onto disks on site was proposed and reference data was made.

Chapter 6

Influence of physico-chemical properties on algae adhesion and lipid production

Abstract

Electrostatic interactions, van der Waals forces and hydrogen bonds are the three types of binding forces involved in algae attachment and biofilm formation. Physico chemical properties were measured for *C. sorokiniana*, *C. vulgaris*, *S. obliquus* and *S. dimorphus* and 7 different substrates including PETG C1 and PETG C3. Two thermodynamic approaches were tested, the first approach looked at work of attachment and the second looked at change in free energy of adhesion. These thermodynamic approaches were tested in order to examine the potential of the model to successfully predict algae adhesion, and therefore make future substrate selection more efficient.

The degree of successful algae biofilm formation was measured by three aspects; the initial attachment, the strength of attachment and the resulting biofilm density. Results showed both thermodynamic approaches failed to predict algae attachment with good accuracy. There was however an observed correlation between lipid content extracted from the harvested biofilms and the physicochemical properties of the corresponding substrates

6.1 Introduction

Physico-chemical approaches can be used to describe microbial adhesive interactions. The thermodynamic approach uses interfacial free energies to determine favourable and unfavourable adhesion from a free energy point of view (Bos et al.1999). Thermodynamic models have been used in different applications to understand microbial adhesion (Absolom et al. 1983; Katsikogianni & Missirlis, 2004). Recently, Cui and Yuan (2013) used a thermodynamic approach comparing dispersive and polar interaction, and found that their experimental data matched their modeling results. This study illustrates the possible use of thermodynamic models in predicting algae adhesion. The ALGADISK system tested primarily on *C. sorokiniana*, and so to cater to other species of algae the disk material and coating may be limited. In order for the end user to select appropriate disk material according to their selected species of algae, a model which can predict adhesion would be valuable, cost-effective and time saving. Therefore, the first section of this chapter focuses on comparing thermodynamic models with experimental results, in order to evaluate the potential for algae attachment prediction.

Plant and animal oil is commonly used today to produce biodiesel. However, microalgae have higher growth rates and oil content than commonly used energy crops such as corn, palm, Jatropha, soybean, etc. (Felizardo et al. 2006; Chisti, 2007; Barnwal & Sharma, 2005). Focus into commercializing microalgae for biodiesel production has now increased due to the increasing price of petroleum and global warming concerns (Gavrilescu & Chisti, 2005).

Although biodiesel production from algae is feasible, the cost of production needs to be reduced in order to compete with petro-diesel (Knothe et al. 1997; Chisti, 2007; Fukuda et al. 2001).

The lipid yield can be manipulated by introducing environmental stresses such as nitrogen limitation, metal components and phosphate (Sheehan et al. 1998; Illman et al. 2000; Liu et al. 2008; Reitan et al. 1994). It is thought that nitrogen limitation causes lipid synthesis to occur from protein synthesis due to changes of the cellular carbon flux (Sheehan et al. 1998). *Chlorella* strains are commonly chosen as candidates for the purpose of biofuel production due to their fast growth rates. Their lipid contents however are relatively low (14-30%) (Illman et al. 2000). A study using *Chlorella vulgaris* showed limiting nitrogen increases lipid content from 20% to 40 % (Illman et al. 2000). However, this method has resulted in low biomass yields and therefore overall lower lipid productivity (Griffiths & Hille, 2014; Feng et al. 2011). Finding alternative ways to increase lipid production would therefore be most beneficial. Johnson and Wen (2009) found lipid content in their algae was highest on polystyrene compared to their other surfaces tested. This could suggest that the substrate selected could influence algal lipid content. Therefore, this chapter later focuses on examining the influence of physico-chemical properties of algae and substrates on resulting lipid content.

6.2 Methodology

6.1 Algae culture

Algae species mentioned in this chapter have been detailed in section 3.2.1 along with their culture conditions. This chapter includes an additional algae species known as *Scenedesmus dimorphus* (CCAP 276/48), which was grown in the same freshwater conditions detailed in section 3.2.1

6.2 Adhesion assays

Initial attachment assays and strength of adhesion assays were carried out in the same fashion as detailed in section 3.2.2.

6.3 Growth tests

Long term growth studies were also carried out in the same procedure detailed in section 3.2.3.

6.4 Substrates

Details of all substrates used in this chapter can be found in section 3.2.5. Silicone rubber substrates were made via Silicone Sealant, Clear, Waterproof (V tech, UK) applied to glass slides with an even thickness of 3 mm. Steel mesh was also used known as Dutch Weave type 80/700 (GKD Solid Weave, Düren, Germany).

6.5 Measuring physico-chemical properties of algae and substrata

6.5.1 Contact angle measurements

Contact angle measurements of substrates and algae were taken with distilled water, diiodomethane (Sigma Aldrich, UK), and glycerol (Sigma Aldrich, UK) in order to obtain surface interfacial free energies. To obtain contact angles of algae, an even layer of algae was prepared on cellulose acetate membrane filter (pore size: 0.45 μm). The algae mats were left to dry for 1 – 3 h before contact angle measurements were taken (Van Loosdrecht et al. 1987). Attension Theta Tensiometer equipment was used to measure contact angles on both substrates and algae.

6.5.2 Thermodynamic models

Thermodynamic approach I

Two thermodynamic approaches were tested simultaneously in order to provide comparison and insight in to physico-chemical factors that are involved in algae attachment. The first approach investigated was finding the work of attachment ($W_{cs,l}$) (1.1) which is described by equation 1. γ_{cl} is the cell and liquid interfacial free energy, γ_{sl} is the surface and liquid interfacial free energy and γ_{cs} is the interfacial free energy between cell and the surface (Ikada et al. 1984). Good's Equation (1.5-1.7), are used to derive these interfacial free energies. Owens/Wendt theory, states surface free energy comprises of both polar and dispersive forces (1.2 – 1.4) (Owens& Wendt., 1969). The subscript s relates to the solid surface, c is the cell and l is the liquid. Equations 1 – 7 can be combined into equation 8 where work of attachment is expressed.

$$W_{cs,l} = \gamma_{cl} + \gamma_{sl} - \gamma_{cs} \quad (1.1)$$

$$\gamma_s = \gamma_s^d + \gamma_s^p \quad (1.2)$$

$$\gamma_c = \gamma_c^d + \gamma_c^p \quad (1.3)$$

$$\gamma_l = \gamma_l^d + \gamma_l^p \quad (1.4)$$

$$\gamma_{cs} = \gamma_c + \gamma_s - 2(\gamma_c^d \gamma_s^d)^{1/2} - 2(\gamma_c^p \gamma_s^p)^{1/2} \quad (1.5)$$

$$\gamma_{cl} = \gamma_c + \gamma_l - 2(\gamma_c^d \gamma_l^d)^{1/2} - 2(\gamma_c^p \gamma_l^p)^{1/2} \quad (1.6)$$

$$\gamma_{sl} = \gamma_s + \gamma_l - 2(\gamma_s^d \gamma_l^d)^{1/2} - 2(\gamma_s^p \gamma_l^p)^{1/2} \quad (1.7)$$

$$W_{cs,l} = 2(\sqrt{\gamma_c^d} - \sqrt{\gamma_l^d})(\sqrt{\gamma_s^d} - \sqrt{\gamma_l^d}) + 2(\sqrt{\gamma_c^p} - \sqrt{\gamma_l^p})(\sqrt{\gamma_s^p} - \sqrt{\gamma_l^p}) \quad (1.8)$$

Thermodynamic approach II

The second thermodynamic approach tested was looking at the change in total free energy (ΔG_{adh}) between the microorganism, substrate and liquid. γ_{sm} , γ_{sl} and γ_{ml} refer to the solid-microorganism, solid-liquid and microorganism-liquid interfacial free energies and is calculated according to equation 2.1. Lifshitz-van der Waals-acid base (LW-AB) approach is used here to calculate γ_{sl} , γ_{sm} , γ_{ml} . The LW-AB approach consists of van der Waals surface free energy and electron donating and accepting parameters. Equation 2.2 illustrates an example of how γ_{sl} is calculated, γ_{sm} , γ_{ml} is calculated in a similar fashion. Equation 2.3 illustrates that total free energy is the sum of both LW and AB components. Equations 2.4 and 2.5 illustrates how both the LW and AB components of surface free energy were derived.

$$\Delta G_{adh} = \gamma_{ms} - \gamma_{ml} - \gamma_{sl} \quad (2.1)$$

$$\gamma_{sl} = (\sqrt{\gamma_s^{LW}} - \sqrt{\gamma_l^{LW}})^2 + 2(\sqrt{\gamma_s^+ \gamma_s^-} + \sqrt{\gamma_l^+ \gamma_l^-} - \sqrt{\gamma_s^- \gamma_l^+} - \sqrt{\gamma_s^+ \gamma_l^-}) \quad (2.2)$$

$$\gamma = \gamma^{AB} + \gamma^{LW} \quad (2.3)$$

$$\Delta G_{adh}^{AB} = 2(\sqrt{\gamma_m^+} - \sqrt{\gamma_s^+})(\sqrt{\gamma_m^-} - \sqrt{\gamma_s^-}) - 2(\sqrt{\gamma_m^+} - \sqrt{\gamma_l^+})$$
$$(\sqrt{\gamma_m^-} - \sqrt{\gamma_l^-}) - 2(\sqrt{\gamma_s^+} - \sqrt{\gamma_l^+})(\sqrt{\gamma_s^-} - \sqrt{\gamma_l^-}) \quad (2.4)$$

$$\Delta G_{adh}^{LW} = -2(\sqrt{\gamma_m^{LW}} - \sqrt{\gamma_l^{LW}})(\sqrt{\gamma_s^{LW}} - \sqrt{\gamma_l^{LW}}) \quad (2.5)$$

6.5.1 Finding degree of hydrophobicity

The extent of substrate or algae hydrophobicity was calculated using equation 3 where surface tension of the interacting surface (S) and water (W) are used to calculate free

energy of interaction. Values of less than zero are considered hydrophobic, and values above 0 indicate the surface is hydrophilic.

$$\Delta G_{SWS} = -2 \left(\sqrt{\gamma_S^{LW}} - \sqrt{\gamma_W^{LW}} \right)^2 + 4 \left(\sqrt{\gamma_S^+ \gamma_W^-} + \sqrt{\gamma_S^- \gamma_W^+} - \sqrt{\gamma_S^+ \gamma_S^-} - \sqrt{\gamma_W^+ \gamma_W^-} \right) \quad (3)$$

6.9 Lipid extraction

In order to measure lipid content from harvested biofilms, algae samples were dried in the oven for 12 h onto glass-fiber paper (0.45 μ m). Dried biomass samples were then weighed before using a fatty acid extraction kit (Sigma Aldrich). 3 mls of the extraction solvent supplied was added before being vortexed for approx. 3 minutes. 0.5 ml of aqueous buffer was added and vortexed again but for only 30 s. A syringe with a filter already supplied with the kit was then used to filter through the solution allowing total lipid extract to be eluted. The total lipids were then measured gravimetrically by evaporating to dryness by washing with 20 mls of 5% (w/v) NaCl solution.

6.3 Results and discussion

6.3.1. Thermodynamic modeling results

Two thermodynamic approaches were calculated from measured physico-chemical properties of algae and substrates. The first being the work of attachment ($W_{cs,l}$) and the second being total free energy of adhesion (G_{adh}).

Table 6.1 lists the surface tension properties of the liquids used to determine different interfacial free energies. Table 6.3.2 shows the physico-chemical properties measured for four different algae species. Their corresponding hydrophobicity was calculated, and

values above 0 corresponded to hydrophilic surfaces while those below 0 were considered hydrophobic. All algae strains tested were hydrophilic except *S. dimorphus*. Table 6.3.3 includes all the physico-chemical properties of the substrates used in this study. Coated PETG had a lowered LW component when compared to uncoated PETG. In addition to this, hydrophobicity values showed coated surfaces were hydrophilic compared to uncoated substrates that were strongly hydrophobic. Table 6.3.4 summarizes the work of attachment ($W_{cs,l}$) and the free energy of adhesion (ΔG_{Adh}) and their corresponding AB and LW components. AB values below 0 for ΔG_{Adh} signified favourable attachment, whereas above 0 signified unfavorable parameters for attachment. All four algae species had the same order of predictive adhesion, from favourable to least favourable: PC > PETG > Silicone rubber > PP > Steel > PETG + C1 > PETG+ C3. The highest observed ΔG_{adh} value was for *S. dimorphus* with substrate PC, due to both their high hydrophobicity.

Values above 0 $W_{cs,l}$ signify favourable adhesion, and below 0 is deemed unfavourable. All four algae species again followed the same trend when $W_{cs,l}$ was considered, which was: Silicone rubber > PP > PETG > PC > PETG+ C1 > PETG + C3 > steel. The highest observed $W_{cs,l}$ value was for *S. obliquus* with silicone rubber, due to their relative dispersive and polar properties.

Table 6.3.1: Surface tension measurements of liquids (mJ m^{-2}) (Van & Good, 1992)

Liquid	γ_{lv}	γ_{lv}^{LW}	γ_{lv}^{AB}	γ_{lv}^{\oplus}	γ_{lv}^{\ominus}
Water	72.8	21.8	51.0	25.5	25.5
Glycerol	64	34	30	3.92	57.4
Diiodomethane	50.8	50.8	~ 0		

Table 6.3.2: Physico chemical properties of algae

Algae	γ^{LW}	γ_s^{\oplus}	γ_s^{\ominus}	θ_w	Hydrophobicity (mJ m^{-2})
<i>C.sorokiniana</i>	31.2	0.01	55.49	40.2	45.83
<i>C.vulgaris</i>	34.3	0.26	39.03	46.5	55.49
<i>S. obliquus</i>	39.2	0	35.59	50.9	8.27
<i>S. dimorphus</i>	38.1	0.01	20.70	64.1	-12.60

Table 6.3.3: Physico chemical properties of surfaces

Surface	γ^{LW}	γ_s \oplus	γ_s^{\ominus}	θ_w	Hydrophobicity (mJ m^{-2})
PETG	46.01	0.41	1.38	83.41	-77.28
PETG + C1	21.21	0.6	49.79	31.21	33.29
PETG + C3	29	0.31	68.88	34.1	58.39
PC	36.51	1.1	0.10	92.01	-79.52
PP	30.2	0	15.94	75.31	-23.29
Steel	34	0.17	28.41	57	72.34
Silicone rubber	28	0.1	3.06	92	-63.27

Table 6.3.4 Interaction energy between substrate and algae

		<i>C. sorokiniana</i>	<i>C. vulgaris</i>	<i>S. obliquus</i>	<i>S. dimorphus</i>
PETG	ΔG_{AB}	-17.20	-24.63	-31.06	-42.77
	ΔG_{LW}	3.87	-5.02	-6.73	-6.35
	ΔG_{adh}	-13.33	-29.65	-37.79	-49.12
	$W_{cs,l}$	14.76	22.82	26.49	23.15
PETG +C1	ΔG_{AB}	40.38	21.73	28.10	15.59
	ΔG_{LW}	1.31	-1.7	-2.28	-2.15
	ΔG_{adh}	41.69	20.03	25.82	13.44
	$W_{cs,l}$	0.84	4.36	4.56	4.09
PETG + C3	ΔG_{AB}	53.73	40.28	41.05	27.68
	ΔG_{LW}	-0.12	0.15	0.21	0.19
	ΔG_{adh}	53.61	40.43	41.26	27.87
	$W_{cs,l}$	-1.57	-1.77	-2.00	-1.72
PC	ΔG_{AB}	-27.66	-33.40	-40.48	-50.86
	ΔG_{LW}	2.52	-3.36	-4.7	-4.13
	ΔG_{adh}	-25.14	-36.66	-45.18	-54.99
	$W_{cs,l}$	14.50	19.52	22.75	19.48
PP	ΔG_{AB}	13.77	2.50	-1.43	-15.52
	ΔG_{LW}	1.52	-1.96	-2.63	-2.48
	ΔG_{adh}	15.29	0.54	-4.06	-18
	$W_{cs,l}$	24.64	26.95	30.38	26.07
Steel	ΔG_{AB}	25.03	13.65	11.33	-1.86
	ΔG_{LW}	2.13	-2.76	-3.7	-3.49
	ΔG_{adh}	27.16	10.89	7.63	-5.35
	$W_{cs,l}$	-10.92	-5.64	-5.62	-4.44
Silicone rubber	ΔG_{AB}	-9.96	-18.63	-24.66	-37.41
	ΔG_{LW}	1.14	-1.48	-1.98	-1.87
	ΔG_{adh}	-8.82	-20.11	-26.64	-39.28
	$W_{cs,l}$	26.23	27.63	31.01	26.56

6.2.1 Experimental growth results and evaluation of the thermodynamic model

Figure 6.3.1 – 6.3.3 is summarized in table 6.3.5 and compared to the model predictions calculated previously. Both the ΔG_{adh} values and $W_{cs,1}$ did not accurately predict order of favourable adhesion. However, $W_{cs,1}$ values did predict silicone rubber to have the highest adhesion, which was the actual case for *S. dimorphus*. However, the remaining order did not match the experimental results. PETG + C3 preformed the best in initial attachment tests for all 4 algae species. It should be noted that this did not necessarily always correlate with the highest strength of attachment or eventual biofilm density (for e.g. *S. obliquus* & *S. dimorphus*). Therefore, other factors that do not affect initial attachment come into play when determining strength of attachment and biofilm yield. Table 6.3.6 lists the Pearson's correlation coefficients found between ΔG_{adh} , ΔW_d , ΔW_p , $\Delta W_{cs,1}$ and resulting initial attachment (IA), strength of attachment (SA) and biofilm density (BD). For all algae species tested there was actually moderate to strong correlation between ΔG_{adh} and IA, SA and BD. As negative values are seen as favourable, these results indicate the opposite. This is in contrast to many microbial studies, whereby there is an apparent link between ΔG_{adh} and higher adhesion (Ozkan and Berberoglu, 2013).

The case with the approach using $\Delta W_{cs,1}$ also followed a similar trend, whereby high $\Delta W_{cs,1}$ did not correlate with overall better attachment for all algae tested, which again is in contrast to previous literature (Cui & Yuan., 2013).

One possible factor contributing to these results are the unaccounted for physico-chemical properties of PE coated substrates. The thermodynamic models do not account for attractive or repulsive electrostatic attractions. It stands to reason that the electrostatic attraction offered by C1 and C3 was stronger than unfavourable surface energy conditions of the substrate. In addition to this, substrates such as PC, which were

predicted by the ΔG_{adh} model to provide the most favourable attachment conditions, did not perform the best after PETG+C1 and PETG + C3. This could imply that PC provided repulsive electrostatic interactions, which is why it experimentally did not perform according to the ΔG_{adh} model.

Another reason as to why the models did not match the experimental results well could be due to the fact that the models do not consider surface roughness. Steel performed a lot better than either thermodynamic approaches predicted. The steel had a mesh structure and so its surface roughness was high. Previous research has indicated that colonisation can increase as a result of surface roughness due to the protection offered and reduced shear forces (Donlan, 2002). As shown in chapter 4 in the present study, the effects of surface roughness were species-dependent and although did not have a significant effect on initial attachment, it did have influence on long-term biofilm growth.

The $W_{cs,1}$ model did predict silicone rubber to have the highest adhesion correctly for *S. dimorphus*. Interestingly, the $W_{cs,1}$ for this interaction was not the highest observed in comparison to all other algae species tested. However, when looking at their hydrophobicity values, *S. dimorphus* was the only hydrophobic strain tested. This could imply this interaction was mediated by favorable hydrophobic interactions, which were stronger than the electrostatic attraction offered by PETG + C3 or PETG + C1.

Other observations found using the $W_{cs,1}$ approach revealed the role of the ΔWd and ΔWp in attachment. For algae strains tested, there was no correlation between ΔWd and ΔWp components and IA, SA and BD except in the case of *C. sorokiniana*. Table 6.3.6 shows *C. sorokiniana* had a strong positive correlation between strength of attachment and ΔWd ($r = 0.82$) and moderate correlation between ΔWd and biofilm density (0.48). There was also weak positive correlation between initial attachment and ΔWd ($r = 0.24$),

which for all other algae species tested was a negative correlation. This indicates for *C. sorokiniana*, attachment was strongly influenced by attractive dispersive forces.

Despite these results, both thermodynamic models did not predict adhesion with good accuracy. Thermodynamic approaches are based on surface free energies of the substratum, algae and liquid medium. The results presented in this study indicates no strong correlation between contact angles and low surface free energies. Although previous research have shown the opposite trends (Cui & Yuan, 2013; Ozkan and Berberoglu, 2013b; Brady & Singer, 2000; Li et al. 2010), there have been alternative studies that agree with the trends observed in the present study. Finlay and colleagues explained that the non-significant effect of wettability on adhesion could be attributed to the presence of EPS. Research looking at EPS production and attachment on substrata with varying surface tensions determined that EPS production is greatest on substrata with surface tensions above 30 mN m⁻¹. However, adhesion of *Amphora coffeaeformis* on both low polytetrafluoroethylene and high (glass) surface tension substrata was equally strong, although EPS production was much greater on glass compared to PFA. Therefore, on surfaces that are hydrophobic, molecules other than EPS become more important for attachment and biofilm formation (Becker, 1996). Ahimou and others found the concentration of EPS correlated strongly with their membrane-aerated biofilm (R = 0.78). They concluded that along with other environmental factors the polysaccharide fraction of EPS plays a significant role in biofilm cohesion (Ahimou et al. 2007).

Other factors that are not concerned with EPS concentration or composition were explored by Shen and colleagues. They assessed the adhesion of six species of freshwater algae. The species with the greatest adhesion biomass productivity (ABP) *Chlorococcum sp.* was then tested on nine different support materials. The study found

that initial total nitrogen concentration, pH, culture volume and culture period are the most significant factors determining ABP (Shen et al. 2013).

The results presented in the present study and previous literature suggests that interfacial energetics are complex and although heavily influenced by algal species and the chemical composition of the specific substrate; other more determining factors play a vital role in attachment.

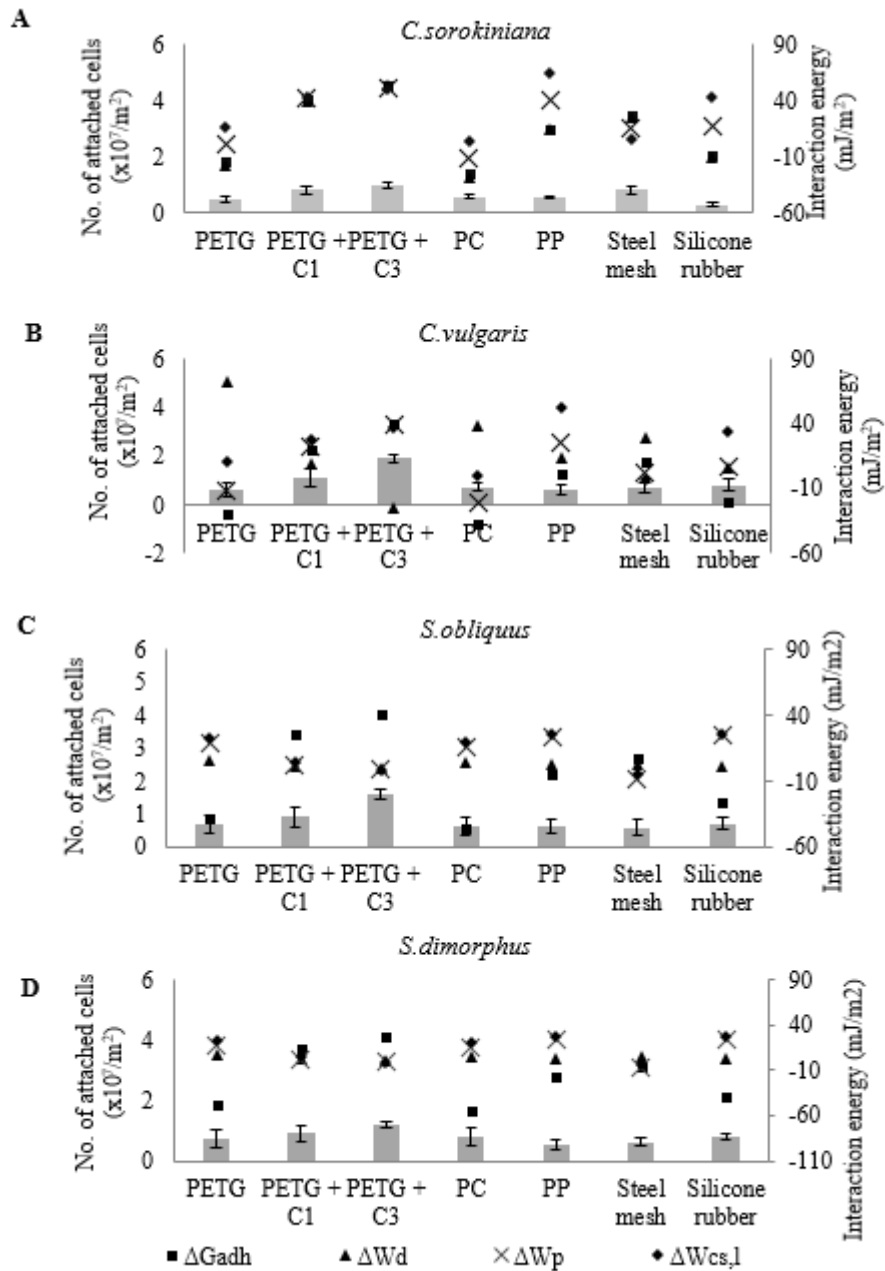


Figure. 6.3.1. Bars show initial attachment of algae after 2h on different surfaces. Error bars show standard deviation of the mean (n=3). ΔG_{adh} is the free energy of adhesion according to AB and LW components. W-d and W-p is the work of attachments due dispersive and polar forces respectively. W is the total work of attachment due to polar and dispersive forces and substrate surface energy.

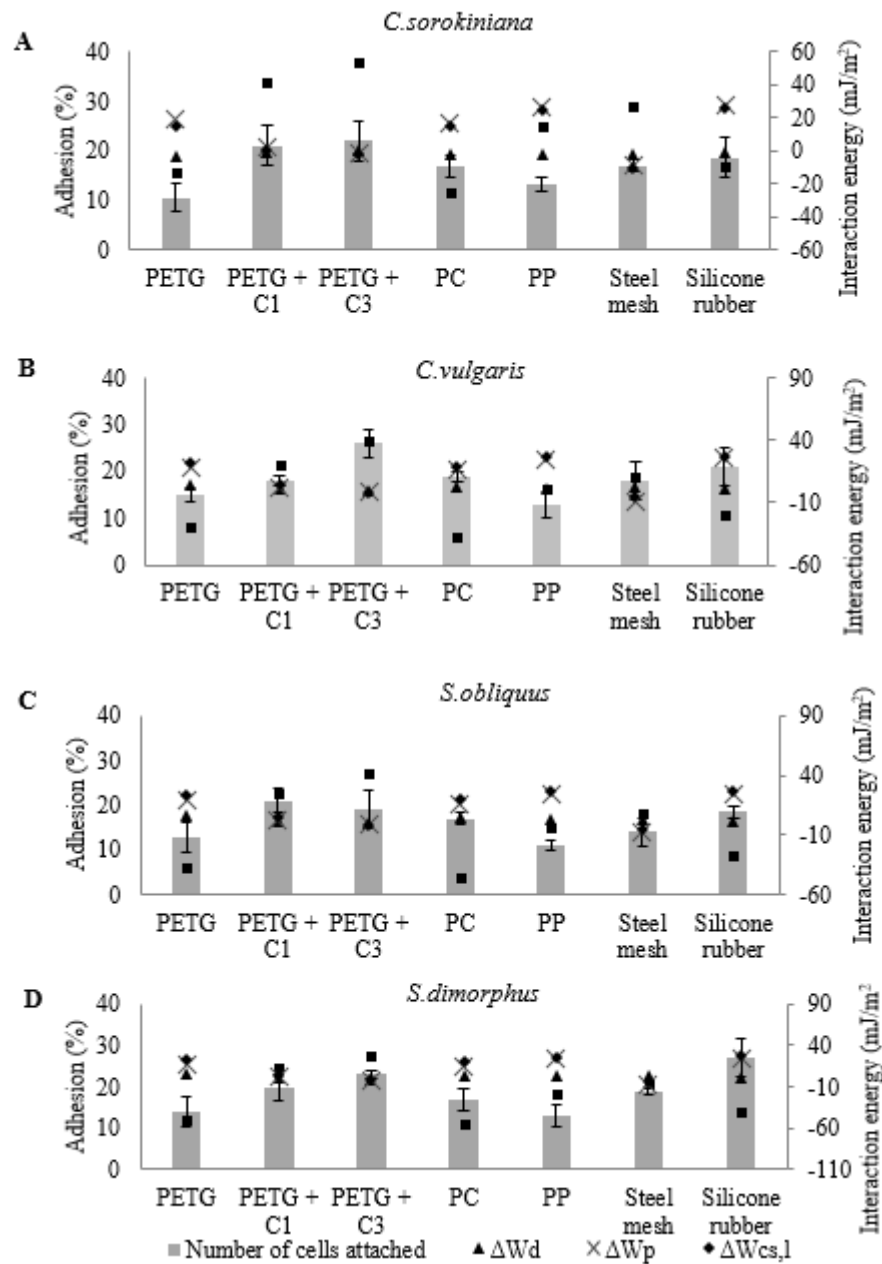


Figure. 6.3.2. Bars show percentage of algal cells after flushing with water on different surfaces. Error bars show standard deviation of the mean (n=3). ΔG_{adh} is the free energy of adhesion according to AB and LW components. ΔW_d and ΔW_p is the work of attachments due dispersive and polar forces respectively. ΔW is the total work of attachment due to polar and dispersive forces and substrate surface energy.

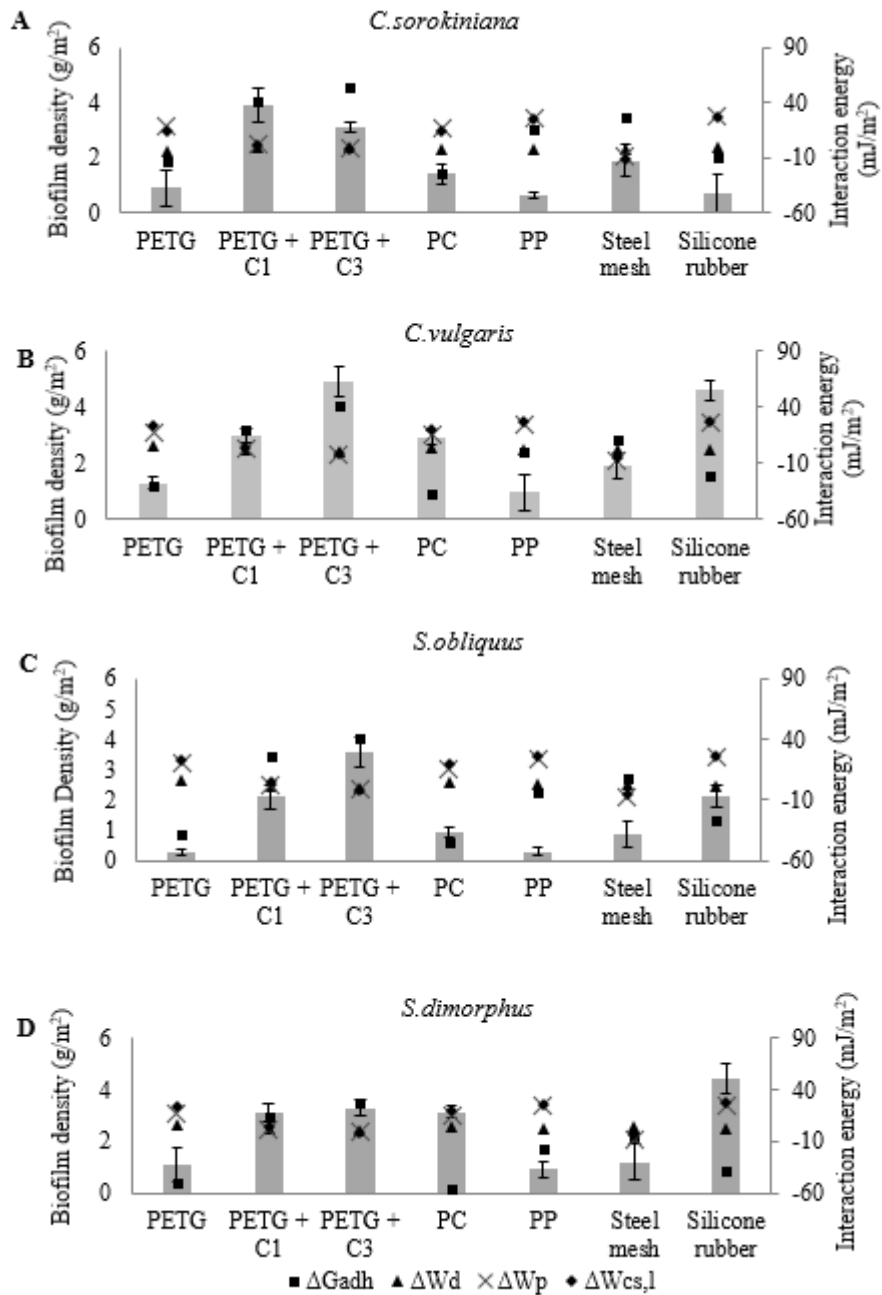


Figure. 6.3.3. Bars show weighted biofilm density found on tested surfaces on different surfaces after 7 days. Error bars show standard deviation of the mean (n=3). ΔG_{adh} is the free energy of adhesion according to AB and LW components. W-d and W-p is the work of attachments due dispersive and polar forces respectively. W is the total work of attachment due to polar and dispersive forces and substrate surface energy.

Table 6.3.5: Comparison of model prediction and experimental results.

<i>Algae</i>		Order of adhesion
<i>C.sorokiniana</i>	$W_{cs,l}$ prediction	Silicone rubber > PP > PETG > PC > PETG+ C1 > PETG + C3 > steel
	ΔG_{adh} prediction	PC > PETG > Silicone rubber > PP > Steel > PETG + C1 > PETG+ C3
	Initial attachment	PETG + C3 > Steel > PETG + C1 > PC > PP > PETG > Silicone rubber
	Strength of attachment	PETG + C3 > PETG + C1 > Silicone rubber > PC > Steel > PP > PETG
	Biofilm density	PETG + C1 > PETG + C3 > Steel > PC > PETG > Silicone rubber > PP
<i>C.vulgaris</i>	$W_{cs,l}$ prediction	Silicone rubber > PP > PETG > PC > PETG+ C1 > PETG + C3 > steel
	ΔG_{adh} prediction	PC > PETG > Silicone rubber > PP > Steel > PETG + C1 > PETG+ C3
	Initial attachment	PETG + C3 > PETG + C1 > Silicone rubber > Steel > PETG > PC > PP
	Strength of attachment	PETG + C3 > Silicone rubber > PC > Steel > PETG + C1 > PETG > PP
	Biofilm density	PETG + C3 > Silicone rubber > PETG + C1 > PC > Steel > PETG > PP
<i>S. obliquus</i>	$W_{cs,l}$ prediction	Silicone rubber > PP > PETG > PC > PETG+ C1 > PETG + C3 > steel
	ΔG_{adh} prediction	PC > PETG > Silicone rubber > PP > Steel > PETG + C1 > PETG+ C3
	Initial attachment	PETG + C3 > PETG + C1 > Silicone rubber > PETG > PC > PP > Steel
	Strength of attachment	Silicone rubber > PETG + C3 > PETG + C1 > Steel > PC > PETG > PP
	Biofilm density	PETG+ C3 > Silicone rubber > PETG + C1 > PC > Steel > PETG > PP
<i>S. dimorphus</i>	$W_{cs,l}$ prediction	Silicone rubber > PP > PETG > PC > PETG+ C1 > PETG + C3 > steel
	ΔG_{adh} prediction	PC > PETG > Silicone rubber > PP > Steel > PETG + C1 > PETG+ C3
	Initial attachment	PETG + C3 > PETG + C1 > Silicone rubber > PETG > PC > Steel > PP
	Strength of attachment	Silicone rubber > PETG + C3 > PETG + C1 > Steel > PC > PETG > PP
	Biofilm density	Silicone rubber > PETG + C3 > PC > PETG + C1 > Steel > PETG > PP

Table 6.3.6: Correlation coefficients calculated from data presented in Figures 6.1 – 6.3.3.

Correlation coefficient (r)					
Algae	Graph	ΔG_{adh}	ΔW_d	ΔW_p	$\Delta W_{cs,l}$
<i>C. sorokiniana</i>	Initial attachment (Fig.6.1 A)	0.68	0.24	-0.76	-0.76
	Strength of attachment (Fig.6.2 A)	0.61	0.82	-0.52	-0.46
	Biofilm density (Fig.6.2 A)	0.77	0.48	-0.76	-0.73
<i>C. vulgaris</i>	Initial attachment (Fig.6.1 B)	0.76	-0.77	-0.51	-0.58
	Strength of attachment (Fig.6.2 B)	0.45	-0.68	-0.41	-0.48
	Biofilm density (Fig.6.3 B)	0.77	-0.64	-0.68	-0.73
<i>S. obliquus</i>	Initial attachment (Fig.6.1 C)	0.70	-0.67	-0.43	-0.51
	Strength of attachment (Fig.6.2 C)	0.38	-0.54	-0.34	-0.37
	Biofilm density (Fig.6.3 C)	0.66	-0.82	-0.41	-0.49
<i>S. dimorphus</i>	Initial attachment (Fig.6.1 D)	0.54	-0.62	-0.39	-0.46
	Strength of attachment (Fig.6.2 D)	0.29	-0.63	-0.17	-0.25
	Biofilm density (Fig.6.3 D)	0.30	-0.57	-0.14	-0.22

6.2.2 Investigating the influence of physico-chemical properties of algae and substrata on lipid content.

Lipid content was measured for all algae samples that were harvested from different substrates, in order to examine the influence of the substrate's physico-chemical properties on lipid production (refer to Fig 6.3.4). Table 6.3.6 lists the correlation coefficients calculated for the data presented in Figure 6.3.4. All algae experienced negative correlation between $\Delta W_{cs,l}$ and lipid content. With the strongest negative correlation observed for *S. obliquus* ($r = -0.75$). All algae experienced positive correlation between ΔG_{adh} and resulting lipid content.

The strongest positive correlation was for *S. dimorphus* ($r = 0.89$). These results generally suggest higher lipid content is found in algae that are attached to substrates that have been predicted to be thermodynamically unfavourable. The differences in lipid content between different substrates were not large but nonetheless a possible trend has been detected. A possible reason as to why there was a found subtle influence of substrate properties on lipid content is offered. The first explanation could be due to the composition and quantity of the EPS being produced. EPS is said to consist of proteins, polysaccharides, and lipids (Vu et al. 2009). Microorganisms are able to change and adapt their EPS and adhesion according to the substrate properties they attach to (Ahimou et al., 2007). A previous study examining bacterial attachment found certain substrates such as pyrite or sulfur involve the lipopolysaccharide fraction of EPS. They also observed the % of lipids found in EPS on pyrite was 53.8 % which was 14.4 % more than in EPS found on sulfur (Gehrke et al. 1998).

It has also been shown that fatty acids from bacterial EPS aid in hydrophobic interactions between the substrate and microorganism. The study also concluded that fatty acids were far more important in membrane fouling than thought previously (Al-Halbouni et al. 2009). An additional study which further confirms this was carried out

by Becker (1996) where *Amphora coffeaeformis* was studied on different substrates with varying surface tensions. Substrates with high surface tensions correlated with high EPS production and resulted in better adhesion.

It should be noted that several other environmental factors have also been found that influence EPS quantity and composition; such as oxygen, temperature, pH, nutrient levels and nitrogen (Mayer et al. 1999).

Therefore, it could be suggested that the higher algal lipid content found in this study was due to increased lipid production for EPS, which is thought to be induced by energetically unfavorable conditions (high surface energy). Coated PETG generally had higher lipid content than the other substrates tested but also had unfavorable predicted interfacial energies. As the cells were attracted to the surface via electrostatic attraction, algal cells once at the surface may have produced more EPS in order to compensate for the lack in AB and LW attractions offered by the substrate. The higher production of EPS would have then aided algae cells to form better attachment. This could also further explain why previous results did not perform according to the thermodynamic model (Fig.6.3.1 – 6.3.3). Future investigations would benefit from characterising the EPS found on the substrate secreted by algae to confirm this suggested explanation.

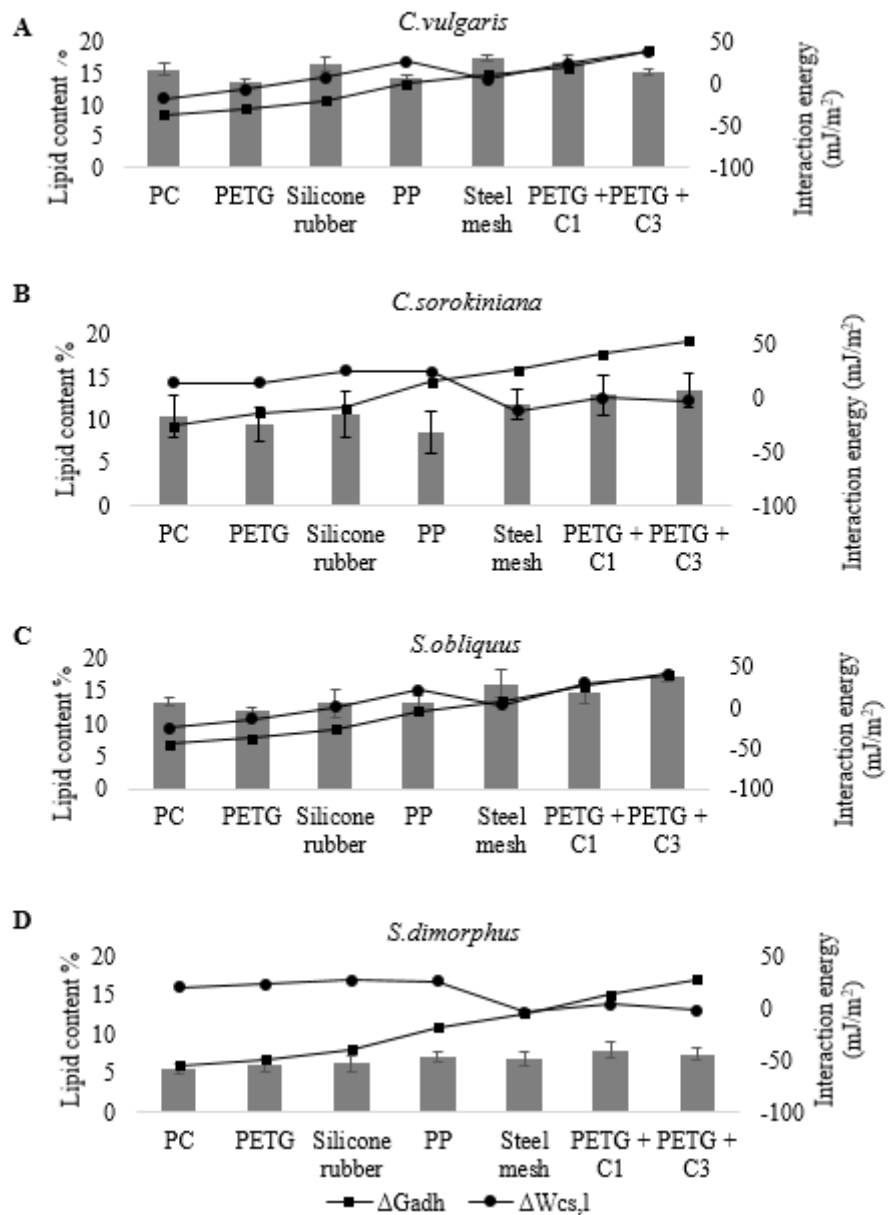


Figure. 6.3.4. Bars show lipid content (%) found on tested surfaces on different surfaces after 7 days. Error bars show standard deviation of the mean (n=3). ΔG_{adh} is the free energy of adhesion according to AB and LW components. W is the total work of attachment due to polar and dispersive forces and substrate surface energy.

Table 6.3.7: Correlation coefficients calculated from data presented in Figure 6.3.4.

Algae	Correlation coefficient (r)	
	ΔG_{adh}	$\Delta W_{cs,l}$
<i>C.sorokiniana</i>	0.710133	-0.7752
<i>C.vulgaris</i>	0.303301	-0.57621
<i>S. obliquus</i>	0.843405	-0.92
<i>S. dimorphus</i>	0.913898	-0.35083

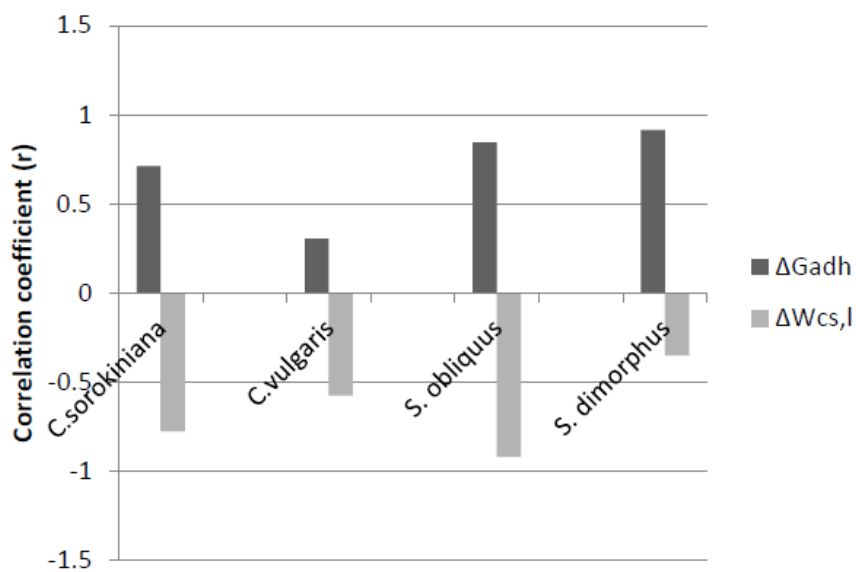


Figure. 6.3.5. Bars show correlation coefficient (refer to table 6.3.7). ΔG_{adh} is the free energy of adhesion according to AB and LW components. W is the total work of attachment due to polar and dispersive forces and substrate surface energy.

6.4 Conclusion

The following can be concluded after investigating the influence of physico-chemical properties of both algae and substrata.

- Both the work of attachment and change in free energy of adhesion approaches tested in this study failed to predict algae adhesion accurately.
- Surfaces with lower interfacial energies generally had better biofilm formation for all algae species tested, except for hydrophobic *S. dimorphus*, where silicone rubber had the highest biofilm density observed.
- The thermodynamic model also neglected to account for electrostatic interactions. Initial attachment to coated substrates are thought to mainly be mediated by electrostatic attraction.
- Charge effects may therefore be more significant than previously thought when determining attachment.
- The strength of attachment for *C. sorokiniana* was shown to be strongly correlated with the dispersal component of work of attachment.
- Physico-chemical properties of the substrate was shown to influence lipid content measured in algal biofilms. A strong correlation between lipid content and unfavourable thermodynamic conditions was observed for *C. sorokiniana*, *S. obliquus* and *S. dimorphus*.

The results presented in this study suggests that while interfacial energetics are complex and are heavily influenced by algal species and the chemical composition of the substrate, other factors may mediate attachment more heavily. Therefore, using thermodynamic models for selecting substrates and predicting adhesion may not be accurately reflective. In addition, further research into attachment factors such as EPS

and substrata influence on algal lipid content may prove beneficial in terms of optimising biofilm growth and stimulating lipid production.

Chapter 7

Conclusions and Recommendations

Chapter 3 revealed the potential of using PE coatings onto commercially available polymers as the carrier substrates for photobioreactors such as the ALGADISK reactor. The degree of attachment was found to be linked with the charge density of the algae species tested. Thereby suggesting attachment was mediated by electrostatic attraction and reduced repulsion. As attachment was measured according to the number of cells found on the surface, the size of the algae species may have had an effect on the number of cells found. Therefore a future recommendation would be to test strength of attachment (% of cells remaining after flushing) instead, to gauge more accurately the effect of charge density on attachment to charged substrates.

Although initial attachments on C1 and C3 coated PETG were high and showed promising applications in the ALGADISK reactor, regrowth between harvests was low and inconsistent. Regrowth was improved by inducing surface roughness onto the substrate prior to coating application via manual sandpapering. A recommendation based on this would be to investigate more textures with varying dimensions. Micro-textured surfaces for example may affect initial attachment or strength of attachment. Three different algae species that ranged in size was tested in chapter 4 when investigating surface roughness. Therefore, the size of the algae in relation to the size of the depressions made would also need to be investigated to gain further insight.

Optimisation of the selected coating (C1) was carried out and suitable parameters were revealed. Developing an airbrushing method rather than dip coating reduced the amount of PE solution needed and reduced the number of steps in the application process. Photo-

cross-linking with UV exposure increased the mechanical strength of the coating. The finalized devised method of coating production and application was implemented in a pilot scale ALGADISK reactor with *C. sorokiniana*. However, due to technical issues a clear conclusion on its performance was not made. A further pilot test after these technical issues are solved would be needed in order to evaluate its performance with the coated disks. In addition to this, the reactor tested freshwater algae species with the coated disks. Therefore, further tests in a marine species environment with the coated disks would have to be tested. A future recommendation would be to test the coated substrates in more alkaline environments to confirm its durability when using marine algae species.

Physicochemical studies showed that the model prediction stated unfavorable parameters for adhesion for C1 and C3. Results indicated that the most thermodynamically unfavorable substrates actually had the highest observed attachment. It was revealed that the thermodynamic model was not able to predict algae adhesion well, but a strong link between lipid content and the substrate was observed. Future recommendations would include testing the extended DVLO model as it accommodates for Lifshitz-van der Waals, electrostatic, Lewis acid-base and Brownian motion forces (Van Oss et al. 1989; Park & Kim, 2015). This model may aid as a better tool for algae adhesion prediction.

In addition to this, the link between lipid content and the substrate should be further examined. The EPS or AOM found on the substrates should be characterised and compared for their lipid content. These results could therefore confirm whether EPS composition, particularly the lipid fractions are influenced by the physico-chemical properties of the substrate. Subsequently it would also be recommended to conduct Fatty acid methyl esters (FAME) analysis of the lipids extracted from biofilm samples via gas

chromatography or high-performance liquid chromatography (HPLC). This would reveal if the substrata influences the quantity and composition of FAME, which are integral components to biodiesel.

The findings observed in the present study have applications in biofilm based photobioreactors as well as designing surfaces for antifouling properties. The conclusions derived from this study state that a higher amount and strength of adhesion occur on surfaces that are oppositely charged to the algae. Thermodynamically unfavorable substrates generally have a higher biofilm lipid content. These findings can be used to select an appropriate substrate to enhance biofilm growth and lipid content.

The coating application method developed in this study has many applications in the coatings field, in particular producing polyelectrolyte coated surfaces on a large scale.

The method developed uses a cost effective airbrushing approach combined with UV light for curing. This technique designed for polyelectrolyte deposition reduces costs and the need for highly trained end users. This was an important aspect towards helping algae production to be commercially viable.

After further development and testing of the ALGADISK reactor, it is hoped to be used by small businesses who aim to produce algae biomass products from industrial emissions.

Appendix

Table 1: M8-a medium used in ALGADISK pilot scale reactor

Compound	Concentration ($\mu\text{mol L}^{-1}$)
KNO_3	$29.67 \cdot 10^3$
$\text{Na}_2\text{PO}_4 \cdot 2 \text{H}_2\text{O}$	$1.46 \cdot 10^3$
KH_2PO_4	$5.44 \cdot 10^3$
$\text{MgSO}_4 \cdot 7 \text{H}_2\text{O}$	$1.62 \cdot 10^3$
$\text{CaCl}_2 \cdot 2 \text{H}_2\text{O}$	88.43
EDTA ferric sodium salt	315.86
H_3BO_3	1.00
$\text{Na}_2\text{EDTA} \cdot 2 \text{H}_2\text{O}$	100.00
$\text{MnCl}_2 \cdot 4 \text{H}_2\text{O}$	65.59
$\text{ZnSO}_4 \cdot 7 \text{H}_2\text{O}$	11.13
$\text{CuSO}_4 \cdot 5 \text{H}_2\text{O}$	7.33

Nomenclature

A	Hamaker constant
a	radius of algae cell, m
b	depth of the parallel plate flow chamber, m
c	distance from the surface of the substrata, m
d	separation distance of algae cell and substrate, m
d ₀	minimum separation distance between two surfaces, m
e	electron charge, 1.6022×10^{-10} C
k	Boltzmann constant, 1.3807×10^{-23} J K ⁻¹
n	concentration of ions, # m ⁻³
N	cell number concentration, # m ⁻³
T	temperature, K
v	hydration layer associated with algal cells, m
w	width of the parallel plate flow chamber, m
z	charge number of ions
PE	Polyelectrolyte
PEM	Polyelectrolyte multilayer

Superscripts

AB	acid-base, i.e., polar component
LW	Lifshitz-van der Waals, i.e., dispersive component
+	refers to electron acceptor parameter
-	refers to electron donor parameter

Subscripts

s substrate

sr surface

l liquid medium

m algae

Greek symbols

γ surface energy, J m⁻²

ζ zeta potential, V

ψ surface potential, V

θ contact angle, degrees

η dynamic viscosity of water at 20°C, 8.9×10⁻⁴ Pa s

ρ density of water at 20 °C, 997 kg m⁻³

$\dot{\gamma}$ wall shear rate, s⁻¹

κ^{-1} double layer thickness, m

λ correlation length of the molecules of the liquid medium, m

Publications

T. Bhaiji, Z.Libor, Sebestyén, P.K.Odolczyk1, Q.Zhang (2015). Enhanced attachment of algae on polymer substrates via polyelectrolyte coatings. *Submitted to the journal of Applied and Environmental Microbiology*.

T.Bhaiji, Qi Zhang. (2015). Devised methodology for large scale production of polyelectrolyte coatings on to polymer substrates. *In preparation*.

T.Bhaiji, Qi Zhang. (2015). Influence of physico-chemical properties on algae adhesion and lipid production. *In preparation*.

W. Blanken, M.Janssen, M.Cuaresma, Z.Libor, **T.Bhaiji**, Wijffels, R.H. (2014). Biofilm growth of *Chlorella sorokiniana* in a rotating biological contactor based photobioreactor. *Biotechnology and Bioengineering* 111 (12) - p. 2436-2445

P. Sebestyén, **T. Bhaiji**, A. Salimbeni, W. Blanken, I. Bacsa, G. Tóth, N. Pomázi, D. Molnár, M. Kozák, P. Kesserű, Q. Zhang, Zs. Libor, M. Janssen (2014). ALGADISK - Novel algae-based solution for co2 capture and biomass production. 22nd European Biomass Conference and Exhibition (Hamburg, Germany, 25 June 2014) – *Conference Proceedings*

References

- ABDEL-RAOUF, N., AL-HOMAIDAN, A. A. & IBRAHEEM, I. B. M. 2012. Microalgae and wastewater treatment. *Saudi Journal of Biological Sciences*, 19, 257-275.
- ABSOLOM, D. R., LAMBERTI, F. V., POLICOVA, Z., ZINGG, W., VAN OSS, C. J. & NEUMANN, A. W. 1983. Surface thermodynamics of bacterial adhesion. *Applied and Environmental Microbiology*, 46, 90-97.
- ABSOLOM, D. R., NEUMANN, A. W., ZINGG, W. & VAN OSS, C. J. 1979. Thermodynamic studies of cellular adhesion. *Trans Am Soc Artif Intern Organs*, 25, 152-8.
- ACIÉN, F. G., FERNÁNDEZ, J. M., MAGÁN, J. J. & MOLINA, E. 2012. Production cost of a real microalgae production plant and strategies to reduce it. *Biotechnology Advances*, 30, 1344-1353.
- ADVINCULA, R., BABA, A. & KANEKO, F. Functional ultrathin multilayer assemblies: Adsorption properties of charged azo dyes and polyelectrolytes investigated using the Quartz Crystal Microbalance (QCM) technique. ABSTRACTS OF PAPERS OF THE AMERICAN CHEMICAL SOCIETY, 1999. AMER CHEMICAL SOC 1155 16TH ST, NW, WASHINGTON, DC 20036 USA, U660-U660.
- AGBAKPE, M., GE, S., ZHANG, W., ZHANG, X. & KOBYLARZ, P. 2014. Algae harvesting for biofuel production: Influences of UV irradiation and polyethylenimine (PEI) coating on bacterial biocoagulation. *Bioresource Technology*, 166, 266-272.
- AHIMOU, F., SEMMENS, M. J., HAUGSTAD, G. & NOVAK, P. J. 2007. Effect of Protein, Polysaccharide, and Oxygen Concentration Profiles on Biofilm Cohesiveness. *Applied and Environmental Microbiology*, 73, 2905-2910.
- AL-HALBOUNI, D., DOTT, W. & HOLLENDER, J. 2009. Occurrence and composition of extracellular lipids and polysaccharides in a full-scale membrane bioreactor. *Water Res*, 43, 97-106.

- ALI, H., CHEEMA, T. A., YOON, H.-S., DO, Y. & PARK, C. W. 2015. Numerical prediction of algae cell mixing feature in raceway ponds using particle tracing methods. *Biotechnology and Bioengineering*, 112, 297-307.
- ANTIPOV, A. A., SUKHORUKOV, G. B., DONATH, E. & MÖHWALD, H. 2001. Sustained Release Properties of Polyelectrolyte Multilayer Capsules. *The Journal of Physical Chemistry B*, 105, 2281-2284.
- BA, C., LADNER, D. A. & ECONOMY, J. 2010. Using polyelectrolyte coatings to improve fouling resistance of a positively charged nanofiltration membrane. *Journal of Membrane Science*, 347, 250-259.
- BA, C., LADNER, D.A. and ECONOMY, J., 2010. Using polyelectrolyte coatings to improve fouling resistance of a positively charged nanofiltration membrane. *Journal of Membrane Science*, 347, 250-259.
- BARBEROUSSE, H., BRAYNER, R., DO REGO, A. M., CASTAING, J. C., BEURDELEY-SAUDOU, P. & COLOMBET, J. F. 2007. Adhesion of facade coating colonisers, as mediated by physico-chemical properties. *Biofouling*, 23, 15-24.
- BARBEROUSSE, H., LOMBARDO, R. J., TELL, G. & COUTE, A. 2006a. Factors involved in the colonisation of building facades by algae and cyanobacteria in France. *Biofouling*, 22, 69-77.
- BARBEROUSSE, H., RUIZ, G., GLOAGUEN, V., LOMBARDO, R. J., DJEDIAT, C., MASCARELL, G. & CASTAING, J. C. 2006b. Capsular polysaccharides secreted by building facade colonisers: characterisation and adsorption to surfaces. *Biofouling*, 22, 361-70.
- BARBOSA, M. J., JANSSEN, M., HAM, N., TRAMPER, J. & WIJFFELS, R. H. 2003. Microalgae cultivation in air-lift reactors: modeling biomass yield and growth rate as a function of mixing frequency. *Biotechnol Bioeng*, 82, 170-9.
- BARNWAL, B. K. & SHARMA, M. P. 2005. Prospects of biodiesel production from vegetable oils in India. *Renewable and Sustainable Energy Reviews*, 9, 363-378.

- BAYOUDH, S., OTHMANE, A., MORA, L. & BEN OUADA, H. 2009. Assessing bacterial adhesion using DLVO and XDLVO theories and the jet impingement technique. *Colloids and Surfaces B: Biointerfaces*, 73, 1-9.
- BECKER, K. 1996. Exopolysaccharide Production and Attachment Strength of Bacteria and Diatoms on Substrates with Different Surface Tensions. *Microb Ecol*, 32, 23-33.
- BEHERA, S., SINGH, R., ARORA, R., SHARMA, N. K., SHUKLA, M. & KUMAR, S. 2014. Scope of algae as third generation biofuels. *Front Bioeng Biotechnol*, 2, 90.
- BENEMANN, J. R. & OSWALD, W. J. 1996. Systems and economic analysis of microalgae ponds for conversion of CO₂ to biomass. Final report. *Other Information: PBD: 21 Mar 1996*.
- BLANKEN, W., JANSSEN, M., CUARESMA, M., LIBOR, Z., BHAIJI, T. & WIJFFELS, R. H. 2014. Biofilm growth of *Chlorella sorokiniana* in a rotating biological contactor based photobioreactor. *Biotechnol Bioeng*, 111, 2436-45.
- BONDESSON PA., GALBE M., ZACCHI G. 2013. Ethanol and biogas production after steam pretreatment of corn stover with or without the addition of sulphuric acid *Biotech. for Biofuels*, 6,11.
- BOROWITZKA, M. 1995. Microalgae as sources of pharmaceuticals and other biologically active compounds. *Journal of Applied Phycology*, 7, 3-15.
- BOROWITZKA, M. 2013. High-value products from microalgae—their development and commercialisation. *Journal of Applied Phycology*, 25, 743-756.
- BOS, R., VAN DER MEI, H. C. & BUSSCHER, H. J. 1999. Physico-chemistry of initial microbial adhesive interactions--its mechanisms and methods for study. *FEMS Microbiol Rev*, 23, 179-230.
- BOWEN, J., PETTITT, M. E., KENDALL, K., LEGGETT, G. J., PREECE, J. A., CALLOW, M. E. & CALLOW, J. A. 2007. *The influence of surface lubricity on the adhesion of Navicula perminuta and Ulva linza to alkanethiol self-assembled monolayers.*

- BP 2014. BP Statistical Review of World Energy 2014. In: PETROLEUM, B. (ed.) *Statistical Review of World Energy* British Petroleum.
- BRADY, R. F. & SINGER, I. L. 2000. Mechanical factors favoring release from fouling release coatings. *Biofouling*, 15, 73-81.
- BUSSCHER, H. J. S., J.; VAN DER MEI, H. 1990. Relative importance of surface free energy as a measure of hydrophobicity in bacterial adhesion to solid surfaces. *Microbial Cell Surface Hydrophobicity*. Washington, DC: American Society for Microbiology,.
- CALLOW M E, JENNINGS A R, BRENNAN A B, SEEGERT C E, GIBSON A, FEINBERG A, BANEY R, CALLOW J A (2002) Microtopographic cues for settlement of zoospores of the green fouling alga *Enteromorpha*. *Biofouling* 18, 237 – 245.
- CALLOW, M. E. & FLETCHER, R. L. 1994. The influence of low surface energy materials on bioadhesion — a review. *International Biodeterioration & Biodegradation*, 34, 333-348.
- CALLOW, M. E., CALLOW, J. A., ISTA, L. K., COLEMAN, S. E., NOLASCO, A. C. & LOPEZ, G. P. 2000. Use of self-assembled monolayers of different wettabilities to study surface selection and primary adhesion processes of green algal (*Enteromorpha*) zoospores. *Appl Environ Microbiol*, 66, 3249-54.
- CAO, X., PETTIT, M. E., CONLAN, S. L., WAGNER, W., HO, A. D., CLARE, A. S., CALLOW, J. A., CALLOW, M. E., GRUNZE, M. & ROSENHAHN, A. 2009. Resistance of polysaccharide coatings to proteins, hematopoietic cells, and marine organisms. *Biomacromolecules*, 10, 907-15.
- CARLOZZI, P. 2003. Dilution of solar radiation through “culture” lamination in photobioreactor rows facing south–north: A way to improve the efficiency of light utilization by cyanobacteria (*Arthrospira platensis*). *Biotechnology and Bioengineering*, 81, 305-315.
- CARVALHO, A. P., MEIRELES, L. A. & MALCATA, F. X. 2006. Microalgal reactors: a review of enclosed system designs and performances. *Biotechnol Prog*, 22, 1490-506.
- CERFF, M., MORWEISER, M., DILLSCHNEIDER, R., MICHEL, A., MENZEL, K. & POSTEN, C. 2012. Harvesting fresh water and marine algae by magnetic separation: screening of

- separation parameters and high gradient magnetic filtration. *Bioresour Technol*, 118, 289-95.
- CHANGE, U. N. F. C. O. C. 2009. Report of the Conference of the Parties on its Fifteenth Session, held in Copenhagen from 7 to 19 December 2009. Part Two: Action taken by the Conference of the Parties at its Fifteenth Session. *United Nations Climate Change Conf. Report 43*. UNFCC.
- CHARAKLIS, W. C. 1990. Microbial fouling and Microbial biofouling Control. In: MARSHALL, W. G. C. K. C. (ed.) *Biofilms*. New York: John Wiley.
- CHEN, W. & MCCARTHY, T. J. 1997. Layer-by-Layer Deposition: A Tool for Polymer Surface Modification. *Macromolecules*, 30, 78-86.
- CHISTI, Y. 2007. Biodiesel from microalgae. *Biotechnol Adv*, 25, 294-306.
- CHRISTENSON, L. B. & SIMS, R. C. 2012. Rotating algal biofilm reactor and spool harvester for wastewater treatment with biofuels by-products. *Biotechnol Bioeng*, 109, 1674-84.
- COOKSEY, K. & WIGGLESWORTH-COOKSEY, B. 1995. Adhesion of bacteria and diatoms to surfaces in the sea: a review. *Aquatic Microbial Ecology*, 9, 87-96.
- CROSS, L. E. 1987. Relaxor ferroelectrics. *Ferroelectrics*, 76, 241-267.
- CUI, Y. & YUAN, W. 2013. Thermodynamic modeling of algal cell–solid substrate interactions. *Applied Energy*, 112, 485-492.
- CUI, Y., YUAN, W. & CHENG, J. 2014. Understanding pH and ionic strength effects on aluminum sulfate-induced microalgae flocculation. *Appl Biochem Biotechnol*, 173, 1692-702.
- DARZINS, A. P., PHILLIP; EDYE, LES. 2010. Current Status and Potential for Algal Biofuels Production. *BioIndustry partners & NREL*, Bioenergy Task 131.
- DECHER, G. 1997. Fuzzy Nanoassemblies: Toward Layered Polymeric Multicomposites. *Science*, 277, 1232-1237.

- DONLAN, R. M. 2002. Biofilms: microbial life on surfaces. *Emerg Infect Dis*, 8, 881-90.
- DUBAS, S. T. & SCHLENOFF, J. B. 1999. Factors Controlling the Growth of Polyelectrolyte Multilayers. *Macromolecules*, 32, 8153-8160.
- EDERTH, T., NYGREN, P., PETTITT, M. E., OSTBLOM, M., DU, C., BROO, K., CALLOW, M. E., CALLOW, J. & LIEDBERG, B. 2008. Anomalous settlement behavior of *Ulva linza* zoospores on cationic oligopeptide surfaces. *Biofouling*, 24, 303-12.
- EDZWALD, J. K. & HAARHOFF, J. 2011. Seawater pretreatment for reverse osmosis: chemistry, contaminants, and coagulation. *Water Res*, 45, 5428-40.
- ERIKSEN, N. 2008. The technology of microalgal culturing. *Biotechnology Letters*, 30, 1525-1536.
- FELIZARDO, P., CORREIA, M. J., RAPOSO, I., MENDES, J. F., BERKEMEIER, R. & BORDADO, J. M. 2006. Production of biodiesel from waste frying oils. *Waste Manag*, 26, 487-94.
- FENG, D., CHEN, Z., XUE, S. & ZHANG, W. 2011. Increased lipid production of the marine oleaginous microalgae *Isochrysis zhangjiangensis* (Chrysophyta) by nitrogen supplement. *Bioresour Technol*, 102, 6710-6.
- FENG, Y., LI, C. & ZHANG, D. 2011. Lipid production of *Chlorella vulgaris* cultured in artificial wastewater medium. *Bioresource technology*, 102, 101-105.
- FINLAY, J. A., CALLOW, M. E., ISTA, L. K., LOPEZ, G. P. & CALLOW, J. A. 2002. The Influence of Surface Wettability on the Adhesion Strength of Settled Spores of the Green Alga *Enteromorpha* and the Diatom *Amphora*. *Integrative and Comparative Biology*, 42, 1116-1122.
- FLETCHER, M. & PRINGLE, J. H. 1985. The effect of surface free energy and medium surface tension on bacterial attachment to solid surfaces. *Journal of Colloid and Interface Science*, 104, 5-14.
- FUKUDA, H., KONDO, A. & NODA, H. 2001. Biodiesel fuel production by transesterification of oils. *Journal of bioscience and bioengineering*, 92, 405-416.

- GALLAGHER, B. J. 2011. The economics of producing biodiesel from algae. *Renewable Energy*, 36, 158-162.
- GAVRILESCU, M. & CHISTI, Y. 2005. Biotechnology-a sustainable alternative for chemical industry. *Biotechnol Adv*, 23, 471-99.
- GEHRKE, T., TELEGGI, J., THIERRY, D. & SAND, W. 1998. Importance of Extracellular Polymeric Substances from *Thiobacillus ferrooxidans* for Bioleaching. *Applied and Environmental Microbiology*, 64, 2743-2747.
- GENDY, T. S. & EL-TEMAMY, S. A. 2013. Commercialization potential aspects of microalgae for biofuel production: An overview. *Egyptian Journal of Petroleum*, 22, 43-51.
- GENIN, S. N., STEWART AITCHISON, J. & GRANT ALLEN, D. 2014. Design of algal film photobioreactors: material surface energy effects on algal film productivity, colonization and lipid content. *Bioresour Technol*, 155, 136-43.
- GOLD J. 2005. Surface modification of biomaterials from an academic research perspective. *Euro Cells and Mater*, 10, 2 .
- GOOD, R. J. 1993. Contact angle, wetting, and adhesion: a critical review. *Journal of adhesion science and technology*, 6, 1269-1302.
- GOOD, R. J. A. V. O., C.J. 1992. The modern theory of contact angles and the hydrogen bond components of surface energies. In: SCHRADER, M. E. A. L., G.I., EDS (ed.) *Modern Approaches to Wettability – Theory and Application* New York: Plenum Press.
- GRANHAG LM1, FINLAY JA, JONSSON PR, CALLOW JA, CALLOW ME. 2004. Roughness-dependent removal of settled spores of the green alga *Ulva* (syn. *Enteromorpha*) exposed to hydrodynamic forces from a water jet. *Biofouling*. 20, 117-22.
- GREENERGY 2010. Second Generation Biofuels. *Greenenergy Perspectives*, 02.
- GRIFFITHS, M., VAN HILLE, R. & HARRISON, S. L. 2012. Lipid productivity, settling potential and fatty acid profile of 11 microalgal species grown under nitrogen replete and limited conditions. *Journal of Applied Phycology*, 24, 989-1001.

- GRIFFITHS, M., VAN HILLE, R. & HARRISON, S. L. 2014. The effect of nitrogen limitation on lipid productivity and cell composition in *Chlorella vulgaris*. *Applied Microbiology and Biotechnology*, 98, 2345-2356.
- GROSS, M. & WEN, Z. 2014. Yearlong evaluation of performance and durability of a pilot-scale Revolving Algal Biofilm (RAB) cultivation system. *Bioresour Technol*, 171, 50-8.
- GROSS, M., HENRY, W., MICHAEL, C. & WEN, Z. 2013. Development of a rotating algal biofilm growth system for attached microalgae growth with in situ biomass harvest. *Bioresour Technol*, 150, 195-201.
- GROSS, M., JARBOE, D. & WEN, Z. 2015. Biofilm-based algal cultivation systems. *Appl Microbiol Biotechnol*, 99, 5781-9.
- GROSS, M., MASCARENHAS, V. & WEN, Z. 2015. Evaluating algal growth performance and water use efficiency of pilot-scale revolving algal biofilm (RAB) culture systems. *Biotechnol Bioeng*.
- GUILLAUME-GENTIL, O., AKIYAMA, Y., SCHULER, M., TANG, C., TEXTOR, M., YAMATO, M., OKANO, T. AND VÖRÖS, J. 2008. Polyelectrolyte Coatings with a Potential for Electronic Control and Cell Sheet Engineering. *Adv. Mater*, 20, 560-565.
- GUIRY, M. D. & SELIVANOVA, O. N. 2007. *Masakiella*, nom. nov. pro *Masakia* N.G. Klochkova (Corallinaceae, Rhodophyta), non *Masakia* (Nakai) Nakai (Celastraceae, Tracheophyta). *Phycologia*, 46, 235-236.
- GUPTA, P. L., LEE, S. M. & CHOI, H. J. 2015. A mini review: photobioreactors for large scale algal cultivation. *World J Microbiol Biotechnol*.
- GURA, T. 2009. Driving biofuels from field to fuel tank. *Cell*, 138, 9-12.
- HAAF, F., SANNER, A. & STRAUB, F. 1985. Polymers of N-vinylpyrrolidone: synthesis, characterization and uses. *Polymer Journal*, 17, 143-152.

- HARUN, R., DANQUAH, M. K. & FORDE, G. M. 2010. Microalgal biomass as a fermentation feedstock for bioethanol production. *Journal of Chemical Technology & Biotechnology*, 85, 199-203.
- HASELBERG, R., FLESCH, F.M., BOERKE, A. and SOMSEN, G.W., 2013. Thickness and morphology of polyelectrolyte coatings on silica surfaces before and after protein exposure studied by atomic force microscopy. *Analytica Chimica Acta*, 779, 90-95.
- HASSAN, M. F., LEE, H. P. & LIM, S. P. 2012. Effects of shear and surface roughness on reducing the attachment of *Oscillatoria* sp. filaments on substrates. *Water Environ Res*, 84, 744-52.
- HASSARD, F., BIDDLE, J., CARTMELL, E., JEFFERSON, B., TYRREL, S. & STEPHENSON, T. 2015. Rotating biological contactors for wastewater treatment – A review. *Process Safety and Environmental Protection*, 94, 285-306.
- HENDERSON, R.K., PARSONS, S.A. & JEFFERSON, B. 2010, "The impact of differing cell and algogenic organic matter (AOM) characteristics on the coagulation and flotation of algae", *Water research*, 44, 617-3624.
- HIRSCH, R. L. 2005. The Inevitable Peaking of World Oil Production. *The Atlantic Council of The United States*, 26, 10.
- HORATH, T. & BACHOFEN, R. 2009. Molecular characterization of an endolithic microbial community in dolomite rock in the central Alps (Switzerland). *Microb Ecol*, 58, 290-306.
- HOSSFELD, S., XIONG, X., KRASDEV, R. 2013. Polyelectrolyte Coatings for Surfaces Modification. *WOMag*, 2, 22.
- HU, Q., KURANO, N., KAWACHI, M., IWASAKI, I. & MIYACHI, S. 1998. Ultrahigh-cell-density culture of a marine green alga *Chlorococcum littorale* in a flat-plate photobioreactor. *Applied Microbiology and Biotechnology*, 49, 655-662.
- HUANG, H.-J., RAMASWAMY, S., AL-DAJANI, W., TSCHIRNER, U. & CAIRNCROSS, R. A. 2009. Effect of biomass species and plant size on cellulosic ethanol: A comparative process and economic analysis. *Biomass and Bioenergy*, 33, 234-246.

- IEA 2014. Key World Energy Statistics 2014. *In*: AGENCY, I. E. (ed.).
- IKADA, Y., SUZUKI, M. & TAMADA, Y. 1984. Polymer Surfaces Possessing Minimal Interaction with Blood Components. *In*: SHALABY, S., HOFFMAN, A., RATNER, B. & HORBETT, T. (eds.) *Polymers as Biomaterials*. Springer US.
- ILLMAN, A., SCRAGG, A. & SHALES, S. 2000. Increase in Chlorella strains calorific values when grown in low nitrogen medium. *Enzyme and microbial technology*, 27, 631-635.
- IRVING, T. E. & ALLEN, D. G. 2011. Species and material considerations in the formation and development of microalgal biofilms. *Appl Microbiol Biotechnol*, 92, 283-94.
- ISTA, L. K., CALLOW, M. E., FINLAY, J. A., COLEMAN, S. E., NOLASCO, A. C., SIMONS, R. H., CALLOW, J. A. & LOPEZ, G. P. 2004. Effect of substratum surface chemistry and surface energy on attachment of marine bacteria and algal spores. *Appl Environ Microbiol*, 70, 4151-7.
- IVÁNOVÁ, D., KADUKOVÁ, J., KAVULIČOVÁ, J. & HORVÁTHOVÁ, H. 2012. Determination of the Functional Groups in Algae Parachlorella Kessleri by Potentiometric Titrations. *Nova Biotechnologica et Chimica*.
- JADA, A. & JRADI, K. 2006. Role of Polyelectrolytes in Crystallogensis of Calcium Carbonate. *Macromolecular Symposia*, 233, 147-151.
- JOHN, W. E. A. 2002. Synthesis and Use of PolyDADMAC for Water Purification. *Biennial Conference of the Water Institute of Southern Africa (WISA)*. South Africa.
- JOHNSON, M. B. & WEN, Z. 2010. Development of an attached microalgal growth system for biofuel production. *Appl Microbiol Biotechnol*, 85, 525-34.
- JONES, C. S. & MAYFIELD, S. P. 2012. Algae biofuels: versatility for the future of bioenergy. *Curr Opin Biotechnol*, 23, 346-51.
- JORQUERA, O., KIPERSTOK, A., SALES, E. A., EMBIRUCU, M. & GHIRARDI, M. L. 2010. Comparative energy life-cycle analyses of microalgal biomass production in open ponds and photobioreactors. *Bioresour Technol*, 101, 1406-13.

- JORQUERA, O., KIPERSTOK, A., SALES, E. A., EMBIRUÇU, M. & GHIRARDI, M. L. 2010. Comparative energy life-cycle analyses of microalgal biomass production in open ponds and photobioreactors. *Bioresource Technology*, 101, 1406-1413.
- KATARZYNA, L., SAI, G. & SINGH, O. A. 2015. Non-enclosure methods for non-suspended microalgae cultivation: literature review and research needs. *Renewable and Sustainable Energy Reviews*, 42, 1418-1427.
- KATSIKOIANNI, M. & MISSIRLIS, Y. F. 2004. Concise review of mechanisms of bacterial adhesion to biomaterials and of techniques used in estimating bacteria-material interactions. *Eur Cell Mater*, 8, 37-57.
- KESAANO, M. & SIMS, R. C. 2014. Algal biofilm based technology for wastewater treatment. *Algal Research*, 5, 231-240.
- KLEINOVÁ, A., CVENGROŠOVÁ, Z., RIMARČÍK, J., BUZETZKI, E., MIKULEC, J. & CVENGROŠ, J. 2012. Biofuels from Algae. *Procedia Engineering*, 42, 231-238.
- KNOTHE, G., DUNN, R. O. & BAGBY, M. O. Biodiesel: the use of vegetable oils and their derivatives as alternative diesel fuels. ACS symposium series, 1997. Washington, DC: American Chemical Society,[1974]-, 172-208.
- KOMMIREDDY, D. S., PATEL, A. A., SHUTAVA, T. G., MILLS, D. K. & LVOV, Y. M. 2005. Layer-by-Layer assembly of TiO₂ nanoparticles for stable hydrophilic biocompatible coatings. *J Nanosci Nanotechnol*, 5, 1081-7.
- KOSTLER, S., DELGADO, A. V. & RIBITSCH, V. 2005. Surface thermodynamic properties of polyelectrolyte multilayers. *J Colloid Interface Sci*, 286, 339-48.
- KROL, S., DEL GUERRA, S., GRUPILLO, M., DIASPRO, A., GLIOZZI, A. & MARCHETTI, P. 2006. Multilayer nanoencapsulation. New approach for immune protection of human pancreatic islets. *Nano Lett*, 6, 1933-9.
- KUDAIBERGENOV, S. E., SADAKBAYEVA, Z. K., TATYKHANOVA, G. S., MEDARD, N., SEITOV, A. S. & ABDULLIN, K. A. 2012. Organosoluble Polyelectrolyte-Surfactant Complexes. *Macromolecular Symposia*, 317-318, 7-17.

- LADAM, G., SCHAAD, P., VOEGEL, J., SCHAAF, P., DECHER, G. & CUISINIER, F. 2000. In situ determination of the structural properties of initially deposited polyelectrolyte multilayers. *Langmuir*, 16, 1249-1255.
- LADAM, G., SCHAAF, P., CUISINIER, F. J., DECHER, G. & VOEGEL, J.-C. 2001. Protein adsorption onto auto-assembled polyelectrolyte films. *Langmuir*, 17, 878-882.
- LEE, D. H. 2011. Algal biodiesel economy and competition among bio-fuels. *Bioresour Technol*, 102, 43-9.
- LEE, K., LEE, S. Y., NA, J. G., JEON, S. G., PRAVEENKUMAR, R., KIM, D. M., CHANG, W. S. & OH, Y. K. 2013. Magnetophoretic harvesting of oleaginous *Chlorella* sp. by using biocompatible chitosan/magnetic nanoparticle composites. *Bioresour Technol*, 149, 575-8.
- LEE, R. A. & LAVOIE, J.-M. 2013. From first- to third-generation biofuels: Challenges of producing a commodity from a biomass of increasing complexity. *Animal Frontiers*, 3, 6-11.
- LEE, Y. C., LEE, K. & OH, Y. K. 2014. Recent nanoparticle engineering advances in microalgal cultivation and harvesting processes of biodiesel production: A review. *Bioresour Technol*.
- LEE, Y.-K. 1997. Commercial production of microalgae in the Asia-Pacific rim. *Journal of Applied Phycology*, 9, 403-411.
- LI, J., LIU, Y., CHENG, J. J., MOS, M. & DAROCH, M. 2015. Biological potential of microalgae in China for biorefinery-based production of biofuels and high value compounds. *N Biotechnol*.
- LI, P., MIAO, X., LI, R. & ZHONG, J. 2011. In Situ Biodiesel Production from Fast-Growing and High Oil Content *Chlorella pyrenoidosa* in Rice Straw Hydrolysate. *Journal of Biomedicine and Biotechnology*, 2011, 8.
- LI, Q., DU, W. & LIU, D. 2008. Perspectives of microbial oils for biodiesel production. *Applied Microbiology and Biotechnology*, 80, 749-756.

- LI, Y., GAO, Y. H., LI, X. S., YANG, J. Y. & QUE, G. H. 2010. Influence of surface free energy on the adhesion of marine benthic diatom *Nitzschia closterium* MMDL533. *Colloids Surf B Biointerfaces*, 75, 550-6.
- LIN, W., GUAN, Y., ZHANG, Y., XU, J. & ZHU, X. X. 2009. Salt-induced erosion of hydrogen-bonded layer-by-layer assembled films. *Soft Matter*, 5, 860-867.
- LIND, J. L., HEIMANN, K., MILLER, E. A., VAN VLIET, C., HOOGENRAAD, N. J. & WETHERBEE, R. 1997. Substratum adhesion and gliding in a diatom are mediated by extracellular proteoglycans. *Planta*, 203, 213-21.
- LIU, T., WANG, J., HU, Q., CHENG, P., JI, B., LIU, J., CHEN, Y., ZHANG, W., CHEN, X., CHEN, L., GAO, L., JI, C. & WANG, H. 2013. Attached cultivation technology of microalgae for efficient biomass feedstock production. *Bioresour Technol*, 127, 216-22.
- LIU, Z.-Y., WANG, G.-C. & ZHOU, B.-C. 2008. Effect of iron on growth and lipid accumulation in *Chlorella vulgaris*. *Bioresource Technology*, 99, 4717-4722.
- LOPEZ, M. C., SANCHEZ EDEL, R., LOPEZ, J. L., FERNANDEZ, F. G., SEVILLA, J. M., RIVAS, J., GUERRERO, M. G. & GRIMA, E. M. 2006. Comparative analysis of the outdoor culture of *Haematococcus pluvialis* in tubular and bubble column photobioreactors. *J Biotechnol*, 123, 329-42.
- LUAN, S., ZHAO, J., YANG, H., SHI, H., JIN, J., LI, X., LIU, J., WANG, J., YIN, J. & STAGNARO, P. 2012. Surface modification of poly(styrene-*b*-(ethylene-co-butylene)-*b*-styrene) elastomer via UV-induced graft polymerization of N-vinyl pyrrolidone. *Colloids Surf B Biointerfaces*, 93, 127-34.
- LVOV, Y., DECHER, G. & SUKHORUKOV, G. 1993. Assembly of thin films by means of successive deposition of alternate layers of DNA and poly(allylamine). *Macromolecules*, 26, 5396-5399.
- MARKOU, G. & NERANTZIS, E. 2013. Microalgae for high-value compounds and biofuels production: A review with focus on cultivation under stress conditions. *Biotechnology Advances*, 31, 1532-1542.

- MARTINELLI, L. A. & FILOSO, S. 2008. Expansion of sugarcane ethanol production in Brazil: environmental and social challenges. *Ecol Appl*, 18, 885-98.
- MATSUKAWA, R., HOTTA, M., MASUDA, Y., CHIHARA, M. & KARUBE, I. 2000. Antioxidants from carbon dioxide fixing *Chlorella sorokiniana*. *Journal of Applied Phycology*, 12, 263-267.
- MAYER, C., MORITZ, R., KIRSCHNER, C., BORCHARD, W., MAIBAUM, R., WINGENDER, J. & FLEMMING, H. C. 1999. The role of intermolecular interactions: studies on model systems for bacterial biofilms. *Int J Biol Macromol*, 26, 3-16.
- MAZIA, D., SCHATTEN, G. & SALE, W. 1975. Adhesion of cells to surfaces coated with polylysine. Applications to electron microscopy. *J Cell Biol*, 66, 198-200.
- MCGLADE, C. & EKINS, P. 2015. The geographical distribution of fossil fuels unused when limiting global warming to 2 [deg]C. *Nature*, 517, 187-190.
- MEIER-HAACK, J., LENK, W., LEHMANN, D. & LUNKWITZ, K. 2001. Pervaporation separation of water/alcohol mixtures using composite membranes based on polyelectrolyte multilayer assemblies. *Journal of Membrane Science*, 184, 233-243.
- MOHR, A. & RAMAN, S. 2013. Lessons from first generation biofuels and implications for the sustainability appraisal of second generation biofuels. *Energy Policy*, 63, 114-122.
- MOODY, J. W., MCGINTY, C. M. & QUINN, J. C. 2014. Global evaluation of biofuel potential from microalgae. *Proc Natl Acad Sci U S A*, 111, 8691-6.
- MOORE, A. 2008. Biofuels are dead: long live biofuels(?) - Part one. *N Biotechnol*, 25, 6-12.
- MORIGUCHI, I., ; FENDLER, J, H. 1998. Characterization and electrochromic properties of ultrathin films self-assembled from poly(diallyldimethylammonium) chloride and sodium decatungstate. *Chem. Materials*, 10, 2205-2211.
- MUJTABA, G., CHOI, W., LEE, C. G. & LEE, K. 2012. Lipid production by *Chlorella vulgaris* after a shift from nutrient-rich to nitrogen starvation conditions. *Bioresour Technol*, 123, 279-83.

- MULBRY, W., KONDRAD, S., PIZARRO, C. & KEBEDE-WESTHEAD, E. 2008. Treatment of dairy manure effluent using freshwater algae: algal productivity and recovery of manure nutrients using pilot-scale algal turf scrubbers. *Bioresour Technol*, 99, 8137-42.
- NADY, N., FRANSEN, M. C., ZUILHOF, H., EL-DIN, M. S. M., BOOM, R. & SCHROËN, K. 2011. Modification methods for poly (arylsulfone) membranes: a mini-review focusing on surface modification. *Desalination*, 275, 1-9.
- NADY, N., SCHROEN, K., FRANSEN, M. C., LAGEN, B., MURALI, S., BOOM, R. M., MOHYELDIN, M. S. & ZUILHOF, H. 2011. Mild and highly flexible enzyme-catalyzed modification of poly(ethersulfone) membranes. *ACS Appl Mater Interfaces*, 3, 801-10.
- NAIK, S. N., GOUD, V. V., ROUT, P. K. & DALAI, A. K. 2010. Production of first and second generation biofuels: A comprehensive review. *Renewable and Sustainable Energy Reviews*, 14, 578-597.
- NORSKER, N.-H., BARBOSA, M. J., VERMUË, M. H. & WIJFFELS, R. H. 2011. Microalgal production — A close look at the economics. *Biotechnology Advances*, 29, 24-27.
- OH, J. K., DRUMRIGHT, R., SIEGWART, D. J. & MATYJASZEWSKI, K. 2008. The development of microgels/nanogels for drug delivery applications. *Progress in Polymer Science*, 33, 448-477.
- ORWOLL, R. A. Y., CHONG S. 1999. Poly(acrylic acid). In: MARK, J. E. (ed.) *Polymer Data Handbook*. Oxford: Oxford University Press, .
- OWEN, N. A., INDERWILDI, O. R. & KING, D. A. 2010. The status of conventional world oil reserves—Hype or cause for concern? *Energy Policy*, 38, 4743-4749.
- OWENS, D. K. & WENDT, R. C. 1969. Estimation of the surface free energy of polymers. *Journal of Applied Polymer Science*, 13, 1741-1747.
- OZKAN, A. & BERBEROGLU, H. 2013a. Adhesion of algal cells to surfaces. *Biofouling*, 29, 469-482.

- OZKAN, A. & BERBEROGLU, H. 2013b. Cell to substratum and cell to cell interactions of microalgae. *Colloids and Surfaces B: Biointerfaces*, 112, 302-309.
- PARK J H, SCHWARTZ Z, NAVARRETE R O, BOYAN B D, AND TANNENBAUM R.2011. Enhancement of Surface Wettability via the Modification of Microtextured Titanium Implant Surfaces with Polyelectrolytes. *Langmuir* , 10, 5976-5985
- PARK, J.-A. & KIM, S.-B. 2015. DLVO and XDLVO calculations for bacteriophage MS2 adhesion to iron oxide particles. *Journal of Contaminant Hydrology*.
- PAUL ABISHEK, M. & PATEL, J. 2014. Algae oil: a sustainable renewable fuel of future. 2014, 272814.
- PIENKOS, P. T. & DARZINS, A. 2009. The promise and challenges of microalgal-derived biofuels. *Biofuels, Bioproducts and Biorefining*, 3, 431-440.
- PIERACCI, J., CRIVELLO, J. V. & BELFORT, G. 1999. Photochemical modification of 10kDa polyethersulfone ultrafiltration membranes for reduction of biofouling. *Journal of membrane science*, 156, 223-240.
- Pivokonsky, M., Kloucek, O. & Pivokonska, L. 2006, "Evaluation of the production, composition and aluminum and iron complexation of algogenic organic matter", *Water research*, 40, 3045-3052.
- POSADAS, E., GARCIA-ENCINA, P. A., SOLTAU, A., DOMINGUEZ, A., DIAZ, I. & MUNOZ, R. 2013. Carbon and nutrient removal from centrates and domestic wastewater using algal-bacterial biofilm bioreactors. *Bioresour Technol*, 139, 50-8.
- POSTEN, C. 2009. Design principles of photo-bioreactors for cultivation of microalgae. *Engineering in Life Sciences*, 9, 165-177.
- PREM RAJAN, A. 2014. Algae Oil: A Sustainable Renewable Fuel of Future. *Biotechnol Res Int*.
- PULZ, O. & GROSS, W. 2004. Valuable products from biotechnology of microalgae. *Appl Microbiol Biotechnol*, 65, 635-48.

- RAGAUSKAS, A. J., WILLIAMS, C. K., DAVISON, B. H., BRITOVSEK, G., CAIRNEY, J., ECKERT, C. A., FREDERICK, W. J., JR., HALLETT, J. P., LEAK, D. J., LIOTTA, C. L., MIELENZ, J. R., MURPHY, R., TEMPLER, R. & TSCHAPLINSKI, T. 2006. The path forward for biofuels and biomaterials. *Science*, 311, 484-9.
- RAMOS, M. J., FERNÁNDEZ, C. M., CASAS, A., RODRÍGUEZ, L. & PÉREZ, Á. 2009. Influence of fatty acid composition of raw materials on biodiesel properties. *Bioresource Technology*, 100, 261-268.
- REDMAN, J. A., WALKER, S. L. & ELIMELECH, M. 2004. Bacterial Adhesion and Transport in Porous Media: Role of the Secondary Energy Minimum. *Environmental Science & Technology*, 38, 1777-1785.
- REINE NEHMÉ, C.P., 2013. Highly Charged Polyelectrolyte Coatings to Prevent Adsorption During Protein and Peptide Analysis in Capillary Electrophoresis. *Meth in Mol Bio*, 984, 191-206.
- REITAN, K. I., RAINUZZO, J. R. & OLSEN, Y. 1994. Effect of nutrient limitation on fatty acid and lipid content of marine microalgae¹. *Journal of Phycology*, 30, 972-979.
- RIJNAARTS, H. H. M., NORDE, W., BOUWER, E. J., LYKLEMA, J. & ZEHNDER, A. J. B. 1995. Reversibility and mechanism of bacterial adhesion. *Colloids and Surfaces B: Biointerfaces*, 4, 5-22.
- RODOLFI, L., CHINI ZITTELLI, G., BASSI, N., PADOVANI, G., BIONDI, N., BONINI, G. & TREDICI, M. R. 2009. Microalgae for oil: strain selection, induction of lipid synthesis and outdoor mass cultivation in a low-cost photobioreactor. *Biotechnol Bioeng*, 102, 100-12.
- ROSENHAHN, A., SCHILP, S., KREUZER, H. J. & GRUNZE, M. 2010. The role of "inert" surface chemistry in marine biofouling prevention. *Physical Chemistry Chemical Physics*, 12, 4275-4286.
- SAFA, M., ALEMZADEH, I. & VOSSOUGH, M. 2014. Biodegradability of oily wastewater using rotating biological contactor combined with an external membrane. *J Environ Health Sci Eng*, 12, 117.

- SCHLENOFF, J. B., DUBAS, S. T. & FARHAT, T. 2000. Sprayed Polyelectrolyte Multilayers. *Langmuir*, 16, 9968-9969.
- SCHLESINGER, A., EISENSTADT, D., BAR-GIL, A., CARMELY, H., EINBINDER, S. & GRESSEL, J. 2012. Inexpensive non-toxic flocculation of microalgae contradicts theories; overcoming a major hurdle to bulk algal production. *Biotechnol Adv*, 30, 1023-30.
- SCHNURR, P. J., ESPIE, G. S. & ALLEN, D. G. 2013. Algae biofilm growth and the potential to stimulate lipid accumulation through nutrient starvation. *Bioresour Technol*, 136, 337-44.
- SCHULZE, K., LOPEZ, D. A., TILLICH, U. M. & FROHME, M. 2011. A simple viability analysis for unicellular cyanobacteria using a new autofluorescence assay, automated microscopy, and ImageJ. *BMC Biotechnol*, 11, 118.
- SCOTT, S. A., DAVEY, M. P., DENNIS, J. S., HORST, I., HOWE, C. J., LEA-SMITH, D. J. & SMITH, A. G. 2010. Biodiesel from algae: challenges and prospects. *Current Opinion in Biotechnology*, 21, 277-286.
- SERIVE, B., KAAS, R., BERARD, J. B., PASQUET, V., PICOT, L. & CADORET, J. P. 2012. Selection and optimisation of a method for efficient metabolites extraction from microalgae. *Bioresour Technol*, 124, 311-20.
- SHARP, E. L., JARVIS, P., PARSONS, S. A. & JEFFERSON, B. 2006. The impact of zeta potential on the physical properties of ferric--NOM flocs. *Environ Sci Technol*, 40, 3934-40.
- SHEEHAN, J. D., T; BENEMANN, J; ROESSLER, P. 1998. A Look Back at the U.S. Department of Energy's Aquatic Species Program—Biodiesel from Algae. U.S. Department of Energy's Office of Fuels Development.
- SHEN, Y. 2014. Carbon dioxide bio-fixation and wastewater treatment via algae photochemical synthesis for biofuels production. *RSC Advances*, 4, 49672-49722.
- SHEN, Y., XU, X., ZHAO, Y. & LIN, X. 2014. Influence of algae species, substrata and culture conditions on attached microalgal culture. *Bioprocess and Biosystems Engineering*, 37, 441-450.

- SIERRA, E., ACIÉN, F. G., FERNÁNDEZ, J. M., GARCÍA, J. L., GONZÁLEZ, C. & MOLINA, E. 2008. Characterization of a flat plate photobioreactor for the production of microalgae. *Chemical Engineering Journal*, 138, 136-147.
- SKJANES, K., REBOURS, C. & LINDBLAD, P. 2013. Potential for green microalgae to produce hydrogen, pharmaceuticals and other high value products in a combined process. *Crit Rev Biotechnol*, 33, 172-215.
- SOROKIN, C. 1959. Tabular comparative data for the low- and high-temperature strains of *Chlorella*. *Nature*, 184, 613-4.
- SOUZA, M. L. D. & FERRAGUT, C. 2012. Influence of substratum surface roughness on periphytic algal community structure in a shallow tropical reservoir. *Acta Limnologica Brasiliensia*, 24, 397-407.
- SPALDING, M. H. 2008. Microalgal carbon-dioxide-concentrating mechanisms: *Chlamydomonas* inorganic carbon transporters. *J Exp Bot*, 59, 1463-73.
- SPOLAORE, P., JOANNIS-CASSAN, C., DURAN, E. & ISAMBERT, A. 2006. Commercial applications of microalgae. *Journal of Bioscience and Bioengineering*, 101, 87-96.
- STANSELL, G., GRAY, V. & SYM, S. 2012. Microalgal fatty acid composition: implications for biodiesel quality. *Journal of Applied Phycology*, 24, 791-801.
- STEWART, S. S., ROLDAN, J. E., LVOV, Y. M. & MILLS, D. K. 2006. Layer-by-Layer adsorption of biocompatible polyelectrolytes onto dexamethasone aggregates. *Conf Proc IEEE Eng Med Biol Soc*, 1, 1474-7.
- SU, B., WANG, T., WANG, Z., GAO, X. & GAO, C. 2012. Preparation and performance of dynamic layer-by-layer PDADMAC/PSS nanofiltration membrane. *Journal of Membrane Science*, 423-424, 324-331.
- SUH, I. & LEE, C.-G. 2003. Photobioreactor engineering: Design and performance. *Biotechnology and Bioprocess Engineering*, 8, 313-321.

- TADMOR, R., HERNANDEZ-ZAPATA, E., CHEN, N., PINCUS, P. & ISRAELACHVILI, J. N. 2002. Debye length and double-layer forces in polyelectrolyte solutions. *Macromolecules*, 35, 2380-2388.
- TAMBURIC, B., ZEMICHAEL, F. W., CRUDGE, P., MAITLAND, G. C. & HELLGARDT, K. 2011. Design of a novel flat-plate photobioreactor system for green algal hydrogen production. *International Journal of Hydrogen Energy*, 36, 6578-6591.
- THIERRY, B., WINNIK, F. M., MERHI, Y., SILVER, J. & TABRIZIAN, M. 2003. Bioactive coatings of endovascular stents based on polyelectrolyte multilayers. *Biomacromolecules*, 4, 1564-71.
- TRUESDAIL, S. E., LUKASIK, J., FARRAH, S. R., SHAH, D. O. & DICKINSON, R. B. 1998. Analysis of bacterial deposition on metal (hydr)oxide-coated sand filter media. *Journal of Colloid and Interface Science*, 203, 369-378.
- TSUJI, H., TAKAI, H., FUKUDA, N. & TAKIKAWA, H. 2006. Non-Isothermal Crystallization Behavior of Poly(L-lactic acid) in the Presence of Various Additives. *Macromolecular Materials and Engineering*, 291, 325-335.
- TSUNEDA, S., AIKAWA, H., HAYASHI, H., YUASA, A. & HIRATA, A. 2003. Extracellular polymeric substances responsible for bacterial adhesion onto solid surface. *FEMS Microbiol Lett*, 223, 287-92.
- UDUMAN, N., QI, Y., DANQUAH, M. K., FORDE, G. M. & HOADLEY, A. 2010. Dewatering of microalgal cultures: A major bottleneck to algae-based fuels. *Journal of Renewable and Sustainable Energy*, 2, 012701.
- UGWU, C. U., AOYAGI, H. & UCHIYAMA, H. 2008. Photobioreactors for mass cultivation of algae. *Bioresource Technology*, 99, 4021-4028.
- ULBRICHT, M. 2006. Advanced functional polymer membranes. *Polymer*, 47, 2217-2262.
- VADAS R L, WRIGHT W A, MILLER S L (1990) Recruitment of *Ascophyllum nodosum*: wave action as a source of mortality. *Mar Ecol Prog Ser* 61, 263 – 272

- VAN LOOSDRECHT, M., LYKLEMA, J., NORDE, W., SCHRAA, G. & ZEHNDER, A. 1987. Electrophoretic mobility and hydrophobicity as a measured to predict the initial steps of bacterial adhesion. *Applied and Environmental Microbiology*, 53, 1898-1901.
- VAN OSS, C. J. 1995. Hydrophobic, hydrophilic and other interactions in epitope-paratope binding. *Mol Immunol*, 32, 199-211.
- VAN OSS, C. J., CHAUDHURY, M. K. & GOOD, R. J. 1989. Mechanism of phase separation of polymers in organic media - apolar and polar systems. *Separation Science and Technology*, 24, 15-30.
- VANCHA, A. R., GOVINDARAJU, S., PARSA, K. V., JASTI, M., GONZALEZ-GARCIA, M. & BALLESTERO, R. P. 2004. Use of polyethyleneimine polymer in cell culture as attachment factor and lipofection enhancer. *BMC Biotechnol*, 4, 23.
- VANDAMME, D., FOUBERT, I. & MUYLAERT, K. 2013. Flocculation as a low-cost method for harvesting microalgae for bulk biomass production. *Trends in Biotechnology*, 31, 233-239.
- VANTHOOR-KOOPMANS, M., WIJFFELS, R. H., BARBOSA, M. J. & EPPINK, M. H. M. 2013. Biorefinery of microalgae for food and fuel. *Bioresource Technology*, 135, 142-149.
- VAZQUEZ, C. P., BOUDOU, T., DULONG, V., NICOLAS, C., PICART, C. & GLINEL, K. 2009. Variation of polyelectrolyte film stiffness by photo-cross-linking: a new way to control cell adhesion. *Langmuir*, 25, 3556-63.
- VÁZQUEZ, C. P., BOUDOU, T., DULONG, V., NICOLAS, C., PICART, C. & GLINEL, K. 2009b. PHOTO-CROSSLINKED POLYELECTROLYTE FILMS OF VARYING MECHANICAL STIFFNESS TO CONTROL CELL ADHESION. *Polymer Preprints*, 50, 33.
- VU, B., CHEN, M., CRAWFORD, R. & IVANOVA, E. 2009. Bacterial Extracellular Polysaccharides Involved in Biofilm Formation. *Molecules*, 14, 2535.
- WANG, S., ZHANG, Y., ABIDI, N. & CABRALES, L. 2009. Wettability and surface free energy of graphene films. *Langmuir*, 25, 11078-11081.

- WANG, X., HAO, C., ZHANG, F., FENG, C. & YANG, Y. 2011. Inhibition of the growth of two blue-green algae species (*Microcystis aruginosa* and *Anabaena spiroides*) by acidification treatments using carbon dioxide. *Bioresour Technol*, 102, 5742-8.
- WANG, Y., HASSAN, M. S., GUNAWAN, P., LAU, R., WANG, X. & XU, R. 2009. Polyelectrolyte mediated formation of hydroxyapatite microspheres of controlled size and hierarchical structure. *Journal of colloid and interface science*, 339, 69-77.
- WIGGLESWORTH-COOKSEY, B., VAN DER MEI, H., BUSSCHER, H. J. & COOKSEY, K. E. 1999. The influence of surface chemistry on the control of cellular behavior: studies with a marine diatom and a wettability gradient. *Colloids and Surfaces B: Biointerfaces*, 15, 71-80.
- WIJFFELS, R. H. & BARBOSA, M. J. 2010. An Outlook on Microalgal Biofuels. *Science*, 329, 796-799.
- WILDHABER, J. H., DEVADASON, S. G., EBER, E., HAYDEN, M. J., EVERARD, M. L., SUMMERS, Q. A. & LESOUEF, P. N. 1996. Effect of electrostatic charge, flow, delay and multiple actuations on the in vitro delivery of salbutamol from different small volume spacers for infants. *Thorax*, 51, 985-8.
- WILEY, P. E., CAMPBELL, J. E. & MCKUIN, B. 2011. Production of biodiesel and biogas from algae: a review of process train options. *Water Environ Res*, 83, 326-38.
- WOOTSCH, A., BULKAI, A., TÓTH, G., MOLNÁR, D., KOZÁK, M., KESSER?, P., KOÓS, A., SEBESTYÉN, P., ZHANG, Q., LIBOR, Z., BLANKEN, W., CUARESMA FRANCO, M., JANSSEN, M., WIJFFELS, R.H. Increasing the competitiveness of European non-energy algal sector by a novel solution for biomass production. 20th European Biomass Conference and Exhibition, 2012 Milan, Italy. 440-449.
- ZAMALLOA, C., BOON, N. & VERSTRAETE, W. 2013. Decentralized two-stage sewage treatment by chemical-biological flocculation combined with microalgae biofilm for nutrient immobilization in a roof installed parallel plate reactor. *Bioresour Technol*, 130, 152-60.
- ZHAI, L., NOLTE, A. J., COHEN, R. E. & RUBNER, M. F. 2004. pH-Gated Porosity Transitions of Polyelectrolyte Multilayers in Confined Geometries and Their Application as Tunable Bragg Reflectors. *Macromolecules*, 37, 6113-6123.

ZIA, K. M., ZIA, F., ZUBER, M., REHMAN, S. & AHMAD, M. N. 2015. Alginate based polyurethanes: A review of recent advances and perspective. *Int J Biol Macromol*, 79, 377-387.

ZITA, A. & HERMANSSON, M. 1997. Effects of bacterial cell surface structures and hydrophobicity on attachment to activated sludge flocs. *Appl Environ Microbiol*, 63, 1168-70.